

Biochemical Investigations of
L-Methionine gamma-lyase 1 from
Trichomonas vaginalis

by

Ignace Adolfo Moya

A thesis
presented to the University of Waterloo
in fulfillment of the
thesis requirement for the degree of
Doctor of Philosophy
in
Chemistry

Waterloo, Ontario, Canada, 2011

© Ignace Adolfo Moya 2011

AUTHOR'S DECLARATION

I hereby declare that I am the sole author of this thesis. This is a true copy of the thesis, including any required final revisions, as accepted by my examiners.

I understand that my thesis may be made electronically available to the public.

ABSTRACT

The enzyme L-methionine γ -lyase (MGL) utilizes a pyridoxal-5'-phosphate-cofactor in order to convert L-methionine to α -ketobutyrate, ammonia and methyl mercaptan. MGL is proposed to be a potential drug target since it is expressed in the human pathogens, *Trichomonas vaginalis* and *Entamoeba histolytica*, but not in humans. There is currently a need to find alternative drug targets for these pathogens, because the misuse and overuse of the currently prescribed drugs of choice, metronidazole and tinidazole, have led to drug resistance.

The overall goal of this thesis was to examine the chemistry of MGL 1 from *T. vaginalis* (TvMGL1) by probing the active site by site-directed mutagenesis and with fluorinated methionine analogs. The mutation of the active site residue Cys113 to Ser led to a 5-fold decrease in turnover rate for L-methionine relative to the wild-type enzyme. The results suggest that the active site C113 residue plays an important role in catalysis and is consistent with literature reports for MGL homologs from *Pseudomonas putida* and *E. histolytica*. Probing the active site of TvMGL1 with the fluorinated methionine analogs, L-difluoromethionine (DFM) and L-trifluoromethionine (TFM), were found to increase the turnover rate of the enzyme with an increase in fluorine substitution. The results suggest that the bulky fluorine atoms do not interfere with the Michaelis-Menten kinetics of the enzyme, and the γ -elimination step is rate determining.

The second goal of this thesis was to identify the reactive intermediates generated by the processing of TFM and the uninvestigated DFM by TvMGL1, and to investigate the theoretical and experimental chemistry and biochemistry of these fluorinated groups (CF₃S- and CF₂HS-). The reactivity of the intermediates, generated from the processing of DFM by TvMGL1 was correlated to the cytotoxicity observed in model organisms expressing TvMGL1, and consistent with the hypothesis that the intermediates will result in the thioformylation of primary amines. The results suggest that cytotoxicity requires thioacylation of a single primary amine, while sequential cross-linking of primary amines is not an absolute requirement. The relationship between the chemical structure of the reactive intermediates produced from the enzymatic processing of these analogs and their cellular toxicity is discussed.

Attempts at the synthesis of 3,3-difluoro-*O*-methyl-L-homoserine were undertaken in order to examine the catalytic mechanism of TvMGL1, since the compound is expected to inhibit the enzyme. To ensure that the oxo moiety does not impede the chemistry of the enzyme, the analog, *O*-methyl-L-homoserine was examined as a potential substrate for TvMGL1. Several synthetic routes to 3,3-difluoro-*O*-methyl-L-homoserine were examined; however, attempts to fluorinate the β-carbon atom of the starting material were unsuccessful.

ACKNOWLEDGEMENTS

I would like to thank my supervisor, Dr. John Honek for his help and support with the project, and improving my understanding of the field. I enjoyed the insightful discussions we had over a cup of coffee and during lunch about medicinal chemistry.

My committee members, Drs. E. Meiering, K. Ma, A. Schwan for their time and critique of my work. Dr. R. Smith (mass spectrometry), C. Myers (mass spectrometry) for obtaining the ESI-MS data. J. Venne (NMR) for running some of my samples, training and for her helpful suggestions. Dr. S. Taylor, Dr. M. Chong and J. Su for their suggestions in trouble shooting the chemical reactions. To our collaborators, Drs. G. Coombs and G. Westrop (University of Strathclyde, Glasgow) for testing the compound on the parasite and critiquing the published manuscript.

I appreciate all of my friends and colleges for their support during my time in Waterloo: T. Trecroce, A. Cavanagh, O. Zhang, J. DaCosta, P. Hang, S. Zhu, V. Azhikannickal, J. Wang, J. Dubrick, Q. Bahtti, M. Grewal, K. Kosar, J. Warren, J. Stewart, K. Mullings, R. Zahoruk, U. Suttisansanee, J. Harris, Dr. E. Daub, Dr. Z. Su, J. Verhoek, M. Vanderkooy, D. Fuhr, R. Clark and E. Ohm.

Special thanks to my former supervisor Dr. Y. Luo (University of Saskatchewan, Saskatoon, SK) and Dr. C. Phenix (TBRRI, Thunder Bay, ON) for their help with editing of my manuscript, suggestions, advice, laboratory training, and past and current mentoring.

DEDICATIONS

Dedicated to my parents and sister for their support in my endeavours. And the early bird that was already in bed while I worked away until the late hours of the night.

TABLE OF CONTENTS

AUTHOR'S DECLARATION	ii
ABSTRACT.....	iii
ACKNOWLEDGEMENTS	v
DEDICATIONS.....	vi
TABLE OF CONTENTS.....	vii
LIST OF FIGURES	xi
LIST OF TABLES.....	xiv
LIST OF ABBREVIATIONS.....	xv
CHAPTER 1 BACKGROUND	1
1.1. Authors' Contributions.....	1
1.2. Introduction	1
1.3. Epidemiology and Treatment for Parasitic Infections.....	3
1.4. Potential Drug Target for Parasitic Infections.....	8
1.5. Superfamilies of PLP-dependent Enzymes	12
1.6. Reactions Catalyzed by L-Methionine γ -lyase.....	19
1.7. Methionine-dependent Tumors	22
1.8. Cysteine Biosynthesis Pathway.....	24
1.8.1. An Overview of Sulfur Biochemistry in Living Organisms	24
1.8.2. Methionine Catabolism	27
1.8.3. Sulfide Biosynthetic Pathway and de novo Cysteine Biosynthesis.....	29
1.9. Purpose of Study	31
CHAPTER 2 ROLE OF THE ACTIVE SITE RESIDUE C113 IN <i>TRICHOMONAS</i> <i>VAGINALIS</i> L-METHIONINE γ -LYASE 1	32
2.1. Authors' Contribution	32
2.2. Introduction	32
2.3. Studies on the Functional Role of the Cysteine Residue	33
2.4. Results and Discussion.....	37

2.5. Conclusion and Future Work	39
2.6. Materials and Methods	40
2.6.1. General Experimental	40
2.6.2. TvMGL1 C113 Mutants	40
2.6.3. Agarose Gel Electrophoresis	42
2.6.4. Cell Culture and Expression of Enzyme	42
2.6.5. Cell Lysis and Protein Purification.....	43
2.6.6. SDS-Polyacrylamide Gel Electrophoresis.....	45
2.6.7. MBTH Assay Method for Detecting α -Ketobutyrate.....	46
CHAPTER 3 MECHANISTIC STUDIES ON THE ENZYMATIC PROCESSING OF FLUORINATED METHIONINE ANALOGS BY TRICHOMONAS VAGINALIS L- METHIONINE γ -LYASE 1	47
3.1. Authors' Contributions.....	47
3.2. Introduction	47
3.3. Pyridoxal Model Systems of Enzymatic Catalytic Reactions.....	48
3.4. Processing of Fluorinated Methionine Analogs by PLP-dependent Enzymes.....	51
3.5. Results	53
3.5.1. Detecting the Products from the Enzymatic Processing of the Fluorinated Methionine Analogs	53
3.5.2. Monitoring the Intermediates Produced from the Processing of TFM and DFM by MPAL	65
3.5.3. Kinetic Parameters for the Enzymatic Processing of the Fluorinated Methionine Analog.....	66
3.5.4. Possible Modes of Inhibition of TvMGL1	69
3.5.5. Cellular toxicity of the Fluorinated Methionine Analogs in Organisms that Express TvMGL1	73
3.6. Discussion	77
3.7. Materials and Methods	83
3.7.1. Materials	83
3.7.2. Protein Purification.....	84

3.7.3. MBTH Assay Method for Detecting α -Ketobutyrate	84
3.7.4. Michaelis-Menten Kinetics	85
3.7.5. ^{19}F -NMR Experiments	85
3.7.6. Theoretical Calculation of the ^{19}F -NMR Chemical Shifts	86
3.7.7. Theoretical Calculations of the Heats of Formation.....	86
3.7.8. Theoretical Calculation of the pK_a Values for the Thiol Compounds.....	87
3.7.9. Cross-linking of MGL Protein Upon Processing of Fluorinated Analogs	88
3.7.10. Model Processing of Fluorinated Analogs	88
3.7.11. Syntheses	89
3.7.12. Cloning of <i>mg11</i> into the pET28b Vector and Cell Inhibition Assay	92
CHAPTER 4 SYNTHETIC ROUTES TO 3,3-DIFLUORO-O-METHYL-L-HOMOSERINE	95
4.1. Authors' Contributions.....	95
4.2. Introduction	95
4.3. Chemical Properties of the Fluorine Atom	97
4.4. Conformational Preference of Fluorinated Molecules.....	98
4.4.1. Models for the Preferred Conformation of Molecules	98
4.5. Fluorination Reagents and Applications	103
4.6. Mechanism Based Inhibitors.....	107
4.7. Results and Discussion.....	111
4.7.1. Synthetic Approaches to 3,3-Difluoro-L-Methionine Analogs.....	111
4.8. Conclusions and Future Work.....	121
4.9. Materials and Methods	123
4.9.1. General Experimental.....	123
4.9.2. MBTH Assay Method for Detecting α -Ketobutyrate.....	124
4.9.3. O-Methyl-L-Homoserine Physical Data.....	125
4.9.4. Titanium-Claisen Condensation Reaction.....	125
4.9.5. Neber Reaction	126

4.9.6. Lithium Diisopropylamide-cross Claisen Condensation Reaction.....	129
4.9.7. Oximation of β -Ketoesters	129
4.9.8. Fluorination of β -Ketoesters with Tetrafluoride Analog Reagents	131
4.9.9. Dithiolane Esters	132
CHAPTER 5 SUMMARY AND FUTURE WORK	135
REFERENCES	139

LIST OF FIGURES

CHAPTER 1 INTRODUCTION

Figure 1.1. Reaction overview for the catalysis of L-amino acids by the PLP-dependent enzyme TvMGL1.	2
Figure 1.2. Antiparasitic prodrugs metronidazole (1.5) and tinidazole (1.6).	4
Figure 1.3. Energy metabolism and metronidazole drug target ferredoxin in <i>T. vaginalis</i>	5
Figure 1.4. Amino acid sequence alignment of MGL from various anaerobic organisms..	11
Figure 1.5. PLP-dependent enzymes fold types I to V, and the PLP cofactor displaying internal aldimine and external aldimine.	13
Figure 1.6. The reactions catalyzed by various PLP-dependent enzymes from fold type I family.	14
Figure 1.7. The domains and secondary structure of a fold-type I family enzyme.	16
Figure 1.8. Structural alignment of TPL and TvMGL1 displaying a potential metal coordination site.	17
Figure 1.9. Hydrogen bonding network established between the bound potassium and the active site residues of CfTPL.	19
Figure 1.10. Overview of the proposed key reaction steps in the γ -elimination of methionine by TvMGL1.	21
Figure 1.11. An overview of the biosynthetic pathways for thiol-containing amino acids in humans, yeast, <i>E. coli</i> , plants, <i>E. histolytica</i> and <i>T. vaginalis</i>	25
Figure 1.12. Forward and reverse transsulfuration pathways.	26
Figure 1.13. Methionine catabolism and <i>de novo</i> cysteine biosynthesis in <i>E. histolytica</i> and <i>T. vaginalis</i>	28

CHAPTER 2 ROLE OF THE ACTIVE SITE RESIDUE C113 IN *TRICHOMONAS VAGINALIS* MGL1

Figure 2.1. The active site of TvMGL1 homodimer.	33
Figure 2.2. Reaction overview of the catalysis of L-homocysteine derivatives by TvMGL1, and modification of active site thiols in enzymes.	35
Figure 2.3. An MBTH (2.6) assay method for detection of α -ketobutyrate (2.7) generated from the turnover of L-methionine by TvMGL1.	38

CHAPTER 3 MECHANISTIC STUDIES ON THE ENZYMATIC PROCESSING OF
FLUORINATED METHIONINE ANALOGS BY *TRICHOMONAS VAGINALIS* L-
METHIONINE γ -LYASE

Figure 3.1. Schematic representation of the reaction catalyzed by the PLP-dependent enzyme MGL.....	48
Figure 3.2. The various nonenzymatic catalytic reactions on an amino acid by pyridoxal. 50	
Figure 3.3. Syntheses of TFM (3.8) and DFM (3.9).	53
Figure 3.4. ^{19}F -NMR spectra for the processing of TFM and DFM by TvMGL1 (externally locked with CFCl_3).	55
Figure 3.5. The proposed reaction for the production of the thioacylating agents using a model pyridoxal system, and syntheses of MPAL and authentic reference standards.	61
Figure 3.6. ^1H -NMR spectra of the extracted compounds from the TFM and DFM PLP model reactions.....	63
Figure 3.7. ESI-MS spectra of the extracted compounds from the TFM and DFM PLP model reaction.	64
Figure 3.8. ^{19}F -NMR spectrum for the processing of TFM by MPAL in a solution of methanol-ethyl acetate (externally locked with CFCl_3).	67
Figure 3.9. Michaelis-Menten kinetics and initial rates for the LDH coupled assay of TvMGL1 processing methionine and its fluorinated analogs.	69
Figure 3.10. The proposed reaction scheme for the production of the thioacylating agents upon processing of the fluorinated methionine analogs by TvMGL1.....	70
Figure 3.11. An SDS-polyacrylamide gel analysis of the intermolecular cross-linking of TvMGL1 with various compounds, and its inhibition with cysteamine <i>in vitro</i>	73
Figure 3.12. The growth inhibition of <i>E. coli</i> cells overexpressing MGL1 and control <i>E. coli</i> cells, and the growth response of <i>T. vaginalis</i>	77
CHAPTER 4 SYNTHETIC ROUTES TO 3,3-DIFLUORO- <i>O</i> -METHYL-L-HOMOSERINE	
Figure 4.1. Hydrogen bonding interactions between water and $\text{C}(\text{sp}^3)\text{-X}$ groups.	97
Figure 4.2. Stereochemistry of a carbohydrate and stabilizing hyper-conjugation effects. 99	
Figure 4.3. The relationship between bond angles of a molecule and percent bonding character of substituted electronegative atoms.....	101
Figure 4.4. Energy difference between trans and gauche conformers.	103

Figure 4.5. Fluorination reagents and deoxyfluorination of molecules.	104
Figure 4.6. Fluorination of β -ketoesters and carbonium ion type rearrangement of pivaldehyde during deoxyfluorination.	106
Figure 4.7. Suicide inhibition mechanism of β - and γ -eliminating PLP-dependent enzymes.	108
Figure 4.8. The synthetic route of 3,3-difluoro-L-methionine (4.25) from the precursor L-ascorbic acid.	109
Figure 4.9. L-Homocysteine (4.22), L-methionine (4.24) and their fluorine derivatives.	110
Figure 4.10. Proposed synthetic route to 3,3-difluoro- <i>O</i> -methyl-L-homoserine (4.23). ..	113
Figure 4.11. Synthetic routes toward α -amido- β -ketoester.	115
Figure 4.12. Side products reported for the deoxyfluorination of β -ketoesters.	117
Figure 4.13. Synthesis of 3,3-difluoro-ester (4.43) from 1,3-dithiolane (4.41).	119
Figure 4.14. Synthesis of 3,3-difluoro-L-amino acid (4.48) <i>via</i> the Neber reaction.	120
CHAPTER 4: SUMMARY AND FUTURE WORK	
Figure 5.1. L-Methionine (5.4), L-homocysteine (5.6) and their fluorine derivatives.	136

LIST OF TABLES

CHAPTER 1: INTRODUCTION

Table 1.1. Sequence and structural identity among MGL and PLP-dependent enzymes. ... 9

CHAPTER 2: ROLE OF THE ACTIVE SITE RESIDUE C113 IN *TRICHOMONAS VAGINALIS* MGL1

Table 2.1. The kinetic parameters of the TvMGL1 constructs and C113S mutant for L-methionine. 38

CHAPTER 3: MECHANISTIC STUDIES ON THE ENZYMATIC PROCESSING OF FLUORINATED METHIONINE ANALOGS BY *TRICHOMONAS VAGINALIS* METHIONINE γ -LYASE

Table 3.1. ^{19}F -NMR theoretical chemical and experimental shifts for various fluorinated molecules. 57

Table 3.2. T1 and G3(MP2) enthalpies of formation at 298 K for the reaction between the thioacylating agents and water or methylamine. 59

Table 3.3. Amount of thioacylating agent trapped and fluoride produced from the PLP model system upon processing of TFM and DFM substrates as determined by NMR spectroscopy. 62

Table 3.4. The kinetic parameters of TvMGL1 for methionine and its analogs. 68

Table 3.5. The EC_{50} values of various compounds for *E. coli* cells expressing TvMGL1 (*E. coli* model) and for *T. vaginalis*. 75

CHAPTER 4: SYNTHETIC ROUTES TO 3,3-DIFLUORO-*O*-METHYL-L-HOMOSERINE

Table 4.1. The kinetic parameters of TvMGL1 for L-methionine and *O*-methyl-L-homoserine (OMHSer). 112

LIST OF ABBREVIATIONS

AAT	Aspartate aminotransferase
AMP	Ampicillin
CA	Cysteamine
CdMGL	<i>Clostridium difficile</i> putative L-methionine- γ -lyase
CfMGL	<i>Citrobacter freundii</i> L-methionine- γ -lyase
CGL	Cystathionine- γ -lyase
CI	Chemical ionization
CGS	Cystathionine γ -synthase
CoA	Coenzyme A
CS	Cysteine synthase
DAST	Diethylaminosulfur trifluoride
DFM	L-Difluoromethionine
DFT	Density functional theory
DGD	2,2-Dialkylglycine decarboxylase
DTT	Dithiothreitol
EDTA	Ethylenediamine tetraacetic acid
EI	Electron ionization
ESI	Electrospray ionization
EhMGL	MGL from <i>E. histolytica</i>
FAD	Flavin adenine dinucleotide
GIAO	Gauge including atomic orbitals
HFT	Hartree-Fock Theory
IPTG	Isopropyl β -D-1-thiogalactopyranoside
KAN	Kanamycin
LB	Luria Bertani

LDA	Lithium diisopropylamide
LDH	Lactate dehydrogenase
MBTH	3-Methyl-2-benzothiazalone hydrazone hydrochloride
MET	L-Methionine
MGL	L-Methionine γ -lyase
MP2	Møeller-Plesset theory level 2
MPAL	<i>N</i> -Methylpyridoxal chloride
NBS	<i>N</i> -Bromosuccinimide
OMHSer	<i>O</i> -Methylhomoserine
PFOR	Pyruvate:ferredoxin oxidoreductase
PLP	Pyridoxal-5'-phosphate
PpMGL	<i>Psuedomonas putida</i> L-methionine- γ -lyase
PGMGL	<i>Pyorphyromonas gingivalis</i> L-methionine- γ -lyase
SAT	Serine <i>O</i> -acetyltransferase
SDH	Serine dehydratase
TAE	Tris Acetate EDTA
TEMED	Tetramethylethylenediamine
TFM	L-Trifluoromethionine
TPL	Tryptophan phenol-lyase
Tris	1,1,1-tris(hydroxymethyl)methylamine
TvMGL1	<i>Trichomonas vaginalis</i> L-methionine- γ -lyase
XtalFluor-E	Diethylaminodifluoro-sulfinium tetrafluoroborate

CHAPTER 1

BACKGROUND

1.1. Authors' Contributions

Some of the material presented in this chapter was reproduced from Moya *et al.* (2009). The reproduced work includes section 1.3 (Epidemiology and Treatment for Parasitic Infections), section 1.8 (Cysteine Biosynthesis Pathways), Figure 1.11 and Figure 1.13. J. Honek wrote parts of section 1.3, and was revised by I. Moya. I. Moya wrote and revised section 1.8.

1.2. Introduction

L-Methionine γ -lyase (MGL) is a pyridoxal-5'-phosphate (PLP; **1.4**)-dependent enzyme that is involved in the γ -elimination reaction of the thiomethyl group of L-methionine (**1.2**) and thiol group from its homologs, such as L-homocysteine (**1.1**) (Figure 1.1a) (Moya *et al.*, 2009). The enzyme is found in parasitic and anaerobic organisms, and is believed to play an important role in energy metabolism and L-cysteine biosynthesis by generating α -ketobutyrate (**1.3**) from L-homocysteine derivatives, and hydrogen sulfide from L-homocysteine, respectively (Figure 1.1a) (Westrop *et al.*, 2006). MGL is also implicated in human pathogenicity, as reported for *Porphyromonas gingivalis*, in which the release of methanethiol from L-methionine and toxic hydrogen sulfide from L-homocysteine are correlated with virulency of this organism (Yoshimura *et al.*, 2002). MGL is proposed to be a

potential drug target for treating anaerobic, parasitic infections since humans do not express MGL (Moya *et al.*, 2009).

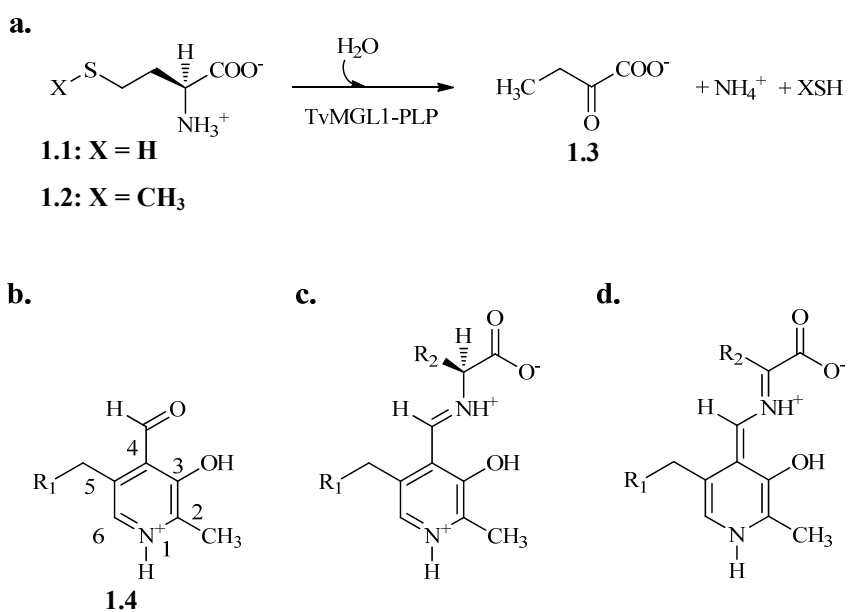


Figure 1.1. Reaction overview for the catalysis of L-amino acids by the PLP-dependent enzyme TvMGL1.

a) Catalysis of L-homocysteine (**1.1**) and L-methionine (**1.2**) by TvMGL1 to produce α -ketobutyrate (**1.3**), ammonium and a mercaptan. **b)** Numbering system for pyridoxal-5'-phosphate (PLP; where $R_1 = \text{OPO}_3^{2-}$, **1.4**), **c)** formation of an aldimine linkage between L-amino acid and PLP, **d)** the quinoid-aldimine intermediate generated from the first step in catalysis of the L-amino acid by the PLP-dependent enzyme, MGL 1 from *T. vaginalis* (TvMGL1-PLP; where $R_2 = \text{Alkyl group}$). The image was generated with ChemDraw Ultra v9.0 (CambridgeSoft, Cambridge, MA).

1.3. Epidemiology and Treatment for Parasitic Infections

In humans, *Trichomonas vaginalis* is a flagellated, sexually transmitted protozoan that has an incidence rate of 5 million new cases per year in the United States (Schwebke, 2002). Infections result in vaginitis in women and urethritis in men; however, men are commonly asymptomatic (Schwebke, 2002). *Entamoeba histolytica* is a pseudopod protozoan that is associated with foodborne illnesses in regions with poor socioeconomic conditions and sanitation (Norhayati *et al.*, 2003; Tarleton *et al.*, 2006). Symptoms range from mild diarrhea to severe dysentery, and the infection results in 100,000 deaths annually worldwide (Ackers *et al.*, 1997).

The current treatment of these parasitic infections is the 5-nitroimidazole class of therapeutics, metronidazole (1.5) and tinidazole (1.6) that are approved by the FDA, while metronidazole is licensed for use in Canada (Figure 1.2) (Moya *et al.*, 2009; Wendel and Workowski, 2007). The lack of alternative drugs for treating these infections is a particular concern, since there are emerging cases of metronidazole-resistant organisms, such as *T. vaginalis* and *Clostridium difficile* (Cudmore *et al.*, 2004; Huang *et al.*, 2009). In the latter case, *Clostridium difficile*, a Gram-positive bacterium is the leading cause of hospital-acquired diarrhea which ranges from mild cases to severe pseudomembranous colitis (Huang *et al.*, 2009). The number of outbreaks has increased since 2003 in part from the emerging hypervirulent *C. difficile* strains 027 and 078 (Bartlett *et al.*, 1978; O'Connor *et al.*, 2009). Most isolates are still susceptible to vancomycin and metronidazole; however, transient and

heteroresistance to metronidazole and other antimicrobial agents have been reported (Huang *et al.*, 2009). Thus, there is a particular interest in identifying alternative drug targets in anaerobic human pathogens in order to avoid future outbreaks of metronidazole resistant strains (Ali and Nozaki, 2007).

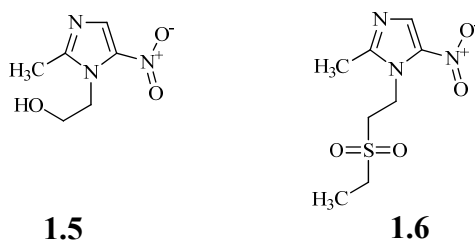


Figure 1.2. Antiparasitic prodrugs metronidazole (1.5) and tinidazole (1.6).

The metronidazole class of drugs, when activated by the anaerobic parasite, impairs the energy production of the pseudo-mitochondria, which is known as the mitosome in *E. histolytica* and the hydrosome in *T. vaginalis* (Tovar *et al.*, 1999). Parasites derive their energy from catalyzing the oxidative decarboxylation of pyruvate to produce CO₂ and acetyl-Coenzyme A (CoA) by pyruvate:ferredoxin oxidoreductase (PFOR; Figure 1.3a) (Aguilera *et al.*, 2008; Kulda, 1999). The two electrons generated from the oxidative decarboxylation of pyruvate are transferred to a [2Fe-2S] ferredoxin, a low molecular weight electron transport protein that has the potential to reduce a variety of cellular enzymes (Figure 1.3 a and c) (Crossnoe *et al.*, 2002). The low redox potential of ferredoxin is reported to reduce metronidazole into its toxic nitro-radical (Figure 1.3b) (Gorrell *et al.*, 1984; Moreno *et al.*,

1984). Activation of the drug is reported to cause breakage of DNA strands, possibly inhibition of DNA repair mechanisms and alkylation of proteins (Edwards, 1980; West *et al.*, 1982).

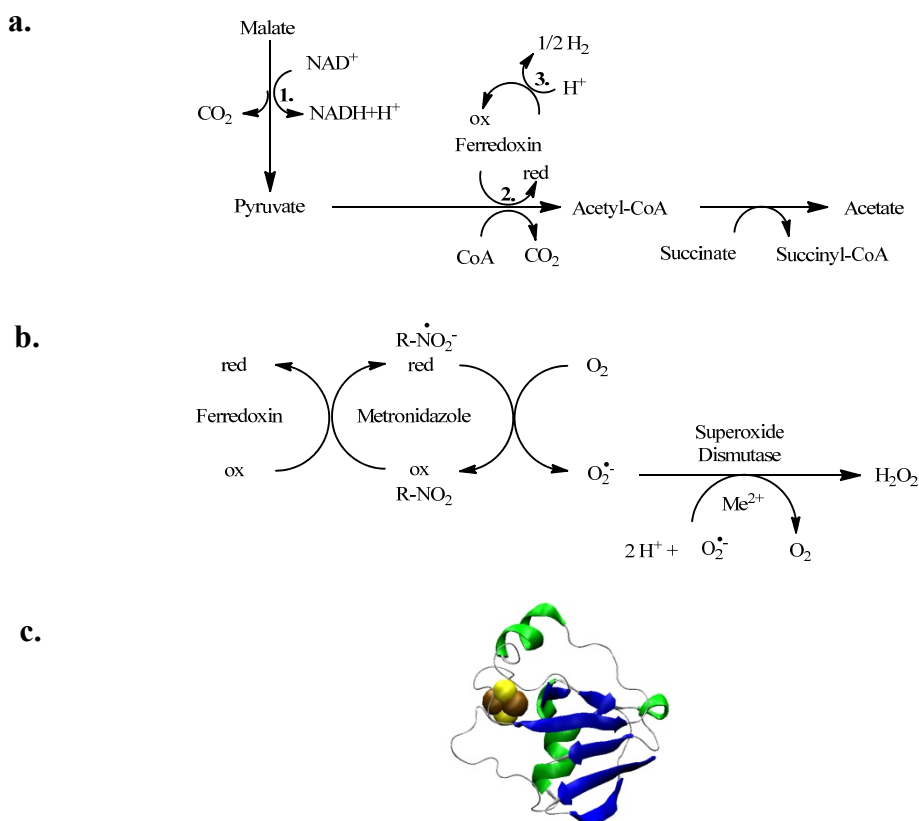


Figure 1.3. Energy metabolism and metronidazole drug target ferredoxin in *T. vaginalis*.

a) Enzymes involved in energy metabolism within the hydrosome: NAD(P) malic enzyme (**1**), pyruvate:ferredoxin oxidoreductase (**2**) and hydrogenase (**3**). **b)** Activation of metronidazole by reduced ferredoxin. The figures were adapted from Kulda (1999). **c)** Crystal structure of ferredoxin from *T. vaginalis* with [2Fe-2S] cluster (brown and yellow, respectively; PDB 1L5P). The ribbon diagram for PDB 1L5P was rendered in Visual Molecular Dynamics v1.9 (Humphrey *et al.*, 1996).

Anaerobic parasitic resistance to the metronidazole class of prodrugs is classified into two categories 1) observed clinical resistance (termed *in vivo* resistance) and 2) laboratory generated resistance (termed *in vitro* resistance) (Dunne *et al.*, 2003). In clinically resistant *T. vaginalis* isolates, the parasites have an increased susceptibility of intracellular oxygen than non-resistant strains, and a higher level of superoxide dismutase activity, but no significant reduction in the transcription levels of ferredoxin (Ellis *et al.*, 1994; Rasoloson *et al.*, 2001; Yarlett *et al.*, 1986). The mechanism for the observed *in vivo* resistance is proposed to occur as follows: 1) metronidazole is reduced by ferredoxin, 2) reduced metronidazole is oxidized by oxygen to produce a superoxide radical, and 3) the superoxide radical is removed from the cell by superoxide dismutase (Figure 1.3b) (Rasoloson *et al.*, 2001). Thus, *in vivo* resistance is proposed to occur by an increase intracellular concentration of oxygen as a result of a defective oxygen scavenging systems in the cytoplasm and hydrosome, which is likely to interfere with the mode of action for metronidazole (Rasoloson *et al.*, 2001). For laboratory generated resistance in *T. vaginalis*, *in vitro* resistance, parasites are normally grown under anaerobic conditions with increasing concentrations of metro-nidazole over several months, resulting in a depleted hydrosomal activity (such as decrease in transcription levels for ferredoxin, PFOR, hydrogenase and malate enzyme) (Kulda *et al.*, 1993; Tachezy *et al.*, 1993). Thus, the *in vitro* resistance model suggests that drug resistance is achieved as through a decrease in hydrosomal enzymes, which are implicated in the activation of the

prodrug (Kulda, 1999). In general, there are discrepancies in the parasite's mode of resistance between *in vitro* and *in vivo* metronidazole-resistant strains.

Microaerophilic conditions with increasing concentrations of metronidazole are believed to accurately represent *in vivo* resistance for laboratory generated *E. histolytica* and *T. vaginalis* strains, because it is hypothesized that the model parasites exhibit an increase in superoxide dismutase activity, in order to neutralize the superoxide anions generated from the reduction of oxygen by the nitro radical (Rasoloson *et al.*, 2001; Samarawickrema *et al.*, 1997; Wassmann *et al.*, 1999). Thus, the microaerophilic conditions for generating the metronidazole-resistant parasites are believed to mimic the elevated oxygen levels within the invaded tissue, and consequently reflect the mode of metronidazole resistance in clinical isolates (Rasoloson *et al.*, 2001; Wassmann *et al.*, 1999). On the other hand, metronidazole-resistant parasites grown under anaerobic conditions, *i.e.*, a depleted pseudo-mitochondrial activity, do not and will not survive *in vivo* because of their strict growth requirement for cysteine (Leitsch *et al.*, 2009; Wassmann *et al.*, 1999).

In *T. vaginalis* and *E. histolytica*, cytosolic nitroreductase is reported to be a target for the activation of metronidazole, while inactivation is believed to occur in the pseudo-mitochondria by nitroimidazole reductase (Pal *et al.*, 2009). On the other hand, intracellular thioredoxin reductase is also implicated in the activation of metronidazole and other nitro compounds (Leitsch *et al.*, 2009; Leitsch *et al.*, 2007). Closer examination of *T. vaginalis* clinical isolates resistant to metronidazole are found to have lower levels of flavin adenine

dinucleotide (FAD), an important cofactor for the activity of thioredoxin reductase, which is not observed in metronidazole sensitive strains (Leitsch *et al.*, 2010). When these cells are supplemented with FAD, the clinical metronidazole resistant cell lines are susceptible to metronidazole (Leitsch *et al.*, 2010). On the other hand, metronidazole sensitive *T. vaginalis* cell lines are found to become resistant to metronidazole when treated with diphenyleneiodonium (an inhibitor of flavin-dependent enzymes), which is consistent with the biochemical features of metronidazole resistance in clinical isolates (Leitsch *et al.*, 2010). Thus, thioredoxin reductase and possibly nitroreductase may potentially activate the metronidazole class of drugs as opposed to PFOR, and the decrease in thioredoxin reductase activity for the laboratory generated strains is consistent with metronidazole-resistance reported in clinical isolates (Leitsch *et al.*, 2010).

1.4. Potential Drug Target for Parasitic Infections

An alternative, potential prodrug to metronidazole is L-trifluoromethionine (TFM), which is reported to be an effective compound against *Trichomonas vaginalis*, *Entamoeba histolytica*, *Pseudomonas putida*, *Clostridium pasteurianum* and *Porphyromonas gingivalis* (Coombs and Mottram, 2001; Tokoro *et al.*, 2003; Yoshimura *et al.*, 2002). The compound is activated by γ -eliminating enzymes, such as MGL (L-methionine- γ -lyase), which are expressed endogenously within the organism (Alston and Bright, 1983; Coombs and Mottram, 2001; Sato *et al.*, 2008). Even though mammals contain a γ -eliminating enzyme, cystathionine- γ -

lyase (CGL), the compound does not appear to be activated in mice since no cytotoxic side-effects were observed over a period of 5 days when mice were injected with L-trifluoromethionine (TFM; 4 μ mol, 0.8 mg) (Yoshimura *et al.*, 2002).

The lack of cytotoxic effects in mammals may be explained by the very high K_m value of mammalian CGL (48 mM) for TFM (Alston and Bright, 1983); and therefore, the enzyme does not readily activate the potential prodrug. This is surprising considering that the sequence identity is ~40% between parasitic protozoan MGL and human CGL (Table 1.1) (McKie *et al.*, 1998; Tokoro *et al.*, 2003). The structures for TvMGL1 (PDB 1E5F) and yeast CGL (PDB 1N8P) are remarkably similar, displaying an RMSD of ~2 Å (Table 1.1), with the exception that the binding pocket of CGL is more polar than MGL (Motoshima *et al.*, 2000). Thus, this may explain why mice do not exhibit any noticeable cytotoxic side-effects when injected with TFM, while parasites expressing MGL are susceptible to the compound (Yoshimura *et al.*, 2002).

Table 1.1. Sequence and structural identity among MGL and PLP-dependent enzymes.

Enzyme	% Sequence identity relative to TvMGL1	RMSD [Å]
TPL (<i>Citrobacter freundii</i>)	13	3.2
CGS (<i>E. coli</i>)	36	1.6
CGL (Yeast)	42	1.7

Sequence identity and structural similarity was calculated with DaliLite (Holm and Park, 2000). Tryptophan phenol-lyase (TPL), cystathionine γ -synthase (CGS) and cystathionine γ -lyase (CGL).

Bioactivity against MGL in *E. histolytica* and *T. vaginalis* may also extend to related enzymes found in anaerobic prokaryotes (Figure 1.4) (Carlton *et al.*, 2007; Loftus *et al.*, 2005; Reeves, 1984; Rosenthal *et al.*, 1997; Stanley, 2005). Analysis of the genome suggests that the genes for MGL (and other genes associated with fermentative metabolism) were acquired through a prokaryote to eukaryote gene transfer (Carlton *et al.*, 2007; Loftus *et al.*, 2005). It is tempting to speculate that the anaerobic environment served as a selection pressure for protozoans to acquire genes from other anaerobic organisms, such that these organisms could better thrive in this environment (Andersson *et al.*, 2006; Ochman *et al.*, 2000). For example, it is believed that glycolytic, catabolic and sulfur metabolic genes were acquired by lateral gene transfer in order to meet the organism's energy demands (Carlton *et al.*, 2007; Loftus *et al.*, 2005) and to better tolerate oxidative molecular species. Thus, compounds that target MGL (or other enzymes related to fermentation) in anaerobic protozoan parasites may potentially target homologous MGL enzymes found in other anaerobic organisms (Figure 1.4), such as the drug resistant isolates of *C. difficile* (a gram-positive bacteria) (Samuelson, 1999; Sebaihia *et al.*, 2006).

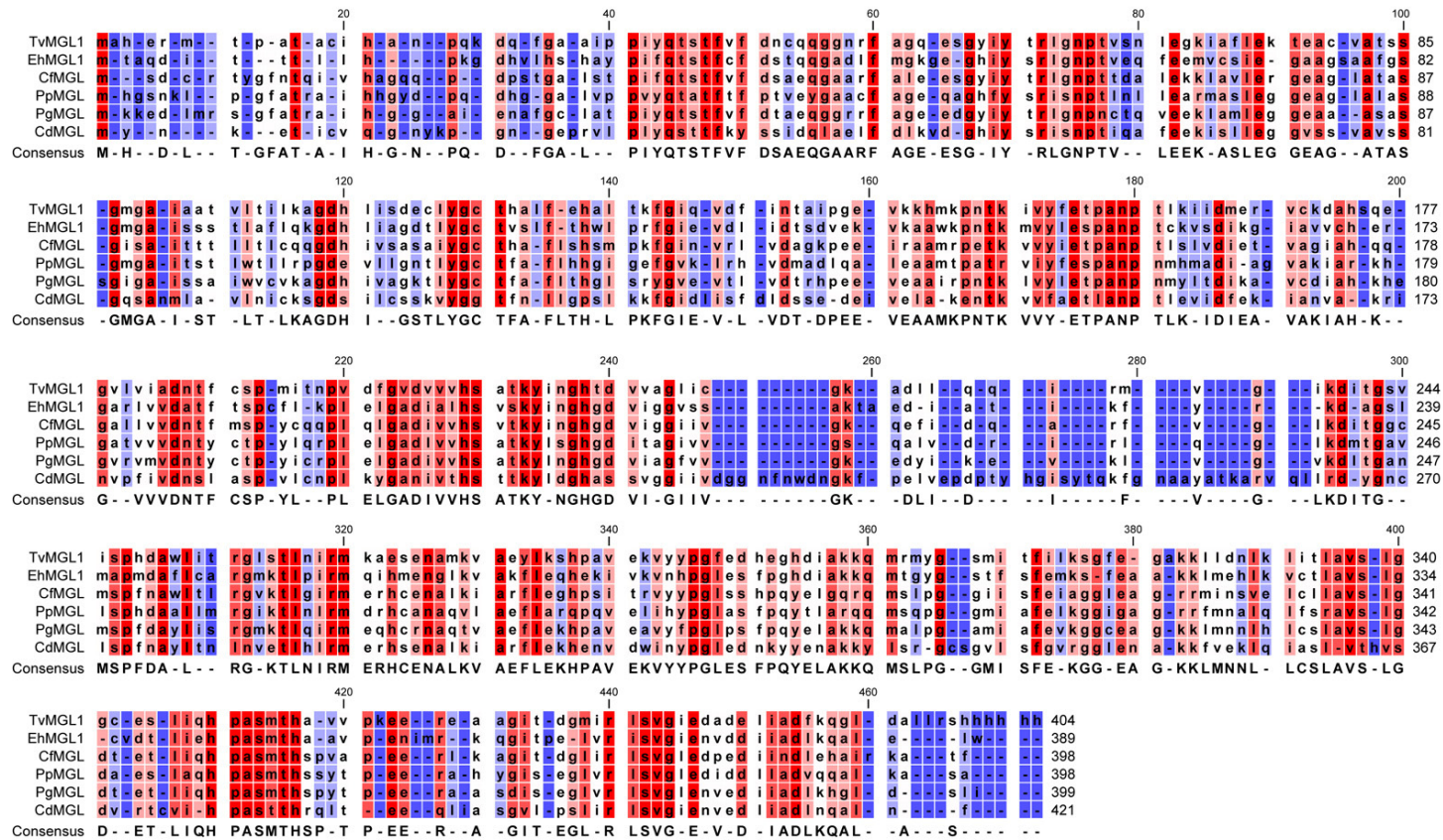


Figure 1.4. Amino acid sequence alignment of MGL from various anaerobic organisms.

The multiple sequence alignment of MGL from *T. vaginalis* (TvMGL1; GI: 15826191), *E. histolytica* (EhMGL1; GI:91522044), *Citrobacter freundii* (CfMGL; GI: 28883481), *Psuedomonas putida* (PpMGL1; GI: 21465428), *Pyorphyromonas gingivalis* (PgMGL; GI: 188995482), *Clostridium difficile* CIP 107932 (CdMGL; putative MGL; GI: 255092847). Colour coding: Red, conserved; White and Grey, lower conservation; Blue, unconserved. Amino acid sequence alignment was generated with CLC Sequence Viewer v6.5.2 (CLC BIO, Toronto, ON).

1.5. Superfamilies of PLP-dependent Enzymes

There are five evolutionarily unrelated superfamilies of PLP-dependent enzymes characterized to date (Grishin *et al.*, 1995), which are classified as fold-type I to V (Figure 1.5 a to e respectively) (Schneider *et al.*, 2000). MGL belongs to the fold type I family, which are reported to catalyze a variety of PLP-dependent reactions such as elimination or replacement (at either α , β or γ positions), decarboxylation, and amino transfer (Figure 1.6).

The chemistry for most of the superfamilies is essentially the same, except for fold-type V family, which appears to utilize the phosphate group of the cofactor for acid-base catalysis (Palm *et al.*, 1990). The basic elements of PLP catalysis involve the covalent linkage of PLP to a lysine residue of the enzyme to form an internal aldimine (Figure 1.5f). This linkage occurs at the *si*-side, which interacts with the β -sheets and where deprotonation of C_α atom and protonation of $C4'$ atom occur in the active site of the enzyme (Christen *et al.*, 1996; Ford *et al.*, 1980). The binding of the L-amino acid substrate exchanges with the internal aldimine at the solvent exposed *re*-side of PLP to form the external aldimine (Figure 1.5g) (Christen and Mehta, 2001; Ford *et al.*, 1980). The π bond established between the C_α atom of the amino acid and the substituent atom is aligned parallel with the π molecular orbital system of PLP. This allows for the π system of the cofactor to extend to the C_α atom, resulting in overlap of the σ - π bonds; thereby promoting bond breakage (Christen and Mehta, 2001).

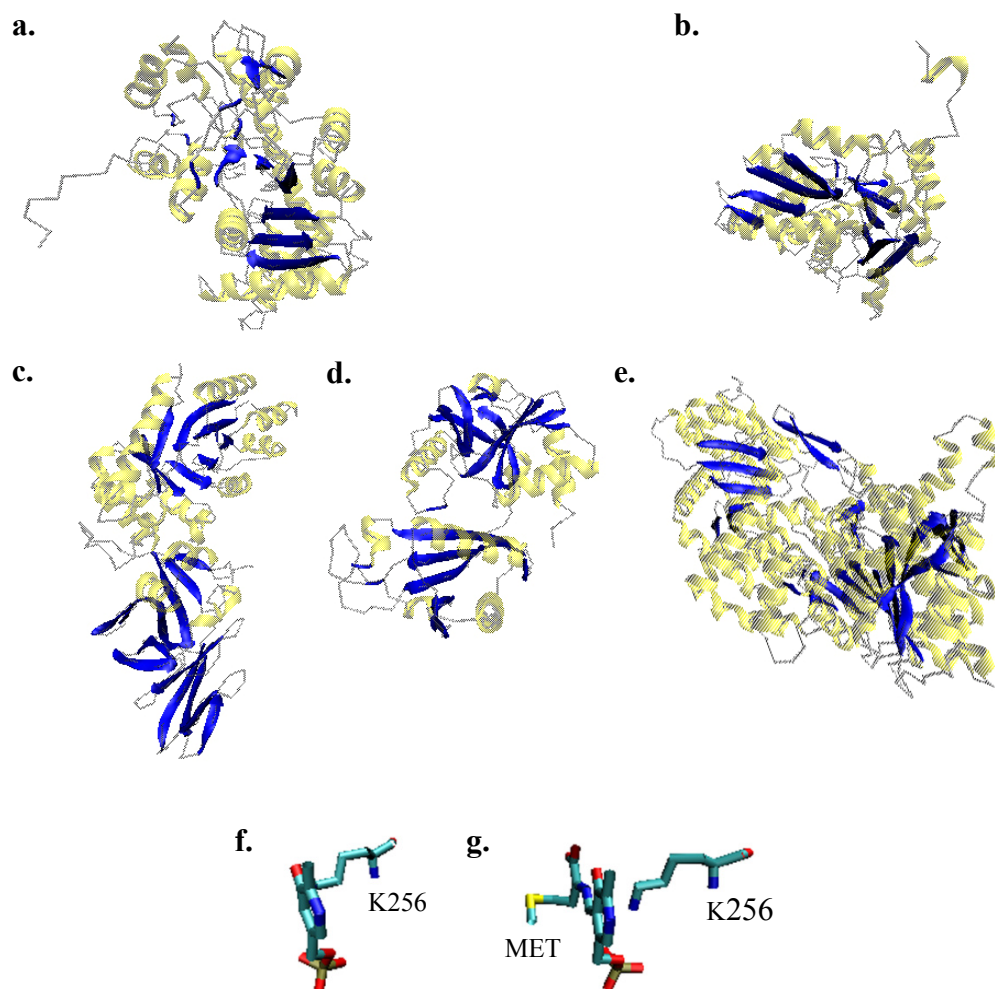


Figure 1.5. PLP-dependent enzymes fold types I to V, and the PLP cofactor displaying internal aldimine and external aldimine.

PLP-dependent enzymes: **a)** fold type I (PDB 3QPG; *Escherichia coli* aspartate transaminase), **b)** fold type II (PDB 1D6S; *Salmonella typhimurium* O-acetylserine sulphydrylase), **c)** fold type III (PDB 3S46, *Streptococcus pneumonia* alanine racemase), **d)** fold type IV (PDB 1DAA, *Bacillus sphaericus* D-amino acid aminotransferase) and **e)** fold type V (PDB 2AZD; *E. coli* maltodextrin phosphorylase). **f)** Lysine 256 side chain of the enzyme forming an internal aldimine at the *si*-side of the PLP cofactor (PDB 2EZ1; *Citrobacter freundii* TPL). **g)** L-Methionine substrate (MET) forming an external aldimine at the *re*-side of the PLP cofactor (PDB 2VLH; *C. freundii* TPL). The images were rendered in Visual Molecular Dynamics v1.9 (Humphrey *et al.*, 1996).

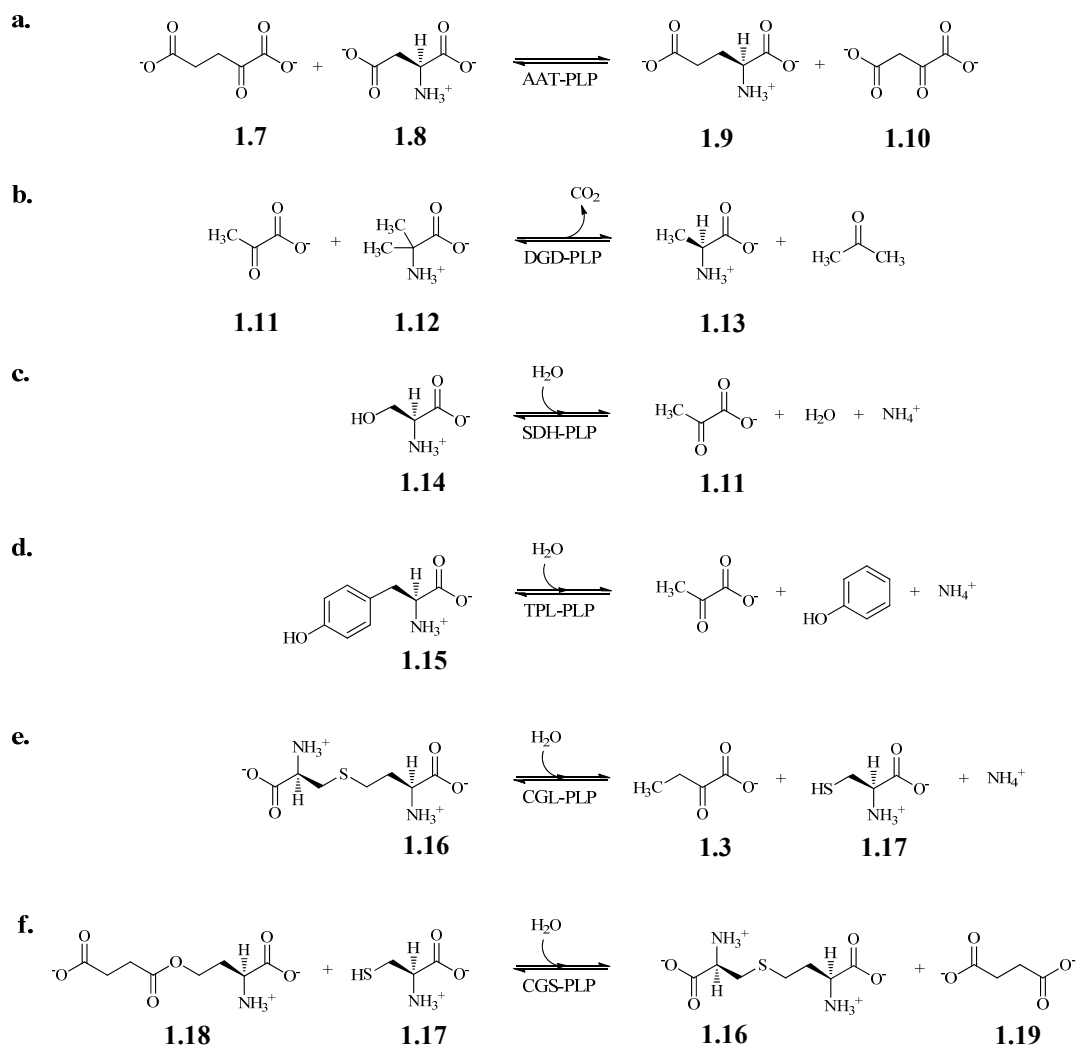


Figure 1.6. The reactions catalyzed by various PLP-dependent enzymes from fold type I family.

a) Aspartate aminotransferase (AAT) catalyzes α -ketoglutarate (**1.7**) and L-aspartate (**1.8**) to L-glutamate (**1.9**) and oxaloacetate (**1.10**). **b)** 2,2-dialkylglycine decarboxylase (DGD) catalyzes pyruvate (**1.11**) and 2,2-dialkylglycine (**1.12**) to carbon dioxide, L-alanine (**1.13**) and acetone. **c)** Serine dehydratase (SDH) breaks down L-serine (**1.14**) to pyruvate (**1.11**), water and ammonia. **d)** Tyrosine phenol-lyase (TPL) breaks down L-tyrosine (**1.15**) to α -ketobutyrate, phenol and ammonia. **e)** Cystathionine γ -lyase (CGL) breaks down L-cystathionine (**1.16**) to α -ketobutyrate (**1.3**), L-cysteine (**1.17**) and ammonia. **f)** Cystathionine γ -synthase (CGS) condenses succinyl-*O*-L-homoserine (**1.18**) and L-cysteine (**1.17**) to L-cystathionine (**1.16**) and succinate (**1.19**). The figure was adapted from Eliot and Kirsch (2004).

L-Methionine γ -lyase belongs to the aspartate aminotransferase family, also known as fold-type I family. The enzyme is catalytically active as homodimers or higher oligomers with two catalytic active sites per homodimer (Schneider *et al.*, 2000). Each monomer has a central domain that is composed of seven-stranded β -sheets, and a C-terminal domain that is composed of three- or four-stranded β -sheets (Schneider *et al.*, 2000) (Figure 1.7a). PLP is covalently attached to the ϵ -amino group of lysine on the central domain, and is situated between the cleft of the central and C-terminal domains (Figure 1.7b). The phosphate moiety of PLP contacts the central domain of the adjacent monomer (Figure 1.7c). The catalytic residues are situated between the cleft of the two domains and at the dimer interface. The domains move significantly upon substrate binding, which is believed to contribute to the substrate specificity and reaction type (Eliot and Kirsch, 2004; Ishijima *et al.*, 2000). Thus, a catalytically active enzyme for fold-type I family requires burial of the PLP cofactor between the two domains and dimerization of the two subunits.

Another feature among the fold-type I family is the metal requirement in order to induce conformations that influence the catalytic activity as reported for 2,2-dialkyl- glycine decarboxylase, tryptophanase and tyrosine phenol-lyase (TPL) (Woehl and Dunn, 1995). Similarly, activation by monovalent metal ions in other as of yet unreported families is expected, considering the high structural similarities with known monovalent-dependent enzymes (Woehl and Dunn, 1995). For example, comparing TvMGL with TPL, the

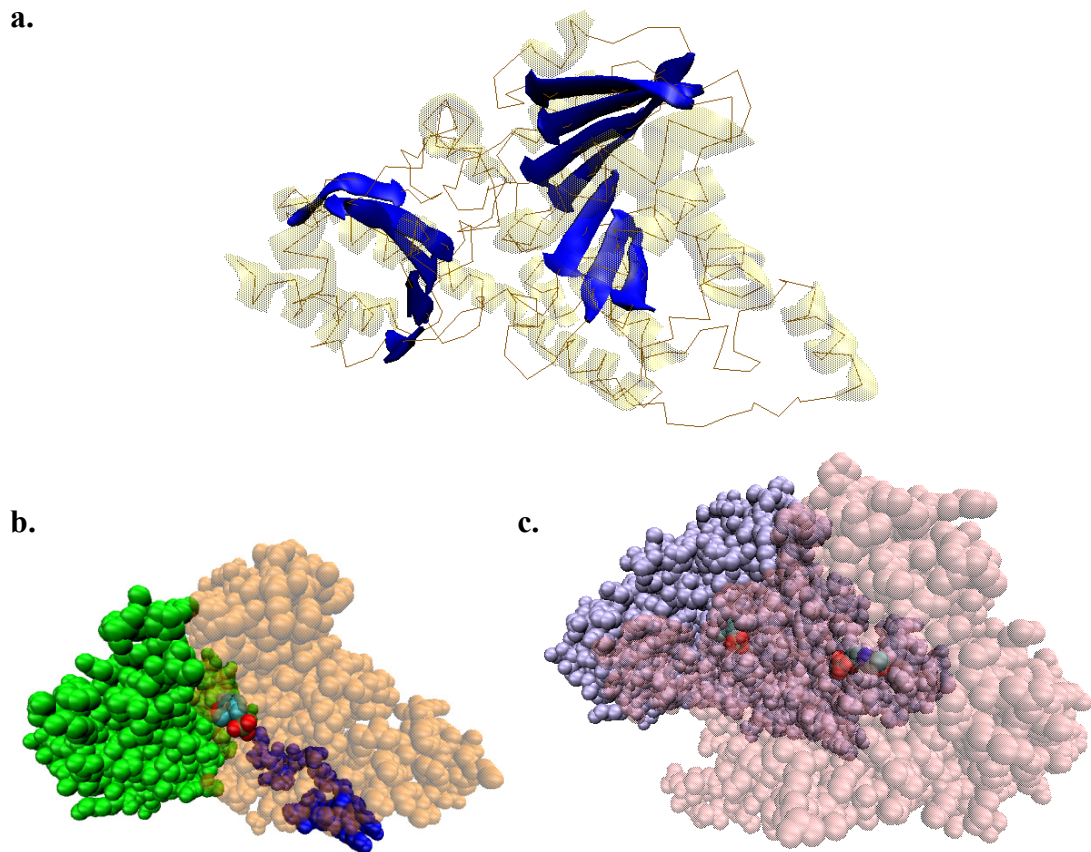


Figure 1.7. The domains and secondary structure of a fold-type I family enzyme.

a) The secondary structure of TvMGL1 displaying β -strands (blue) and α -helices (grey; transparent). **b)** The space fill structure displaying the N-terminal (blue), central (orange, transparent) and C-terminal (green) domains of TvMGL1, and PLP cofactor (light blue and red). **c)** The space fill structure of the PLP cofactor (light blue and red) is situated in the middle of the central and C-terminal domain (silver), which is kept in place by an internal aldimine linkage and dimerization of the adjacent subunit (transparent, pink). The images (PDB 1E5F) were rendered in Visual Molecular Dynamics v1.9 (Humphrey *et al.*, 1996).

respective γ and β -eliminating enzymes, have a very low sequence identity but they are structurally similar (an RMSD of 3.2 Å; I. Moya, unpublished observations). The potential ligands to coordinate a monovalent cation in MGL may involve the side chains of Q31 (from an adjacent subunit) and D249, and the carbonyl backbone of D216. These predictions are based on the structural alignment with TPL, where potassium is coordinated to the carbonyl backbone of G52 (from an adjacent subunit) and E69, and the carbonyl side chain of Q262 (Figure 1.8) (I. Moya; unpublished observations).

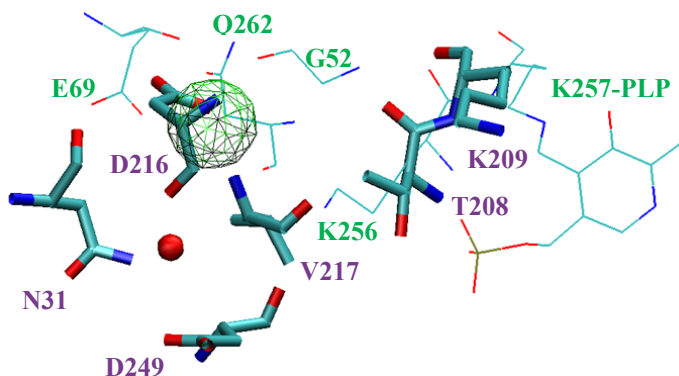


Figure 1.8. Structural alignment of TPL and TvMGL1 displaying a potential metal coordination site.

TPL (thin lines; PDB 2V1H) displaying chelating residues (G52, E69 and Q262; labeled green) coordinated to potassium (wire mesh), and its catalytic residue K257. TvMGL1 (thick lines; PDB 1E5F) displaying potential chelating residues (N31, D216 and D249; labeled purple) coordinated to water 207 (red sphere); and its catalytic residue (K209). The images were rendered in Visual Molecular Dynamics v1.9 (Humphrey *et al.*, 1996).

Based on structural and kinetic studies of tyrosine phenol-lyase (TPL) and tryptophan indole-lyase, monovalent cations are known to increase the affinity of the apoenzyme for the cofactor, strengthen intersubunit interactions, and help in labilization of the C_α proton for the external aldimine complex (Honda and Tokushige, 1986; Kumagai *et al.*, 1970; Toraya *et al.*, 1976). For example, a pentagonal bipyramidal coordinated potassium ion (in *C. freundii* TPL) forms a hydrogen bonding network with S51, and as a result this residue is proposed to maintain the basicity of the catalytic residue K257 and proper orientation of the PLP cofactor (Figure 1.9) (Demidkina *et al.*, 2009). The latter idea is consistent with the predictions of Ivanov and Karpeisky (1966) for aspartate aminotransferase, in which the positioning of the coenzyme establishes an optimal active-center conformation for catalysis. In other words, a change in the position of the cofactor will alter the protonation state of the aldimine (internal or external), and in turn influence the intermediate structures of the enzyme associated with substrate binding and catalysis (Hayashi *et al.*, 1998). Thus, the coordination of a monovalent cation serves as an allosteric effector for β-lyase enzymes in the catalysis of the substrate (Woehl and Dunn, 1995), but there are no reports of such a requirement in γ-eliminating enzymes such as MGL.

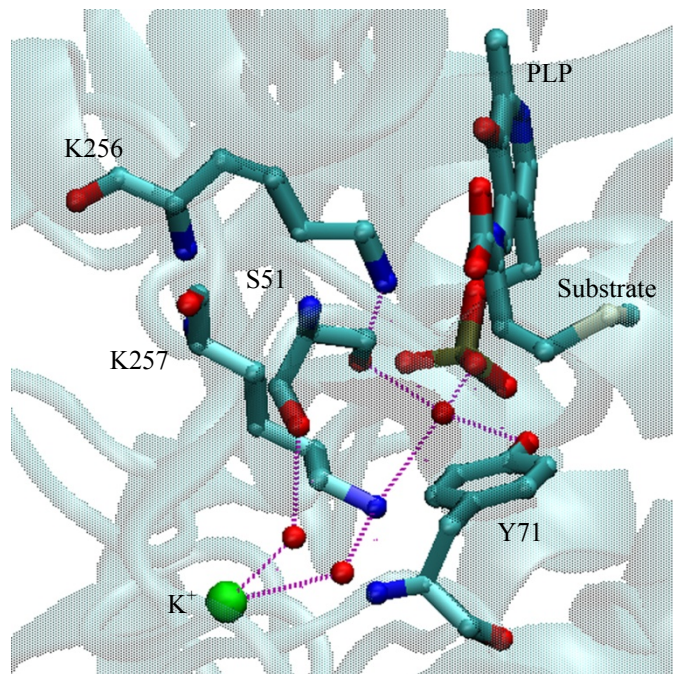


Figure 1.9. Hydrogen bonding network established between the bound potassium and the active site residues of CFTPL.

The hydrogen bonding network (dashed purple lines) is believed to play an important role in catalysis for CFTPL, which is established among potassium (green sphere), water molecules (red sphere), S51, K256, K257, Y71 and PLP-methionine aldimine linkage (ball and stick; P in yellow; O in red; C in turquoise; N in blue; S in grey) as previously reported by Demidkina *et al.* (2009). The image was rendered in Visual Molecular Dynamics v1.9 by aligning CFTPL structures PDB 2V1H and PDB 2EZ1 (Humphrey *et al.*, 1996).

1.6. Reactions Catalyzed by L-Methionine γ -lyase

In the literature, homologous L-methionine γ -lyases are known to carry out two or more of the following reactions: α,γ -elimination, α,γ -replacement, α,β -elimination and α,β -replacement of the respective *S*-homocysteine and *S*-cysteine derivatives (Dias and Weimer, 1998; Lockwood and Coombs, 1991; Manukhov *et al.*, 2006; Sato *et al.*, 2008; Tanaka *et al.*,

1977; Tokoro *et al.*, 2003). For example, *P. putida* (Pp)MGL is the only enzyme studied to date that catalyzes both γ -replacement of *O*-substituted homoserine derivatives to produce *S*-substituted homocysteine derivatives, and β -replacement of *O*-substituted serine derivatives to produce *S*-substituted cysteine derivatives (Inoue *et al.*, 2000; Takada *et al.*, 1988). However, there are no reports of the enzyme displaying CGS activity, *i.e.*, the γ -replacement reaction involved in the biosynthesis of L-cystathionine from L-cysteine and *O*-succinyl-homoserine (Sato and Nozaki, 2009).

The catalytic mechanism of the enzyme is proposed to follow a series of deprotonation and reprotonation steps at the C_α and C_β atoms as reported for the orthologous cystathionine γ -lyase enzyme, and homologous PpMGL enzyme (Figure 1.10) (Esaki *et al.*, 1985; Messerschmidt *et al.*, 2003). Briefly, the enzyme forms an internal aldimine linkage (**1.21**) between PLP and the catalytic active site residue, lysine (Figure 1.10 a). The binding of L-amino acid facilitates transaldimination with lysine to form an external aldimine linkage (**1.22**) between PLP and the amino acid, thereby freeing the lysine side chain for general acid-base catalysis. Thus, the free lysine side chain is able to labilize the α - and β -hydrogen atoms of the amino acid, which leads to a shift of electrons in the conjugated π -system (Figure 1.10 b and c). The catalytic tyrosine is believed to aid in the elimination of the thiol group as reported for PpMGL, and the hydrolysis of the ketimine (**1.24**) is believed to occur off the enzyme (Inoue *et al.*, 2000; Johnston *et al.*, 1981).

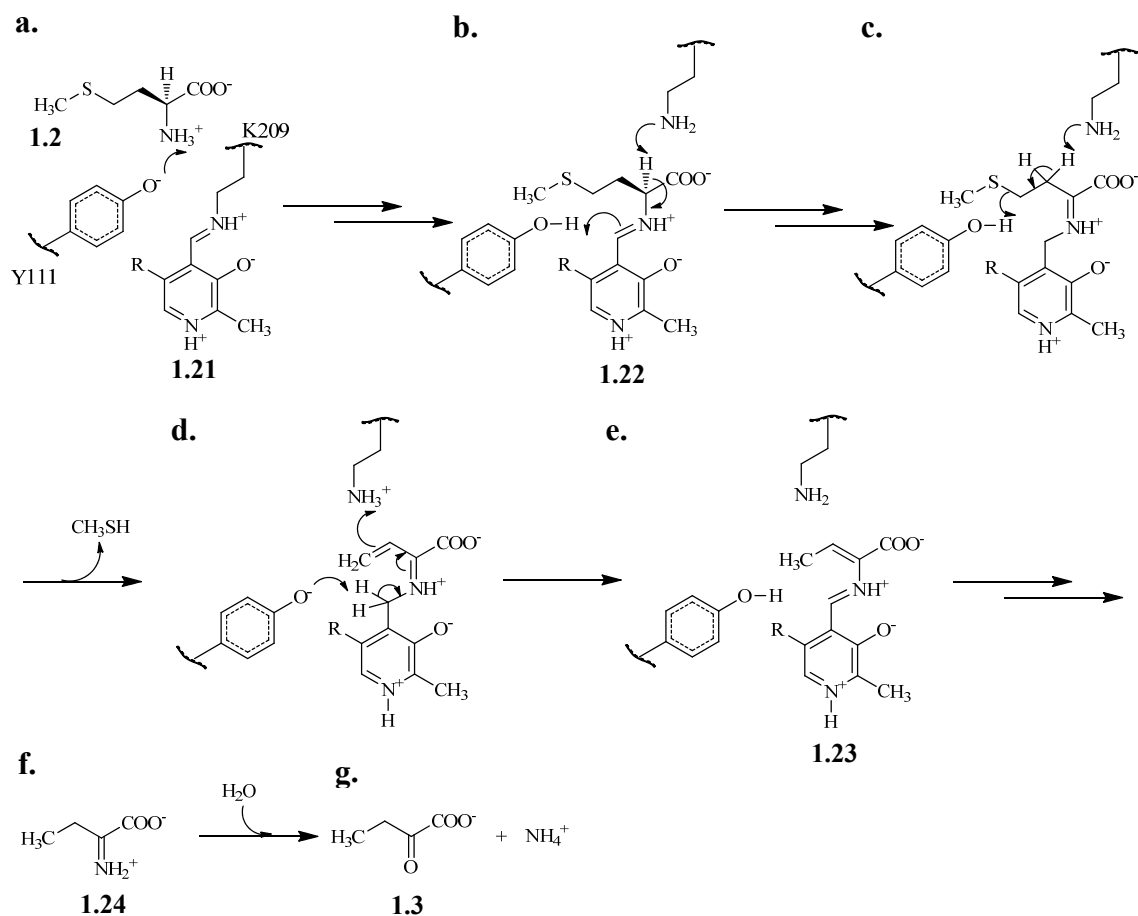


Figure 1.10. Overview of the proposed key reaction steps in the γ -elimination of methionine by TvMGL1.

a) The aldehyde group of PLP forms an internal aldimine (**1.21**) linkage with K209. The linkage is replaced by the incoming L-methionine substrate (**1.2**) to form **b)** an external aldimine (**1.22**). Deprotonation of the α -carbon atom and subsequent **c)** β -carbon atom of the amino acid lead to the γ -elimination of the methanethiol moiety. **d)** Deprotonation of the C4' proton and shift of electrons are believed to form **e)** an iminoacrylate (**1.23**). The compound undergoes transaldimination with lysine to release **f)** α -iminobutanoate (**1.24**). The non-enzymatic hydrolysis of the ketimine (**1.24**) produces **g)** the final end products, α -ketobutyrate (**1.3**) and ammonia. The reaction mechanism was adapted from Esaki *et al.* (1985) and Messerschmidt *et al.* (2003) for PpMGL and orthologous yeast CGL enzymes, respectively.

Based on $^1\text{H-NMR}$ for the catalysis of L-methionine by PpMGL, the rate of α -proton abstraction is 2-fold greater than the β -deprotonation step, and 40-fold greater than the γ -elimination step (Esaki *et al.*, 1985), which is similar to reports for the orthologous CGL and CGS enzymes (Guggenheim and Flavin, 1969; Posner and Flavin, 1972; Washtien *et al.*, 1977). The rate determining step is believed to occur after the elimination of the thiol group, which is consistent with the reports for CGS from *Salmonella typhimurium* (Johnston *et al.*, 1979). Both CGL and CGS enzymes are reported to be stereospecific for one of the β -hydrogens on L-homocysteine; however, the stereochemistry was not identified (Posner and Flavin, 1972; Washtien *et al.*, 1977). On the other hand, MGL did not exhibit any stereospecificity for the β -hydrogen atoms of L-methionine nor S-methyl-L-cysteine (Esaki *et al.*, 1985), and there is currently no explanation for this lack of stereospecificity.

1.7. Methionine-dependent Tumors

A characteristic of many cancer cell lines is their absolute requirement for plasma L-methionine, while normal cells are able to tolerate a restriction of exogenous L-methionine (Cellarier *et al.*, 2003). Methionine-dependent tumor cells have an abnormally high rate of methionine utilization for methylation reactions, and therefore, require more methionine than the cells can synthesize from homocysteine during methionine starvation (Coalson *et al.*, 1982; Stern and Hoffman, 1984; Tisdale, 1980). Thus, when these tumor cells are deprived

of methionine in homocysteine-containing medium *in vitro*, they reversibly arrest in the late S/G2 phase of the cell cycle (Guo *et al.*, 1993; Hoffman and Jacobsen, 1980).

A therapeutic approach to deplete methionine from tumors is to treat the cells with recombinant MGL from *Pseudomonas putida* (PpMGL). The growth of human tumors *in vivo* and *in vitro* (xenographed in nude mice) is reported to be inhibited upon treatment with recombinant PpMGL when compared to normal cells (Tan *et al.*, 1997). Therapeutic efficacy is found to improve when recombinant PpMGL is combined with anticancer drugs such as cisplatin, 5-fluorouracil, nitrosourea, and vincristine (Hu and Cheung, 2009; Kokkinakis *et al.*, 2001; Tan *et al.*, 1999; Yoshioka *et al.*, 1998). Reduction in cell growth is also achieved by integrating *P. putida mgl* gene into human lung cancer cells by using a retroviral vector and treatment with exogenous recombinant ppMGL, in order to deplete intracellular and extracellular methionine levels (Miki *et al.*, 2000; Miki *et al.*, 2001). Treatment of the transduced cells with exogenous selenomethionine is found to inhibit tumor cell growth, since the processing of selenomethionine by MGL is implicated in the release of methylselenol, a catalyst for generating reactive oxygen species and in turn oxidize intracellular thiols (Chaudiere *et al.*, 1992; Clark *et al.*, 1996; Miki *et al.*, 2001; Yan and Spallholz, 1993). Coupling the recombinant PpMGL to methoxypolyethylene glycol succinimidyl glutarate was found to improve the pharmacokinetics and reduce immunogenicity in primates relative to the unmodified enzyme (Yang *et al.*, 2004). Thus, there is evidence to suggest that methionine depletion by PpMGL and in combination with a chemotherapeutic agent may be an effective anticancer therapeutic strategy.

1.8. Cysteine Biosynthesis Pathway

1.8.1. An Overview of Sulfur Biochemistry in Living Organisms

In living organisms, L-methionine and L-cysteine play essential roles in protein synthesis, methylation reactions, polyamine biosynthesis (*e.g.*, proper cell development), anti-oxidative stress defense (glutathione/trypanothione), and iron-sulfur cluster biosynthesis (*e.g.*, energy metabolism) (Ali and Nozaki, 2007; Ravanel *et al.*, 1998; Sekowska *et al.*, 2000; Stipanuk, 1986; Thomas and Surdin-Kerjan, 1997). The strategy that organisms utilize in order to biosynthesize sulfur-containing amino acids varies from organism to organism (Figure 1.11). In humans, L-methionine must be incorporated into the diet in order to biosynthesize L-cysteine; this occurs through the forward transsulfuration pathway (Stipanuk, 1986). In yeast, either cysteine or methionine can be supplemented to its diet in order to biosynthesize methionine or cysteine, respectively (Thomas and Surdin-Kerjan, 1997). Alternatively, the organism may synthesize the sulfur-containing amino acids by utilizing inorganic sulfate *via de novo* cysteine biosynthesis pathway (Thomas and Surdin-Kerjan, 1997). Thus, yeast have a forward transsulfuration pathway (Figure 1.12a), a reverse transsulfuration pathway (Figure 1.12b) and a sulfide biosynthetic pathway (sulfate to sulfide). *Escherichia coli* and plants utilize the forward transsulfuration pathway such that methionine is biosynthesized from cysteine, or may utilize inorganic sulfate *via de novo* cysteine biosynthesis (Ravanel *et al.*, 1998; Sekowska *et al.*, 2000). On the other hand, *E. histolytica* and *T. vaginalis* do not have a

forward or a reverse transsulfuration pathway, but have a methionine catabolic pathway (and elements of a *de novo* sulfide biosynthetic pathway for cysteine biosynthesis in *E. histolytica*) (Carlton *et al.*, 2007; Loftus *et al.*, 2005). These differences in cysteine metabolism between humans and parasites are of particular interest, especially for the future development of anti-parasitic compounds.

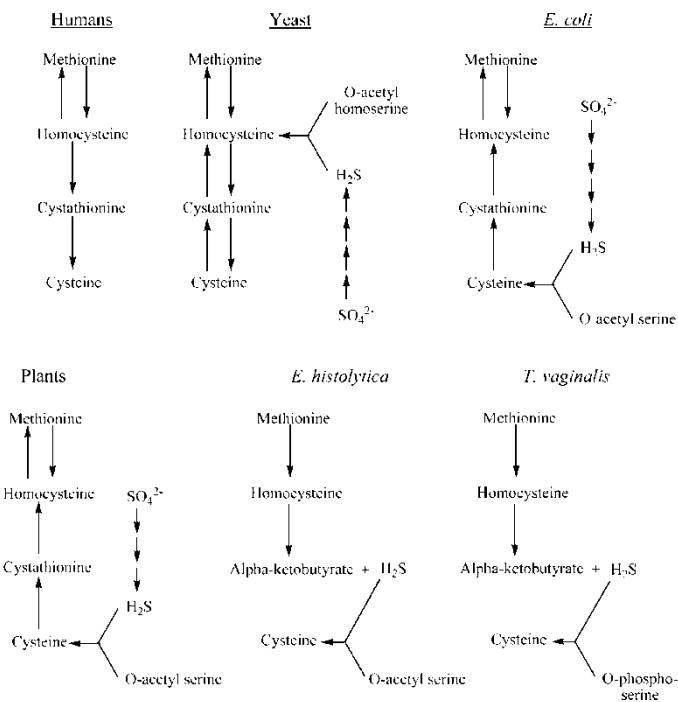


Figure 1.11. An overview of the biosynthetic pathways for thiol-containing amino acids in humans, yeast, *E. coli*, plants, *E. histolytica* and *T. vaginalis*.

The forward transsulfuration pathway is present in humans and yeast. The reverse transsulfuration pathway is present in yeast, plants and *E. coli*. The sulfide and *de novo* cysteine/homocysteine biosynthesis is present in yeast, plants and *E. coli*. The methionine catabolic pathway is present in *E. histolytica* and *T. vaginalis*. The figure was adapted from Moya *et al.* (Moya *et al.*, 2009) and based on several studies (Carlton *et al.*, 2007; Loftus *et al.*, 2005; Ravanel *et al.*, 1998; Sekowska *et al.*, 2000; Stipanuk, 1986; Thomas and Surdin-Kerjan, 1997).

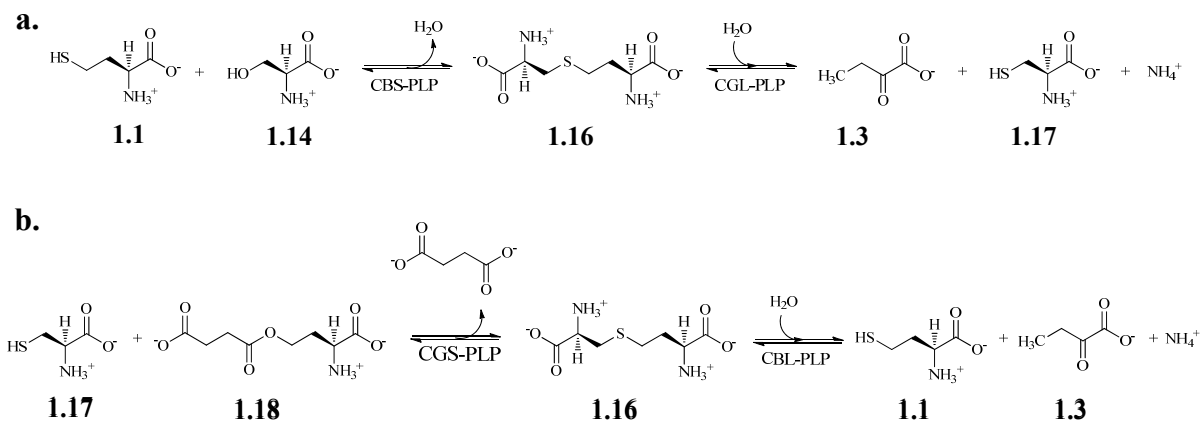


Figure 1.12. Forward and reverse transsulfuration pathways.

a) Forward transsulfuration pathway in humans: cystathionine β -synthase (CBS) condenses L-homocysteine (**1.1**) and L-serine (**1.14**) to L-cystathionine (**1.16**), and cystathionine γ -lyase (CGL) breaks down L-cystathionine (**1.16**) to α -ketobutyrate (**1.3**), ammonium and L-cysteine (**1.17**). **b)** Reverse transsulfuration pathway in *E. coli*: cystathionine γ -synthase (CGS) condenses L-cysteine (**1.17**) and *O*-succinyl-L-homoserine (**1.18**) to succinate and L-cystathionine (**1.16**), and cystathionine β -lyase (CBL) breaks down L-cystathionine (**1.16**) to L-homocysteine (**1.1**), α -ketobutyrate (**1.3**) and ammonium.

1.8.2. Methionine Catabolism

In *E. histolytica* and *T. vaginalis*, L-cysteine is an essential nutrient for growth and for tolerance to reactive oxygen species (Bruchhaus *et al.*, 1998; Coombs *et al.*, 2004; Trussell, 1946; Vicente *et al.*, 2008). The anaerobic parasites are known to catabolize methionine to homocysteine, but lack enzymes to convert homocysteine to cysteine and *vice versa* (Figure 1.13 a and b); thus, the parasites lack a forward and a reverse transsulfuration pathway, respectively (Figure 1.12 a and b) (Carlton *et al.*, 2007; Loftus *et al.*, 2005). In the forward transsulfuration pathway in humans for example, the enzyme cystathionine β -synthase condenses homocysteine (1.1) and serine (1.14) to produce cystathionine, which is utilized by cystathionine γ -lyase to produce cysteine (1.17) and α -ketobutyrate (1.3; Figure 1.12a) (Stipanuk, 1986).

The absence of a forward transsulfuration pathway in the two parasitic protozoans is expected to result in an accumulation of homocysteine, and consequently interfere with cellular methylation reactions due to an imbalance in their methionine:homocysteine ratios. Analysis of the parasite's genome suggests that homocysteine cannot be converted to methionine because the organism lacks methionine synthase genes (Anderson and Loftus, 2005; Carlton *et al.*, 2007; Loftus *et al.*, 2005; Westrop *et al.*, 2006). A possible solution in preventing the accumulation of homocysteine in a parasite may be resolved by MGL (4; a pyridoxal-dependent enzyme involved in the α,γ -elimination reactions), since the enzyme is

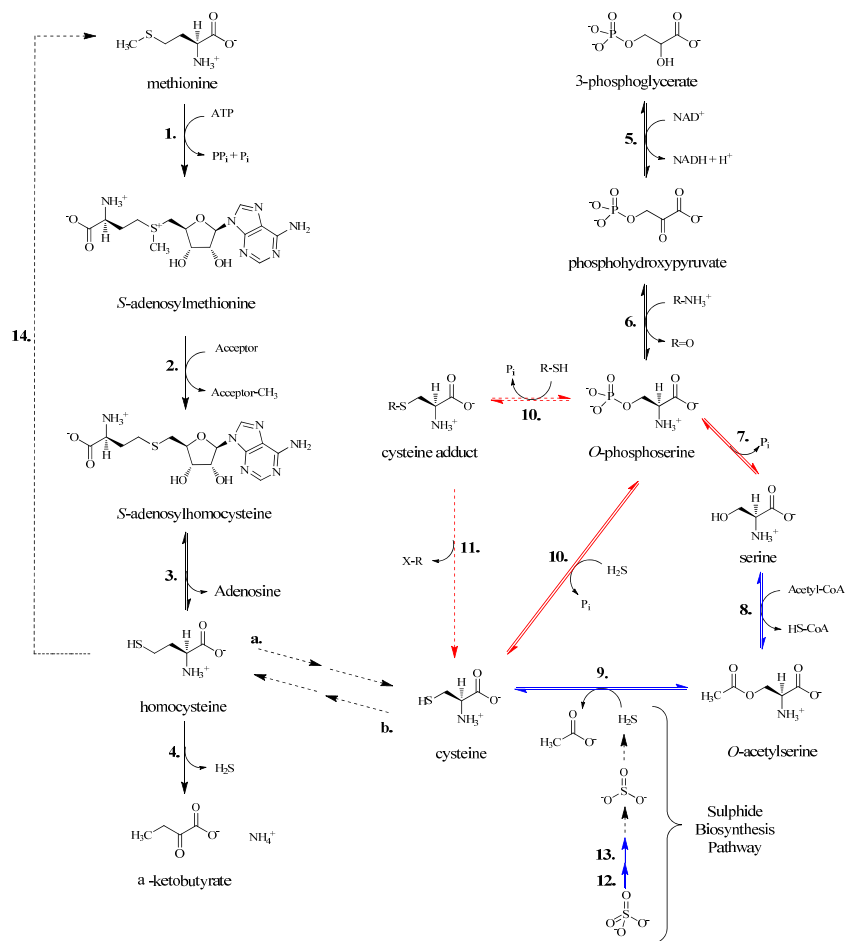


Figure 1.13. Methionine catabolism and *de novo* cysteine biosynthesis in *E. histolytica* and *T. vaginalis*.

The solid black arrow indicates that the enzyme is present in *E. histolytica* and *T. vaginalis*, while the dashed black arrow indicates that the enzyme is absent in both parasites. The solid blue arrow indicates that the enzyme is present in *T. vaginalis*. The solid red arrow indicates that the enzyme is present in *E. histolytica*, while the red dashed arrow is a proposed route in *E. histolytica*. The protozoan parasites lack both **a**) a forward transsulfuration pathway and **b**) a reverse transsulfuration pathway. **1**) methionine adenosyltransferase, **2**) S-adenosyl-L-methionine dependent methyltransferase, **3**) S-adenosyl-L-homocysteine hydrolase, **4**) L-methionine γ -lyase, **5**) phosphoglycerate dehydrogenase, **6**) phosphoserine aminotransferase, **7**) phosphoserine phosphatase, **8**) serine O-acetyltransferase, **9**) type A cysteine synthase, **10**) Type B cysteine synthase, **11**) zinc-dependent metallo-protease/thioredoxin reductase, **12**) ATP sulfurylase, **13**) APS kinase, **14**) methionine synthase. The figure was adapted from Moya *et. al.* (2009).

able to catabolize both L-methionine and L-homocysteine (Figure 1.13) (Lockwood and Coombs, 1991; Tokoro *et al.*, 2003). The turnover of L-homocysteine by MGL produces H₂S, which is proposed to be incorporated into the *de novo* biosynthesis of cysteine (Sato *et al.*, 2008). The α -keto by-products generated from MGL may serve as an energy source for the organism (Brown *et al.*, 1999; Samarawickrema *et al.*, 1997). Thus, imbalances in methionine/homocysteine ratios may be restored by the activity of MGL, and the by-products generated may be incorporated into *de novo* cysteine biosynthesis and energy metabolism.

1.8.3. Sulfide Biosynthetic Pathway and de novo Cysteine Biosynthesis

Based on genomic analysis of *T. vaginalis* and *E. histolytica*, the two genomes have been found to contain remnants of the *de novo* cysteine biosynthetic pathway (Carlton *et al.*, 2007; Loftus *et al.*, 2005), and remnants of the sulfide biosynthetic pathway (**12** and **13**) in *E. histolytica* (Figure 1.13). For the *de novo* cysteine biosynthetic pathway in *E. histolytica*, the parasite produces *O*-acetylserine from serine by serine *O*-acetyltransferase (SAT, **8**), and is subsequently converted to cysteine by cysteine synthase (CS, **10**; Figure 1.13) (Nozaki *et al.*, 1998; Nozaki *et al.*, 1999). *Entamoeba histolytica* lacks genes for *O*-phosphoserine phosphatase (**7**), which is involved in the dephosphorylation of *O*-phosphoserine to serine; but are present in *T. vaginalis* (Figure 1.13) (Carlton *et al.*, 2007; Westrop *et al.*, 2006). On the other hand, *T. vaginalis* lacks SATs and enzymes involved in *de novo* sulfide biosynthesis (Loftus *et al.*, 2005; Westrop *et al.*, 2006). Thus, in *E. histolytica*, cysteine

synthase is likely to biosynthesize L-cysteine from *O*-L-acetylserine. However, in *T. vaginalis*, the preferred substrate for CS in order to biosynthesis L-cysteine is uncertain.

Analysis of the genes encoding for CS in the two parasites indicate different CS isoenzymes. *E. histolytica* encodes for three type A CS enzymes (**9**), while *T. vaginalis* encodes for six type B CS enzymes (**10**; Figure 1.13) (Westrop *et al.*, 2006). Even though the two types of isoenzymes carry out β -replacement reactions and accept *O*-L-acetylserine and sulfide as substrates, type B CS isoenzymes are known to accept thiosulfate or other larger thiol donors (Nozaki *et al.*, 2000; Westrop *et al.*, 2006).

In *T. vaginalis*, the genome lacks SAT genes and there are no reports of cysteine biosynthesis from *O*-L-acetylserine. There are genes in the parasite that encode for 3-phosphoglycerate dehydrogenase and an *O*-phosphoserine aminotransferase in order to biosynthesize *O*-L-phosphoserine precursor (Carlton *et al.*, 2007; Westrop *et al.*, 2006). Type B CS from *T. vaginalis* (**10**) is reported to utilize *O*-L-phosphoserine (a K_M of 230 mM) as substitute for *O*-L-acetylserine (a K_M of 40 mM) in the biosynthesis of cysteine (Figure 1.13) (Westrop *et al.*, 2006), which has been reported for CS from *Aeropyrum pernix* (Mino and Ishikawa, 2003). In *Mycobacterium tuberculosis*, *O*-phosphoserine is utilized as a substrate for type B CS enzyme, *via* a novel cysteine biosynthetic pathway (Agren *et al.*, 2008; Burns *et al.*, 2005). The enzyme is characterized as an *O*-phosphoserine sulfhydrylase that accepts *O*-L-phosphoserine as a substrate, and its sulfur donor is a small protein (CysO) that is thiocarboxylated at the C-terminus (CysO-SH, **10**; Figure 1.13) (Agren *et al.*, 2008). The enzyme produces a CysO-cysteine adduct, and in turn is cleaved by a zinc-dependent

metalloprotease (**11**) to produce cysteine and CysO (Figure 1.13) (Agren *et al.*, 2008). Thus, type B CS enzymes in *T. vaginalis* may have an *O*-phosphoserine sulfhydrylase activity, and belong to a similar pathway as described for *M. tuberculosis*. The absence of type A CS and SAT enzymes in *T. vaginalis* should not be ruled out because the sequence of its (entire) genome is incomplete.

1.9. Purpose of Study

The overuse and misuse of metronidazole family of drugs for treating human protozoan infections have led to an increased incidence of drug resistant strains. The enzyme, MGL is proposed to be an alternative, potential drug target in order to treat human protozoan infections. The purpose of the thesis is to understand the chemistry of the enzyme, TvMGL in respect to its reaction mechanism by utilizing fluorinated L-methionine analogs as probes and by site-directed mutagenesis. The chemistry of the products generated from the processing of the fluorinated methionine analogs by TvMGL1 was examined by ¹⁹F-NMR spectroscopy, high level thermochemistry calculations, PLP model studies, cross-linking studies and cellular toxicity assays. The knowledge gained from this study will be applied to a second generation of fluorinated methionine analogs that takes into consideration the mechanism of the enzyme and chemistry of the fluorinated substitution within the compound.

CHAPTER 2

ROLE OF THE ACTIVE SITE RESIDUE C113 IN *TRICHOMONAS* *VAGINALIS* L-METHIONINE γ -LYASE 1

2.1. Authors' Contribution

Dr. G. Coombs provided the *mgll* gene from *Trichomonas vaginalis* G3. I. Moya cloned the *mgll* gene and mutants into the pET28b vector. Dr. Richard Smith performed the ESI-MS experiments for the enzymes. Jessica Dubrick generated the TvMGL1 mutants, C113S and C113A. All other work was performed by I. Moya. Dr. J. Honek conceived the project and discussed the data with I. Moya.

2.2. Introduction

The active site residue C113 in TvMGL1 is proposed to aid in the catalytic efficiency of the enzyme such as substrate specificity and a general acid as indicated by site-directed mutagenesis studies and X-ray crystallography structures (Figure 2.1) (Sato and Nozaki, 2009). The active site cysteine is conserved in homologous MGLs from bacteria to protozoa, but dispensable in orthologous γ -eliminating enzymes such as cystathionine γ -lyase and cystathionine γ -synthase (McKie *et al.*, 1998; Nakayama *et al.*, 1988a). In this chapter, we

present numerous reports that address the role of the catalytic cysteine, and our own work on the mutation of this residue.

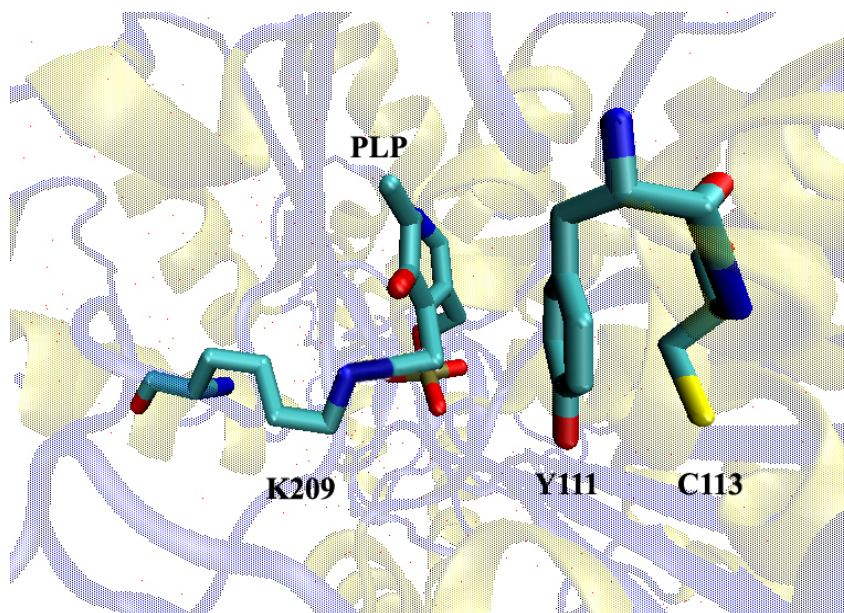


Figure 2.1. The active site of TvMGL1 homodimer.

The active site of TvMGL1 displaying the catalytic residues: K209 bound to the PLP cofactor, Y111 and C113 (PDB 1E5E; unpublished crystal structure). The image was rendered in Visual Molecular Dynamics v1.9 (Humphrey *et al.*, 1996).

2.3. Studies on the Functional Role of the Cysteine Residue

In TvMGL1, site-directed mutagenesis studies on C113 suggest that the side chain plays an important role in the catalysis of L-homocysteine (2.1) and L-methionine (2.2) (McKie *et al.*, 1998). Mutating the residue C113 to Gly, which is conserved among orthologous α,γ -eliminating enzymes, leads to a reduction in both α,β elimination and α,γ eliminating

reactions, a 3-fold reduction in the turnover rate of L-cysteine and a 13-fold reduction in the turnover rate of L-methionine, respectively (McKie *et al.*, 1998). The mutations do not enable the enzyme to utilize cystathionine nor facilitate α,γ -replacement reactions, considering that the requirement is likely to be dictated by the polarity of the binding pocket and not by a single amino acid side chain in the active site (Motoshima *et al.*, 2000). In a similar study, the equivalent cysteine residue in PpMGL is implicated in catalysis, as suggested by inactivation of the enzyme as a result of the covalent modification of cysteine residues by *N*-(bromoacetyl) pyridoxamine phosphate (**2.3**; Figure 2.2b) (Nakayama *et al.*, 1988b). Further studies with a thiol specific cyanylating reagent, 2-nitro-5-thiocyanobenzoic acid (**2.4**; Figure 2.2c), suggest that the active-site cysteine residue is essential for α,γ -elimination but not α,β -elimination reactions (Nakayama *et al.*, 1988a). The α,γ -elimination activity of thiocyanylated enzymes (**2.5**) can be restored with L-homocysteine derivatives; it is believed that the mercaptan leaving group exchanges with the cyanyl group of the modified cysteine within the active site. These findings are also consistent with the modification of the cysteine residue of PpMGL by the mechanistic-based inhibitor, 2-amino-4-chloro-5-(*p*-nitrophenylsulfinyl)pentanoic acid (Johnston *et al.*, 1980). Thus, the active site cysteine residue in MGL is implicated in the catalysis of α,γ -elimination reactions.

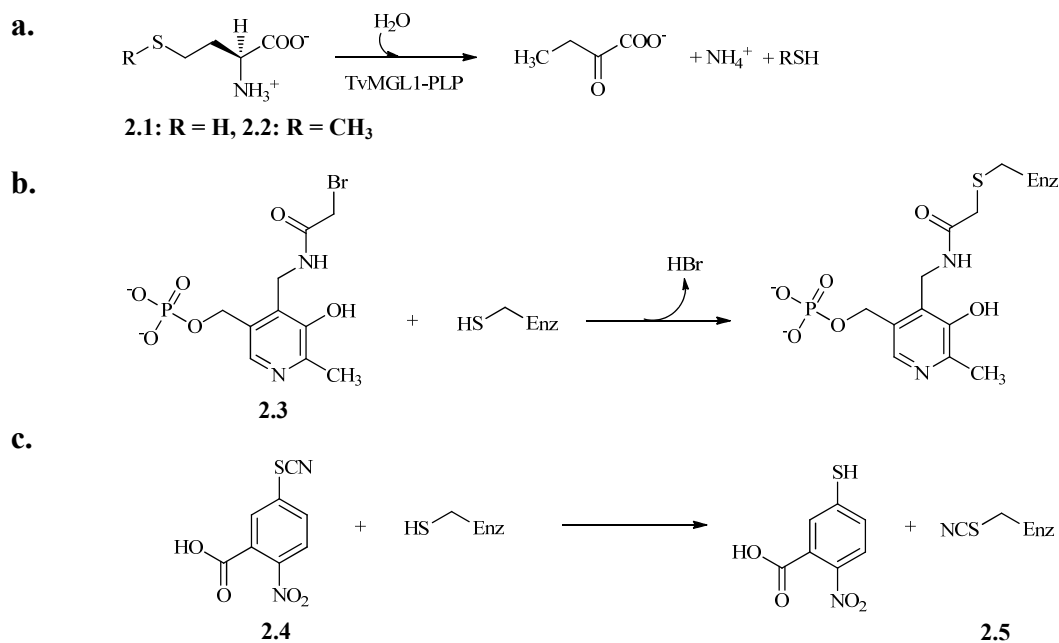


Figure 2.2. Reaction overview of the catalysis of L-homocysteine derivatives by TvMGL1, and modification of active site thiols in enzymes.

a) Reaction overview of the catalysis of L-homocysteine (**2.1**) and L-methionine (**2.2**) by TvMGL1. **b)** Inactivation of the active site cysteine of an enzyme by *N*-(bromoacetyl)-pyridoxamine 5'-phosphate (**2.3**). The figure was adapted from Higgins and Miles (1978). **c)** Cyanylation of the active site cysteine to thiocyanate (**2.5**) by 2-nitro-5-thiocyanobenzoic acid (**2.4**). The figure was adapted from Patchornik *et al.* (1970).

With the removal or inactivation of the catalytic cysteine residue of MGL, the enzyme's α,β -elimination activity remains (McKie *et al.*, 1998; Sato and Nozaki, 2009). The pH-dependencies of the main kinetic parameters of *Citrobacter freundii* (Cf)MGL suggest that the elimination reactions are aided by two general acids that have a pK_a of 8.7 (Faleev *et al.*, 2009). The authors propose that Y58 in CfMGL acts as the general acid in the catalysis of α,β -reactions of substrates such as *S*-methyl-L-cysteine (Y56 equivalent in TvMGL1), while Y113 acts as a general acid in the catalysis of α,γ -reactions for substrates such as L-

methionine (Y111 equivalent in TvMGL1) because of its proximity to the thiol leaving group (Figure 2.1). However, the authors ruled out the possibility that the catalytic C115, adjacent to Y113, acts as a general acid because it is not within hydrogen bonding distance to the methanethiol leaving group of methionine, as indicated by their structural model (Faleev *et al.*, 2009).

The catalytic cysteine is implicated in substrate specificity as reported for EhMGL, TvMGL and PpMGL (Kudou *et al.*, 2008; Kudou *et al.*, 2007; McKie *et al.*, 1998; Sato *et al.*, 2008). The crystal structure of PpMGL suggests that the catalytic residue C116 forms an extensive H-bonding network within the active site, such as the hydrogen bonding network established between Y114 and residues on the adjacent subunit (K240, D241 and R61) (Kudou *et al.*, 2007). The notion is supported by site-directed mutagenesis on the catalytic C116 residue in PpMGL (Kudou *et al.*, 2008). For one of the substitutions, the C116H mutant increases the turnover rate of β -elimination by ~20-fold for the cysteine substrate, while the γ -elimination turnover rate decreases by ~300-fold for the methionine substrate when compared to wild-type enzyme (Kudou *et al.*, 2008). Thus, catalytic residue C116 in PpMGL is not only important in the α,γ -elimination reaction, but may influence substrate specificity due to its hydrogen bonding network within the active site.

The goal of this study was to examine the catalytic role of C113 in TvMGL1 by site-directed mutagenesis (C113S mutant) and its relation to previous studies (Kudou *et al.*, 2008; McKie *et al.*, 1998; Sato *et al.*, 2008). The particular mutation was to allow for a similar

structure of the side chain but alter the thiol group, which was replaced by a hydroxyl group. To our knowledge, this type of mutation has never been studied for the TvMGL enzyme.

2.4. Results and Discussion

The *mgl1* gene from pGL14, which was a gift from Dr. G. Coombs (University Strathclyde, Glasgow, UK), was cloned into the pET28b vector possessing an inducible promoter for overexpression, and a thrombin-cleavable site upstream of the hexahistidine tag, which was incorporated at the C-terminus of the enzyme (termed TvMGL1p28). The enzyme was overexpressed in *E. coli* and purified by a Ni²⁺-chelating resin. The latter construct was used as a template to generate TvMGL1 C113S, termed TvMGL1p28 C113S (presented here); and TvMGL1 C113A, termed TvMGL1p28 C113A (not examined in this study).

The Michaelis-Menten Kinetics of the enzyme were determined by a 3-methyl-2-benzothiazolone hydrazone hydrochloride (MBTH; 2.6) assay method as previously reported (Figure 2.3) (Soda, 1968). Compared to TvMGL1 from the pGL14 construct, TvMGL1p28 had a 1.2-fold lower turnover rate of L-methionine and the Km value for the substrate was within experimental error (Table 2.1). The cause of the slightly lower activity is currently unclear (trace amounts of impurities, linker region, or a truncated N-terminus), but in general the enzyme has a comparable activity when compared to TvMGL1 from the pGL14 construct.

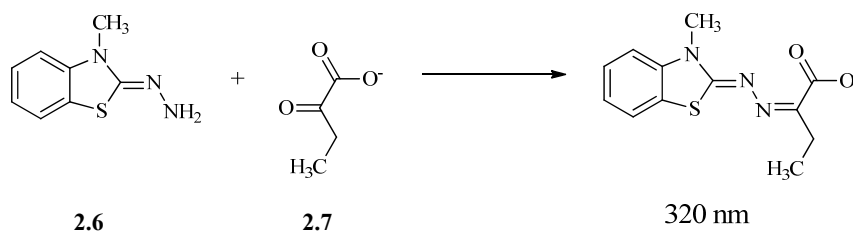


Figure 2.3. An MBTH (2.6) assay method for detection of α -ketobutyrate (2.7) generated from the turnover of L-methionine by TvMGL1.

Table 2.1. The kinetic parameters of the TvMGL1 constructs and C113S mutant for L-methionine.

Enzyme Construct	K_m mM	k_{cat} min^{-1}
TvMGL1 (pGL14)	0.22 ± 0.05	416 ± 15
	$0.19 \pm 0.01^*$	$403 \pm 12^*$
	ND	$453 \pm 14^{**}$
TvMGL1p28	0.17 ± 0.03	347 ± 17
TvMGL1p28 C113S	0.19 ± 0.11	50 ± 2

The standard errors were obtained from three independent experiments. *As reported by Moya *et al.* (2011), and **estimated value from Mckie *et al.* (1998). ND, not determined.

Comparing the TvMGL1p28 C113S mutant with TvMGL1p28, the turnover rate of L-methionine was reduced by approximately 7-fold, with no significant difference in its K_m value for the substrate (Table 2.1). In a previous study, TvMGL1 C113G mutant is reported to have an approximately 6-fold reduction in the turnover rate of L-homocysteine, and no significant changes in its K_m value when compared to the wild-type enzyme (McKie *et al.*, 1998). However, the study did not examine the Michaelis-Menten values for the mutant in the presence of L-methionine. EhMGL1 C110S mutant is reported to have a 2-fold reduction

in its turnover rate of L-methionine and no significant changes in its K_m value when compared to the wild-type enzyme (45% sequence identity) (Sato *et al.*, 2008). The equivalent mutation in PpMGL, C116S is reported to have a 14-fold reduction in turnover rate of L-methionine and an 8-fold reduction in K_m value for the substrate when compared to the wild-type enzyme (42% sequence identity) (Kudou *et al.*, 2008). Overall, TvMGL1 C113 side chain plays an important role in catalysis and is consistent with homologous enzymes studied to date, while dispensable among reported orthologous enzymes such as cystathionine γ -lyase and cystathionine γ -synthase (Sato and Nozaki, 2009).

2.5. Conclusion and Future Work

The activity of TvMGL1p28 is slightly lower than TvMGL1 from the pGL14 construct. Despite these concerns, the single mutation for the pET28 constructs (all things being equal) allowed for direct comparison of the effect of the C113S mutation. The mutant, TvMGL1p28 C113S had a reduced turnover rate relative to the wild type enzyme, which might suggest that the side chain plays an important role in the activity of the enzyme. This notion is consistent with proposals reported for homologous MGLs (Kudou *et al.*, 2008; McKie *et al.*, 1998; Nakayama *et al.*, 1988a; Sato *et al.*, 2008), and C113 proximity to Y111 in the crystal structure of TvMGL1 (a distance of 3.7 Å; PDB 1E5F, unpublished structure). However, a definitive understanding into the exact role of C113 side chain, such as its role in substrate

specificity, will require structural and biophysical data in order to substantiate the kinetic values, which has not been reported for MGL enzymes studied to date.

2.6. Materials and Methods

2.6.1. General Experimental

The *mgll* gene from *T. vaginalis* was a gift from Dr. G. Coombs (University of Strathclyde). Derivatizing agent, MBTH and pyridoxal 5'-phosphate-HCl were purchased from Sigma Aldrich (Milwaukee, WI). Buffers, isopropyl β -D-1-thiogalactopyranoside (IPTG), and dithiothreitol (DTT) were purchased from Bioshop Canada Inc. (Burlington, ON). Kanamycin (KAN) and ampicillin (AMP) were purchased from EMD Chemicals Inc. (Gibbstown, NJ).

Bradford assay for measuring protein concentration was prepared according to procedures reported by Bradford (1976).

2.6.2. TvMGL1 C113 Mutants

The *mgll* gene, previously cloned into the pET28b vector (Novagen, Madison, WI) (Moya *et al.*, 2011), was used as a template to generate the C113A and C113S mutants. The C113A mutant was generated by overlap extension PCR with Pwo SuperYield DNA polymerase (Roche Applied Science, Indianapolis, IN) as described by Sambrook and Russell (2001).

The primer pair (Invitrogen, Burlington, ON) termed “MGL1 forNcoI” (5'-GATATACCATGGCGCACGAGAGAATGAC-3') and “MGL1 C113A Rev” (5'-GCATGTGTggcGCCATAAAGGCACTC-3') generated the N-terminal fragment, which contained the *NcoI* restriction site (underlined) and alanine codon (lower case letters), respectively. The primer pair termed “MGL1 C113A For” (5'-CTTTATGGCgccACACATGCTCTCTTTG-3') and “MGL1 rev1bXhoI” (5'-GTAAATCTCGAGGCTACCACGTGGCACCAGAC-3') generated the C-terminal fragment, which introduced the alanine codon (lowercase letters) and the *XhoI* site (uppercase lettering and underlined), respectively. The N-terminal fragment and C-terminal fragment were combined and amplified with the primer pair termed “MGL1 forNcoI” and “MGL1 rev1bXhoI”, in order to generate the ORF of *mgII*. Amplification of the PCR products was carried out under the following conditions: denatured at 95°C, 1'; 18 cycles (95°C, 1'; 63°C, 1'; 72°C, 1'45"); and 11 cycles (95°C, 1'; 63°C, 1'; 72°C, 1' 35") and 72°C, 5'. The PCR products were recovered using a Silica Bead DNA Gel Extraction Kit (Fermentas Inc., Hanover, MD). The PCR products and the pET28b vector were double digested with *NcoI* and *XhoI* restriction enzymes (NEB, Ipswich, MA), purified using the Silica Bead DNA Gel Extraction kit, and ligated with T4 DNA ligase (NEB). The ligation mixture was transformed into electrocompetent XL-1 Blue cells (Stratagene, La Jolla, CA) and selected on LB-agar media with 35 mg/L kanamycin (KAN). The plasmids with the insert were purified from the transformed cells using a QIAGEN miniprep kit (QIAGEN, Valencia, CA), and then transformed into electrocompetent BL21 (DE3) cells. The procedure to generate the C113S mutant was similar as the methods

described above for the C113A mutant, except that primer termed “TvMGL1 C113S For” (5'-CCTTTATGGCtccACACA-TGCTCTCTTTG-3') was used for generating the N-terminal fragment, and the primer termed “TvMGL1 C113S Rev” (5'-AGCATGTGTgga-GCCATAAAGGCACTC-3') was used for generating the C-terminal fragment. All of the gene sequences for the MGL1 constructs were verified by DNA sequencing (DNA Sequencing Facility, Department of Biology, University Waterloo, Waterloo, ON).

2.6.3. Agarose Gel Electrophoresis

The DNA samples were mixed in a final concentration of 1X loading buffer [0.04% (w/v) bromophenol blue, 5% (v/v) glycerol], and ~4 μ L of the mixture was loaded into the agarose gel. The samples were resolved at 120 volts for 12 min in 1X TAE buffer (40 mM Tris-acetate, 1 mM EDTA, pH 8.0), and visualized with a UV lamp at 365 nm. The agarose gels consisted of 1.0% to 1.4% (w/v) agarose, 1X TAE buffer, and 0.5 μ g/ml ethidium bromide.

2.6.4. Cell Culture and Expression of Enzyme

The pET28b construct containing the gene of interest (*mgll* or *mgll* C113A, *mgll* C113S) was transformed into *E. coli* BL21 (DE3) (Stratagene) by electroporation (5 msec at 1,600 volts), and recovered in 1 mL LB media for one hour at 37°C. The transformants were inoculated into 10 mL LB media supplemented with 35 μ g/mL KAN, and grown overnight in a shaking incubator at 37°C. The overnight culture was inoculated in 1 L LB media

supplemented with 35 µg/mL KAN, grown to an OD₆₀₀ of 0.6 at 37°C, and subsequently induced with 0.12 mM IPTG for 3 hr in a shaking incubator at 37°C. The cultures were harvested by centrifugation at 4,600 xg for 20 min at 10°C, and the cell pellets were stored at -20°C for future use. The growth conditions for MGL1p28 was modified as follows: the overnight culture was inoculated in 1 L Terrific Broth media supplemented with 50 µg/mL KAN and 0.8% glucose, grown to an OD₆₀₀ of 0.6 at 37°C, and subsequently induced with 0.12 mM IPTG for 3 hr in a shaking incubator at 21°C.

2.6.5. Cell Lysis and Protein Purification

The cell pellets containing the His-tagged recombinant enzyme (TvMGL1p28 or mutant) were thawed at 22°C and suspended in ice-cold binding buffer A [30 mM 4-(2-hydroxyethyl)-1-piperazineethanesulfonic acid (HEPES), pH 7.5, 500 mM NaCl]. The cell suspension was homogenized four-times on ice by sonication (3” pulse, 6” rest; 90” total) and then centrifuged at 21,000 xg for 30 min at 10°C. The DNA and cell debris was removed from the supernatant with the DE52 anion exchange column (Sigma Chemicals CO, St. Louis, MO), which was pre-equilibrated with binding buffer A. The flow through from the anion exchange column was loaded onto the Ni²⁺-NTA superflow resin (Qiagen) column that was pre-equilibrated with the Binding buffer. The Ni²⁺-chelating column was washed with five column volumes of Wash buffer (40 mM imidazole, pH 7.4 and 500 mM NaCl); and the bound enzyme was eluted with two column volumes of elution buffer (30 mM HEPES-NaOH, 100 mM imidazole, pH 7.5 and 500 mM NaCl). Fractions with the highest

protein yield were pooled together as determined by visualization on a 15% (w/v) SDS-polyacrylamide gel that was stained with Coomassie Brilliant Blue. An additional purification step for TvMGL1p28 was introduced into the procedure, as a result of an impurity (ESI observed $45,860 \pm 5$ Da). Following ammonium sulfate precipitation (as described below), the enzyme was suspended in buffer B (50 mM phosphate buffer, 1 M NaCl) and resolved on a Superdex 75 chromatography column (GE Healthcare, Piscataway, NJ), which was pre-equilibrated with buffer B. The fraction containing the enzyme was dialyzed, concentrated and stored at -80°C as described below.

The enzyme was precipitated with 35% (w/v) ammonium sulphate at 4°C for 15 hr, and spun down at 21,000 $\times g$ for 30 min at 10°C . The precipitate was suspended in dialysis buffer (1 mL; 100 mM sodium phosphate, 10 mM EDTA, pH 7.2, 200 mM NaCl, 2 mM DTT and 100 μM PLP), The sample was spun down to remove debris and insoluble enzyme at 15,000 $\times g$ for 1 min at 22°C . The enzyme was dialyzed (4 x 1 L) against dialysis buffer in a 10k MWCO dialysis tubing, over a period of 15 hr at 4°C . The samples were concentrated to 25 to 30 mg mL^{-1} with a 10k MWCO centrifuge tube (Sartorius Stedim Biotech & Corning), flash frozen in liquid nitrogen and stored at -80°C for future use (stable for more than 5 months).

ESI-MS for TvMGL1p28 calculated 44 625.33 Da (N-terminal residues MAH removed) and 44 127.75 Da (N-terminal residues MAHERMT removed and ammonium ion present), observed $44\ 621 \pm 5$ Da and $44\ 128 \pm 4$ Da. The enzyme was buffered in 10 mM ammonium

acetate, pH 7.2, prior to ESI-MS analysis. Total amount of enzyme obtained from 1 L culture was 4.5 mg.

ESI-MS for TvMGL1p28 C113S mutant calculated 44 609.26 Da (N-terminal residues MAH removed), observed 44 606±5 Da. The enzyme was buffered in 10 mM ammonium acetate, pH 7.2, prior to ESI-MS analysis. Total amount of enzyme obtained from 1 L culture was 30 mg.

2.6.6. SDS-Polyacrylamide Gel Electrophoresis

The protein sample (6 µL total volume) was mixed with a final concentration of 1X loading buffer [50 mM Tris-HCl pH 6.8, 1% (v/v) β-mercaptoethanol, 2% (w/v) SDS, 0.1% (w/v) bromophenol blue, 10% (v/v) glycerol], and boiled in a water bath for 10 min. The sample was loaded onto an SDS polyacrylamide gel and resolved at 200 volts for ~60 min. The resolving gel was composed of 14% (w/v) acrylamide mix (acrylamide/bis-acrylamide, 30:0.8), 380 mM Tris-base pH 8.8, 0.1% (w/v) SDS, 0.1% (w/v) ammonium persulfate, and 0.04% (v/v) tetramethylethylenediamine (TEMED). The stacking gel was composed of 5% (w/v) acrylamide mix, 130 mM Tris-HCl pH 6.8, 0.1% (w/v) SDS, 0.1% (w/v) ammonium persulfate, and 0.1% (v/v) TEMED. The protein bands were visualized by staining the gel with Coomassie Brilliant Blue.

The procedures for visualizing the proteins bands on the SDS-polyacrylamide gels consisted of: staining solution (0.1% Coomassie Brilliant Blue R, 25% isopropanol, 10%

acetic acid) for 1 hr at 21°C; destaining solution (25% isopropanol, 10% acetic acid) for 15 hr at 21°C.

2.6.7. MBTH Assay Method for Detecting α -Ketobutyrate

The activity of MGL was monitored by utilizing the MBTH assay as described by Soda *et al.* (1968). Briefly, the reaction mixture (50 μ L) for the turnover of methionine consisted of: 60 mM HEPES-NaOH, pH 8.0, 10 μ M PLP, 0.05 to 3.0 mM substrate, and 0.1 μ M enzyme. For the C113S mutant, the reaction mixture was the same as above except that the final enzyme concentration consisted of 1.0 μ M TvMGL1p28 C113S. The reaction was initiated with the enzyme, proceeded for 2 min at 37°C, and stopped with the addition of 10 μ L 12.5% (v/v) trichloroacetic acid. The solution was centrifuged at 15 000 xg for 10 min at 4°C, and the supernatant (50 μ L) was incubated with 140 μ L of 1.0 M acetate buffer at pH 5.0 containing 1.33 mM MBTH at 50°C for 30 min. The amounts of the derivatized samples were determined by a standard curve, which consisted of measuring the absorbance at 320 nm with sodium 2-oxobutyrate supplemented in the enzyme reaction mixture (instead of L-methionine).

CHAPTER 3

**MECHANISTIC STUDIES ON THE ENZYMATIC PROCESSING OF
FLUORINATED METHIONINE ANALOGS BY TRICHOMONAS
VAGINALIS L-METHIONINE γ -LYASE 1**

3.1. Authors' Contributions

The work presented in this chapter was reproduced and revised from Moya *et al.* (2011). Dr. G. Coombs provided the *mgll* gene from *Trichomonas vaginalis* G3. Dr. R. Smith obtained the ESI-MS data for the enzyme and reported compounds. Jan Venne assisted with the ^{19}F -NMR experiments. Dr. J. Honek obtained the theoretical calculations for the heats of formation and the majority of the ^{19}F -NMR chemical shifts. Drs G. Westrop and G. Coombs obtained and analyzed the data for the model pathogen, *T. vaginalis* G3. I. Moya and Dr. J. Honek designed the project, discussed the data, and wrote the paper. All other work was performed by I. Moya such as syntheses, data analysis and enzyme assays.

3.2. Introduction

L-Methionine γ -lyase is a pyridoxal-5'-phosphate (PLP)-dependent enzyme, which catalyzes the α,γ -elimination reaction of L-methionine (**3.1**) to produce methanethiol, ammonia and α -

ketobutyrate (**3.2**; Figure 3.1) (Lockwood and Coombs, 1991; Tanaka *et al.*, 1977). The catalytic α,γ -elimination reaction is driven by the PLP cofactor, as reported by studies using a modified PLP derivative that mimics the catalytic reaction mechanism of the enzyme (Johnston *et al.*, 1981; Karube and Matsushima, 1977). The reaction rate of the catalytic cofactor is enhanced by the environment of the enzyme as a result of conformational strain imposed on the Schiff-base and planarity of external aldimine linkage, and proximity effects of catalytic side chains (Dubnovitsky *et al.*, 2005; Hayashi *et al.*, 2003; Zabinski and Toney, 2001). Thus, MGL provides an appropriate environment for the PLP cofactor to facilitate the α,γ -elimination reaction of L-methionine.

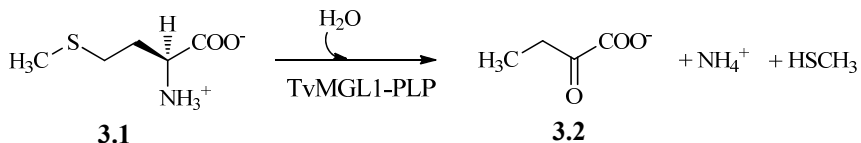


Figure 3.1. Schematic representation of the reaction catalyzed by the PLP-dependent enzyme MGL.

3.3. Pyridoxal Model Systems of Enzymatic Catalytic Reactions

The vitamin B₆ cofactor, pyridoxal, is known to catalyze racemization, decarboxylation, transamination, elimination and substitution reactions of amino acids; and believed to mimic the mechanism of PLP-dependent enzyme-catalyzed reactions (Figure 3.2) (Metzler *et al.*, 1954a). The initial steps for these reactions involve the formation of an aldimine linkage with the amino acid and chelation of a metal ion (**3.3**; Figure 3.2). This establishes a planar

conjugated system from the amino acid to the pyridine ring of pyridoxal, and favours the labilization of the α -hydrogen atom of the amino acid to produce the ketimine-quinoid intermediate (**3.4**; Figure 3.2) (Metzler *et al.*, 1954a).

For racemization of the amino acid by pyridoxal, the proton is removed and then reintroduced at the opposite face of the C_α atom, which is favoured at pH 10 (Figure 3.2a) (Olivard *et al.*, 1952). Transamination is favoured at pH 5, where the $C4'$ atom of the aldimine is protonated followed by hydrolysis of the ketimine to yield pyridoxamine (**3.6**) and the α -ketoester (**3.7**; Figure 3.2f) (Matsuo, 1957; Olivard *et al.*, 1952). Elimination of the amino acid side chain requires reorientation of the side chain, antiparallel to the planar conjugated system (Figure 3.2b) (Christen and Mehta, 2001). This has been observed for the splitting of threonine and serine to produce glycine, and their respective acetaldehyde and aldehyde leaving groups (Metzler *et al.*, 1954b). Elimination reaction of a β -substituted electron attracting group from the side chain of an amino acid, such as hydroxyl and thiol functional groups, involves the deprotonation of the C_α atom and a shift of electrons in the conjugated system to produce an imino acrylate (**3.5**; Figure 3.2d) (Metzler and Snell, 1952; Thomas *et al.*, 1968). Elimination of a γ -substituted electron attracting group from an amino acid, such as hydroxyl and thiol functional group, involves the deprotonation of the C_β atom and a shift of electrons in the conjugated system (Figure 3.2e) (Metzler *et al.*, 1954a). Substitutions at the C_α atom of glycine occurs readily for acetaldehyde and aldehyde, which follows the reverse direction for an elimination reaction (Metzler *et al.*, 1954b). Substitutions

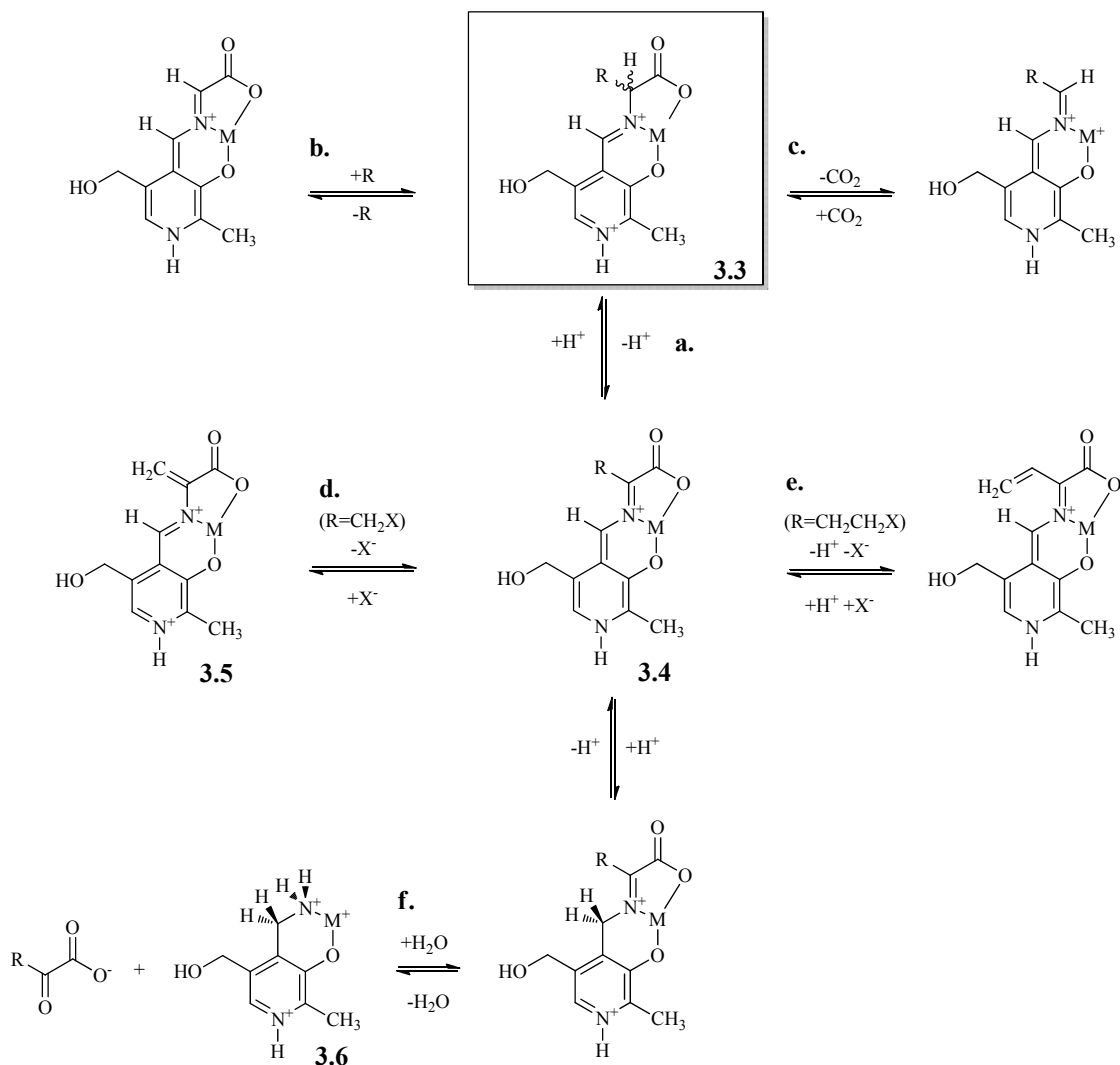


Figure 3.2. The various nonenzymatic catalytic reactions on an amino acid by pyridoxal.

Pyridoxal catalysis of various reactions on an amino acid by **a**) racemization of the C_α atom, **b**) elimination of the amino acid side chain (where R = CH₃(CO)H or formaldehyde), **c**) decarboxylation at the C_α atom, **d**) elimination of the electron attracting group at the C_β atom (where X = thiol or hydroxy functional group), **e**) elimination of the electron attracting group at the C_γ atom (where X = thiol or hydroxy functional group) and **f**) transamination. Adapted from Metzler *et al.* (1954a). Where M is a chelated metal ion.

at the C_β atom do not proceed readily, as reported for the non-enzymatic synthesis of tryptophan from serine and indole (Metzler *et al.*, 1954a), and substitutions at the C_γ atom are reported for a modified pyridoxal cofactor (Karube and Matsushima, 1977). For amino acids to undergo decarboxylation, the carboxylate group is reorientated antiparallel to the plane of the conjugated system, which may proceed in the absence of metal ions (Figure 3.2c) (Kalyankar and Snell, 1962; Zabinski and Toney, 2001). Thus, pyridoxal may catalyze several types of reactions depending on the functional groups present and the reaction conditions.

3.4. Processing of Fluorinated Methionine Analogs by PLP-dependent Enzymes

Previous studies have suggested that the methionine analog L-trifluoromethionine (TFM; **3.8**) may act as a potential prodrug in organisms that express γ -eliminating enzymes, such as MGL (Alston and Bright, 1983). The processing of TFM is hypothesized to produce trifluoromethanethiol, which spontaneously decomposes to thiocarbonyl difluoride (**3.15**), a chemically reactive molecule that results in cellular toxicity. The bioactivity of TFM was later confirmed in antimicrobial screens against microorganisms that contain MGL, such as *Entamoeba histolytica*, *T. vaginalis*, and *Porphyromonas gingivalis* (Coombs and Mottram, 2001; Tokoro *et al.*, 2003; Yoshimura *et al.*, 2002).

Previous investigations on the effects of fluorination on methionine analog biochemistry indicated alterations in its electronic, as well as steric properties when incorporated within

enzymes (Duewel *et al.*, 2001) (and references therein). Therefore, it was of interest to evaluate the effects of increasing fluorination at the thiomethyl moiety of the methionine analog on the efficiency of enzymatic processing by MGL, and the effect of fluorination on antiparasitic activity. For example, the processing of the analog, DFM would likely act as a thioformylating agent. Thus, it would be of interest to determine if this type of conversion could also be lethal to a parasite containing MGL, which may lead to future modulation of the activity of the fluorinated compound by introducing other moieties into the fluorinated methanethiol group.

To date, the production of a thioacylating agent upon the processing of TFM and DFM by MGL has not been experimentally confirmed. To identify these very reactive agents, the fluorinated methionine analogs were studied with the recombinant MGL enzyme as well as a model pyridoxal system, which is known to mimic the γ -elimination of the TvMGL1 enzyme itself (Johnston *et al.*, 1981; Karube and Matsushima, 1977). To investigate the differences in cytotoxicity between TFM and DFM, the levels of cell growth inhibition for the two fluorinated methionine analogs were examined with *Escherichia coli* expressing TvMGL1 as well as with the intact human pathogen, *T. vaginalis*.

3.5. Results

3.5.1. Detecting the Products from the Enzymatic Processing of the Fluorinated Methionine Analogs

The recombinant TvMGL1 was previously cloned into a pQE vector possessing an inducible promoter for overexpression, and with a hexahistidine tag incorporated at the C-terminus of the enzyme (McKie *et al.*, 1998). The enzyme was overexpressed in *E. coli* and purified by a Ni²⁺-chelating resin. The syntheses of DFM (**3.9**) and TFM (**3.8**) from L-homocystine (**3.7**; Figure 3.3) were adapted from reported procedures (Houston and Honek, 1989; Tsushima *et al.*, 1990).

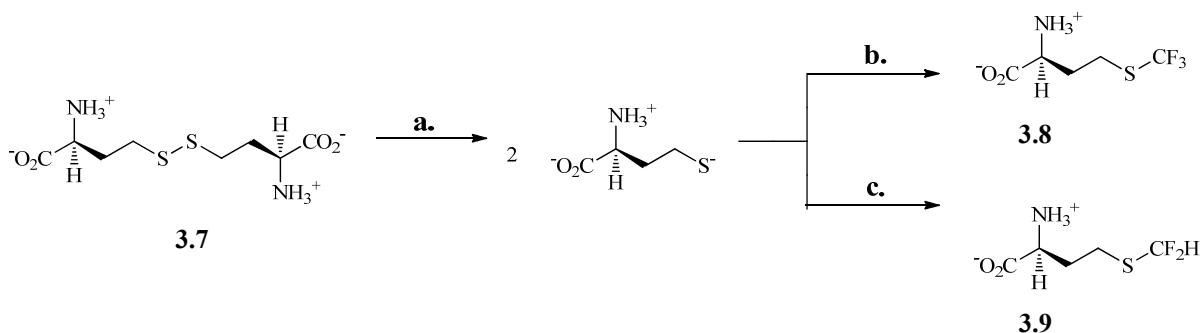


Figure 3.3. Syntheses of TFM (3.8) and DFM (3.9).

a) Sodium metal, liquid ammonia, -78°C, 20 min; **b)** potassium *t*-butoxide, iodotrifluoromethane, ethanol, 21°C, 15 hr with photolysis; **c)** potassium *t*-butoxide, chlorodifluoromethane, ethanol, 21°C, 15 hr.

The processing of DFM and TFM by the recombinant enzyme was monitored by ^1H decoupled ^{19}F -NMR and ^{19}F -NMR, respectively, for changes in the chemical shift of the fluorine nuclei of the compounds, as described previously for the processing of TFM by cystathionase (a γ -eliminating PLP-dependent enzyme) (Alston and Bright, 1983). A total of 144 scans were taken with a sweep width of +100 to -125 ppm, in order to cover the region where the calculated and experimental fluorine signals were expected to appear (Table 3.1). In the negative control experiments (incubation without enzyme), a ^{19}F NMR resonance signal was observed at -41.4 ppm, which corresponded to the fluorine nuclei in TFM (Figure 3.4a), and in a separate experiment, at -93.3 ppm for the fluorine nuclei in DFM (Figure 3.4c). Upon the addition of the enzyme, a second ^{19}F NMR resonance was observed at -119.8 ppm for both TFM and DFM samples (Figure 3.4 b and d), which coincided with the chemical shift of the fluoride ion under similar conditions (Figure 3.4e). All of the ^{19}F -NMR chemical shifts in the current experiments were consistent with the literature values for TFM, DFM and the fluoride ion previously reported (Düewel *et al.*, 1997; Gerken *et al.*, 2002; Soloshonok *et al.*, 1992; Vaughan *et al.*, 1999).

No other ^{19}F -NMR chemical shifts were observed for the intermediates proposed for the enzymatic processing of TFM and DFM, during the timeframe and sweep width of the experiments. The reported literature values for the ^{19}F -NMR chemical shifts for the fluorine nuclei of trifluoromethanethiol (**3.16**) and thiocarbonyl difluoride (**3.15**; the proposed products in the enzymatic processing of TFM) occur at -31.4 and +41.2 ppm, respectively, in

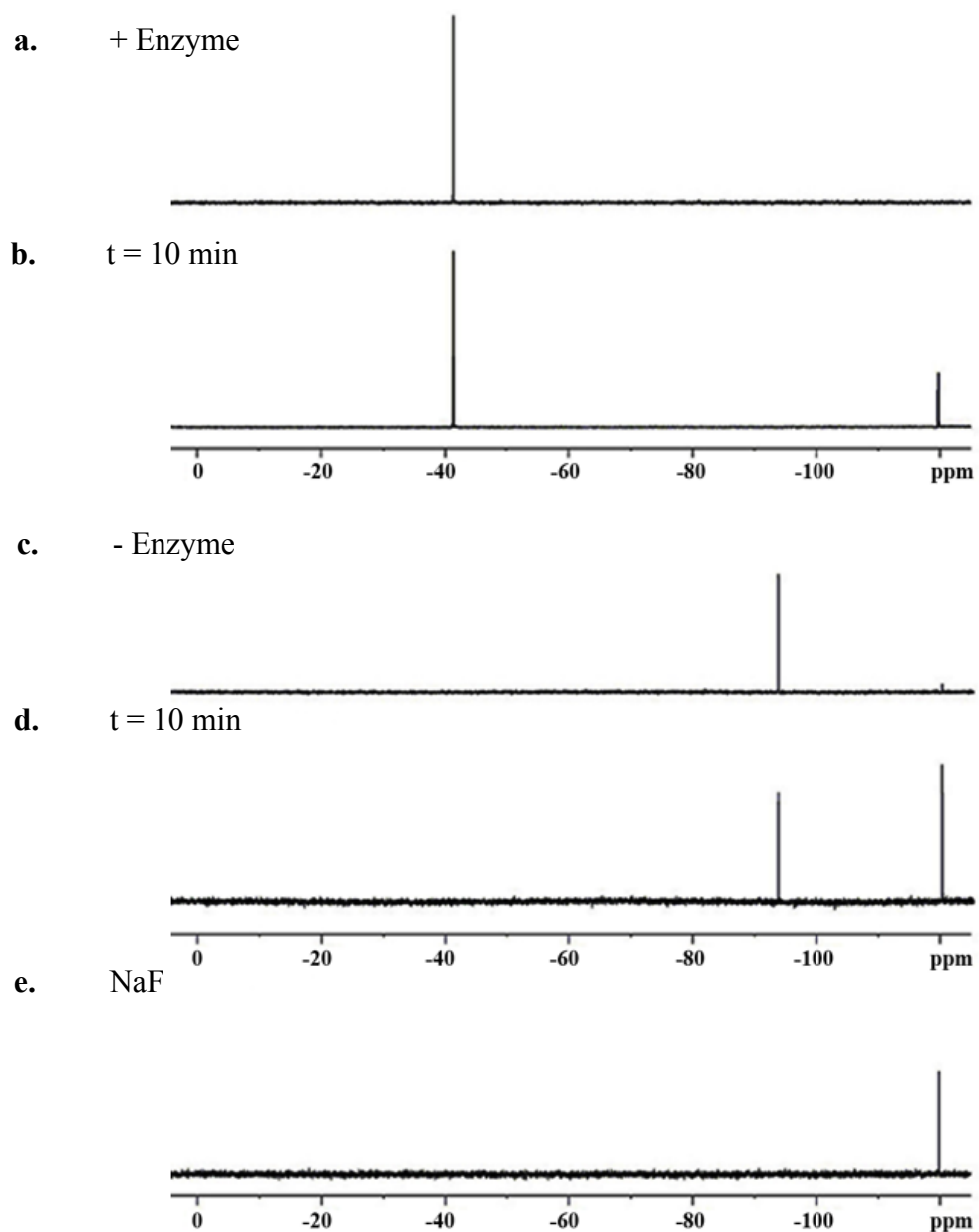


Figure 3.4. ^{19}F -NMR spectra for the processing of TFM and DFM by TvMGL1 (externally locked with CFCl_3).

The processing of TFM (δ : -41.4 ppm) in **a**) the absence and **b**) the presence of the enzyme; the processing of DFM (δ : -93.3 ppm) in **c**) the absence and **d**) the presence of the enzyme; and **e**) the control, 2.0 mM sodium fluoride (δ : -119.8 ppm).

CFCl_3 (Table 3.1) (Adams *et al.*, 1998; Haas and Wanzke, 1987). However, there are no known reports of the ^{19}F -NMR chemical shifts for the fluorine nuclei of difluoromethanethiol (**3.15**) and thioformyl fluoride (**3.19**), the proposed products in the enzymatic processing of DFM.

The accuracy of the theoretical ^{19}F -NMR chemical shifts was higher for the geometry optimized DFT (rms error 8.5 ppm) and MP2 (rms error 10.8 ppm) basis sets than the geometry optimized HFT basis set (rms error 19.5 ppm) (Table 3.1). Overall, the basis sets used for the theoretical calculations were in good agreement with the experimental values, even though solvation effects were not taken into account. Thus, the scanning region selected for the ^{19}F NMR experiment was likely appropriate for monitoring the expected fluorine nuclei of the nonenzymatic decomposition products, generated from the enzymatic reactions.

Table 3.1. ^{19}F -NMR theoretical chemical and experimental shifts for various fluorinated molecules.

Entry	Compound	^{19}F -NMR HFT ppm	^{19}F -NMR MP2 ppm	^{19}F -NMR DFT ppm	Exptl (lit) ppm
3.10	CFCl_3	0.0 (12.3)	0.0 (199.9)	0.0 (179.2)	0.0 (REF)
3.11	$\text{CH}_3\text{C}(\text{O})\text{F}$	51.7	36	56.2	50 ^a
3.12	$\text{FC}(\text{O})\text{OCH}_3$	9.7	4.1	-30.3	-18.7 ^b
3.13	CF_2HSCH_3	-91.5	-103	-107.5	-97.3 ^c
3.14	CF_3SCH_3	-34.6	-48.1	-57.8	-45 ^d
3.15	CHF_2SH	-74.6	-84.5	-87.2	
3.16	CF_3SH	-22.8	-35.4	-44	-31.4 ^e
3.17	$\text{HC}(\text{O})\text{F}$	51.3	36.6	45.6	42.8 ^f
3.18	$\text{FC}(\text{O})\text{F}$	5.4	-34	-28.2	-23 ^g
3.19	$\text{HC}(\text{S})\text{F}$	88.3	70.7	98.1	
3.20	$\text{FC}(\text{S})\text{F}$	69.9	31.1	44.2	41.2 ^h
3.21	$\text{FC}(\text{S})\text{OH}$	59.7	40.8	49.0	
3.22	$\text{FC}(\text{S})\text{OCH}_3$	70.2	28.8	36.8	
3.23	$\text{FC}(\text{S})\text{N}(\text{CH}_3)_2$	39.8	10.9	14.9	13.37 ⁱ
3.24	$\text{FC}(\text{S})\text{NC}_4\text{H}_8\text{O}$	37.9	3.0	5.5	

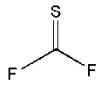
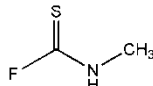
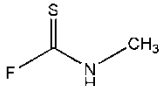
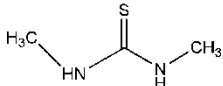
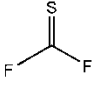
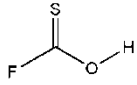
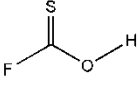
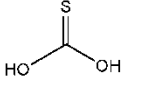
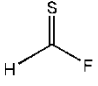
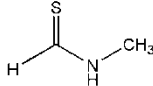
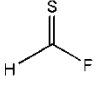
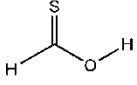
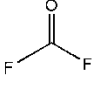
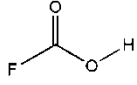
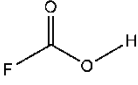
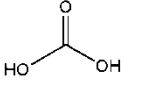
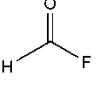
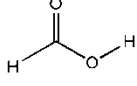
The experimental values are from: ^aKirij *et al.* (2000), ^bAppelman *et al.* (1985) and Bock *et al.* (1968), ^cLange and Shreeve (1985), ^dYu *et al.* (1974), ^eHaas and Wanzke (1987), ^fde Rege *et al.* (1997), ^gDowns (1962), and ^hAdams *et al.* (1998), ⁱTyrra (2001).

HFT: Hartree-Fock Theory, HFT/6-311+G(d,p)//B3LYP/6-31G(d) gauge including atomic orbitals (GIAO); MP2: Møller-Plesset theory, MP2/6-311++G(2d,p)//B3LYP/6-311++G(2d,p) GIAO; DFT: density functional theory, B3LYP/6-31+G(df,p)//B3LYP/6-31+G(df,p) GIAO. HFT calculations utilized Spartan '08 software (Wavefunction Inc., Irvine, CA, USA) (Shao *et al.*, 2006). MP2 and DFT level GIAO calculations were carried out utilizing Gaussian 03 and Gaussview v3.0.9 for structure drawing and calculation setup (Frisch *et al.*, 2003a; Frisch *et al.*, 2003b). The theoretically calculated chemical shifts of the compounds were referenced to the theoretically calculated chemical shielding constant of CFCl_3 (in brackets).

To examine whether the decomposition of the thioacylating agents were thermodynamically favorable, the heats of formation were calculated using T1 and G3 (MP2) high level thermochemical methods (Curtiss *et al.*, 1999; Ohlinger *et al.*, 2009). The nucleophiles methylamine and water were chosen for the calculations as a model for the ϵ -amines in lysine found on the surface of the homodimer (45 out of a total 52 lysines; PDB code 1E5F, unpublished crystal structure) and the water present in the reaction mixture, respectively. Analyses of the theoretical calculations indicated that the heats of formation for the reactions between the thioacylating agent and the nucleophiles (methylamine or water) were thermodynamically extremely favorable (Table 3.2).

To examine the stabilities of the methylmercaptan products generated from the enzymatic reaction, the theoretical pK_a values of the thiols were calculated using previously reported computational methodologies (Klicic *et al.*, 2002). The pK_a values were found to decrease as follows: methanethiol (pK_a 10.6) > difluoromethanethiol (pK_a 5.2) > trifluoromethanethiol (pK_a 2.8) which were consistent with the previously reported trend for their theoretical gas phase acidities (Burk *et al.*, 2000). Thus, analysis of the predicted pK_a values indicated that the thiolate forms of trifluoromethanethiol and difluoromethanethiol would be the predominant ionized forms at physiological pH, and the instability should eject a fluoride ion upon collapse.

Table 3.2. T1 and G3(MP2) enthalpies of formation at 298 K for the reaction between the thioacylating agents and water or methylamine.

					T1 (kJ/mol)	G3(MP2) (kJ/mol)
	+ NH ₂ CH ₃	→		+ HF	-101.50	-101.50
	+ NH ₂ CH ₃	→		+ HF	-61.75	-60.73
	+ H ₂ O	→		+ HF	-30.72	-31.30
	+ H ₂ O	→		+ HF	-43.74	-41.45
	+ NH ₂ CH ₃	→		+ HF	-102.83	-99.30
	+ H ₂ O	→		+ HF	-46.13	-42.82
	+ H ₂ O	→		+ HF	-35.62	-37.46
	+ H ₂ O	→		+ HF	-29.04	-24.04
	+ H ₂ O	→		+ HF	-27.60	-26.54

Spartan '08 software (Wavefunction Inc., California, USA) was utilized for structure drawing and thermochemical calculations using the default protocols for the T1 and G3(MP2) thermochemical recipes as employed in this program. Choice of the exact structures (e.g., syn versus anti) utilized in these calculations were made based on utilizing the lowest energy structures found from geometry optimization calculations at the B3LYP/6-31G* level to determine the starting geometries for the thermochemical recipes (Shao *et al.*, 2006).

The difficulty in confirming the existence of the thioacylating agent, produced from the enzymatic processing of the fluorinated methionine analogs, was the heterogeneity of potential nucleophiles within the reaction mixture, such as buffer, water and enzyme. To trap the thioacylating products, the complexity of the reaction was reduced by using a PLP model system (Figure 3.5); thus, avoiding protein and extra buffers. It has been previously demonstrated that *N*-methylpyridoxal chloride (MPAL, **3.29**) in a KOH/methanol solution can mechanistically mimic the γ -elimination reaction catalyzed by the intact MGL enzyme (Johnston *et al.*, 1981; Karube and Matsushima, 1977). It was hypothesized that the fluorinated methionine analogs would be processed by MPAL to produce the reactive thioacylating agents (Figure 3.5 a and b). Morpholine (**3.25**) was selected as the trapping agent in this study because its alkyl groups are restrained, and it is a strong nucleophilic amine (Moltzen *et al.*, 1987). The synthesis of MPAL was adapted according to the methods reported by Heyl (1951) and Johnston (1981), and the syntheses of the authentic reference standards for the trapped thioacylating agents were followed according to previously reported procedures (Beerheide *et al.*, 2000; Mills, 1986) (Figure 3.5).

The conditions for the PLP model system were followed according to the methods previously described by Karube and Matsushima (1977) for normal substrates. The reaction mixture containing synthetic MPAL and the fluorinated methionine analogs were treated with morpholine. Any reaction products trapped by morpholine were extracted by washing the aqueous reaction mixture with ethyl acetate or CHCl_3 . The major products for the DFM and TFM reactions were consistent with the authentic reference standards (4-thioformyl-morpholine (**3.26**) and 4,4'-thiocarbonyl-dimorpholine (**3.27**), respectively, in terms of their

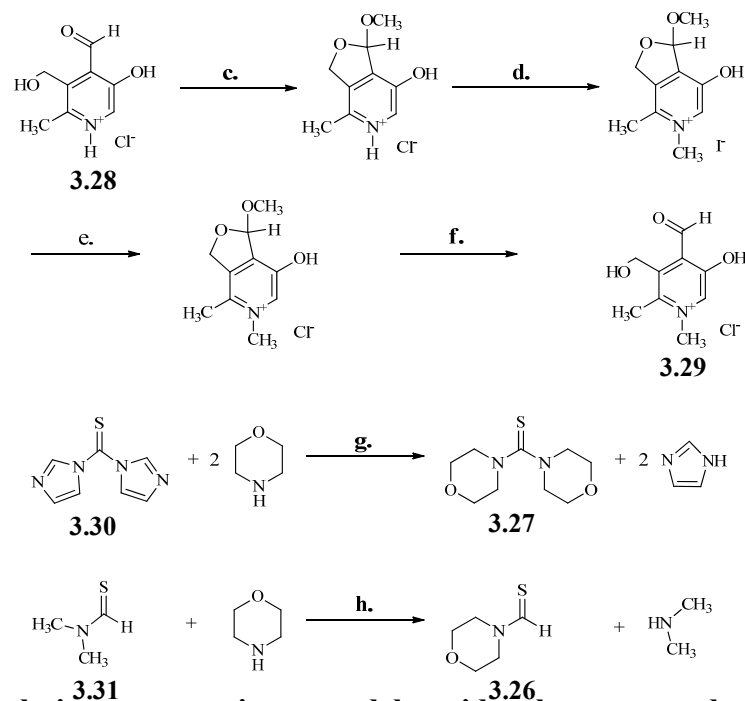
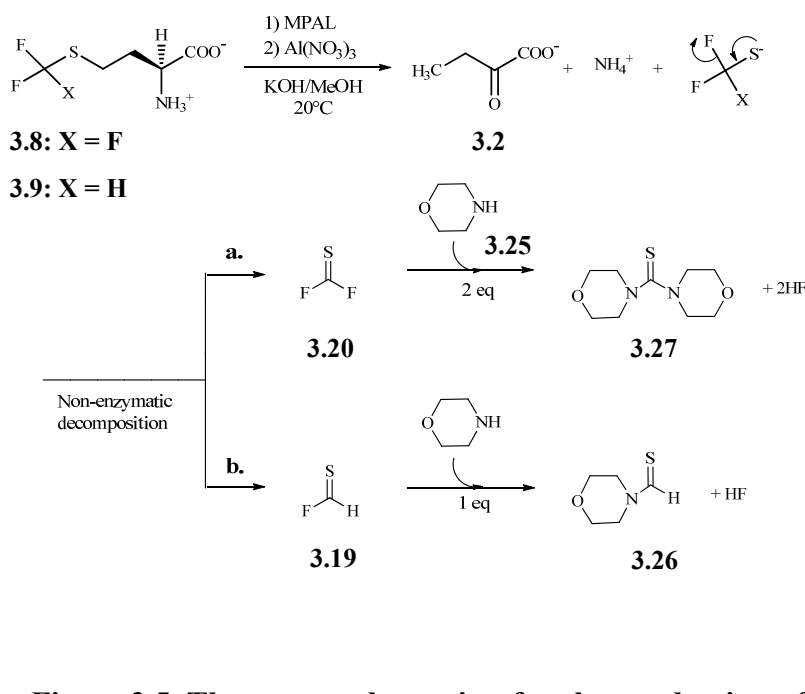


Figure 3.5. The proposed reaction for the production of the thioacylating agents using a model pyridoxal system, and syntheses of MPAL and authentic reference standards.

Catalytic processing of TFM (**3.8**) and DFM (**3.9**) by MPAL and generation of **a**) thiocarbonyl difluoride when X = F (**3.20**) and **b**) thioformyl fluoride when X = H (**3.19**). The capture of thiocarbonyl difluoride and thioformyl fluoride with morpholine (**3.25**) to afford 4,4'-thiocarbonyldimorpholine (**3.27**) and 4-thioformylmorpholine (**3.26**), respectively. Synthesis of MPAL (**3.29**) from pyridoxal chloride (**3.28**): **c**) methanol; **d**) iodomethane, benzene, 21°C, 24 hr; **e**) silver chloride, 21°C, 2 hr; **f**) dilute HCl. Synthesis of 4,4'-thiocarbonyldimorpholine (**3.27**) from 1,1'-thiocarbonyldiimidazole (**3.30**): **g**) triethylamine, methylene chloride, 4°C to 21°C, 4 hr. Synthesis of 4-thioformylmorpholine (**3.26**) from *N,N*'-dimethyl thioformamide (**3.31**): **h**) toluene refluxed at 115°C, 15 hr.

R_f values by TLC (see Materials and Methods), $^1\text{H-NMR}$ spectroscopic properties (Figure 3.6) and their electrospray mass spectra (Figure 3.7). The amount of product trapped was 50% for thiocarbonyl fluoride and 16% for thioformyl fluoride as estimated by $^1\text{H-NMR}$ spectroscopy (Table 3.3). Thus, the intermediates trapped from the processing of DFM and TFM by MPAL were thioformyl fluoride and thiocarbonyl difluoride, respectively.

Table 3.3. Amount of thioacylating agent trapped and fluoride produced from the PLP model system upon processing of TFM and DFM substrates as determined by NMR spectroscopy.

		TFM Reaction (mM)	DFM Reaction (mM)
$^{19}\text{F-NMR}$	$[\text{Substrate}]_i$	1.00	1.00
	$[\text{Substrate}]_f$	0.15	0.29
	Fluoride	2.45	1.66
$^1\text{H-NMR}$	Trapped	0.50	0.16

Samples were locked with D_2O for $^1\text{H-NMR}$ experiment and externally locked with CFCl_3 for $^{19}\text{F-NMR}$ experiment using a 300 MHz NMR (Bruker) spectrometer. $[\text{Substrate}]_i$ is the initial concentration of substrate amino acid analogue. $[\text{Substrate}]_f$ is the final concentration of substrate amino acid analogue.

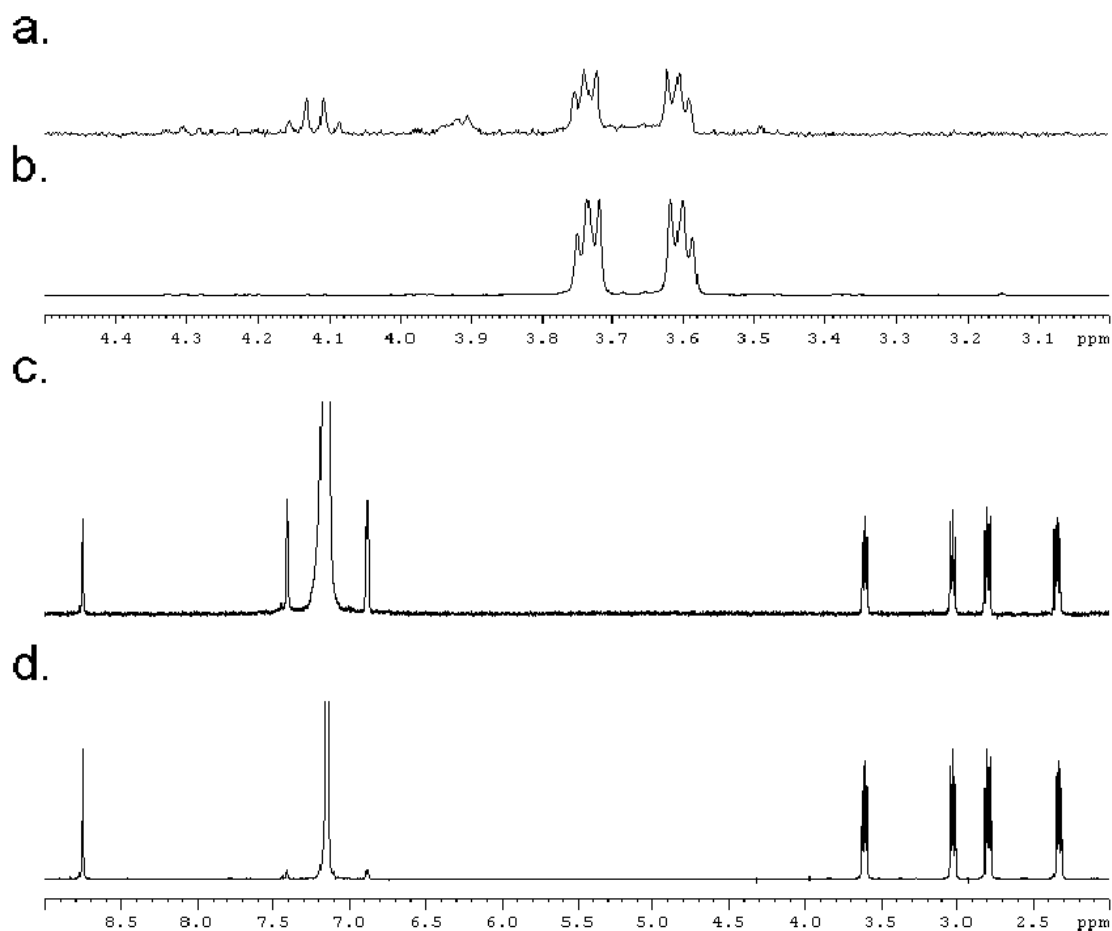


Figure 3.6. $^1\text{H-NMR}$ spectra of the extracted compounds from the TFM and DFM PLP model reactions.

The NMR spectra (locked with CDCl_3) for **a**) the extracted compound from the TFM reaction and **b**) the authentic reference standard, 4,4'-thiocarbonyldimorpholine (δ : 3.59, 3.72 ppm). The NMR spectra (locked with C_6D_6) for **c**) the extracted compound from the DFM reaction and **d**) the authentic reference standard, 4-thioformylmorpholine (δ : 2.33, 2.80, 3.03, 3.61, 8.76 ppm). The likely impurity in the spectrum for TFM PLP model reaction is ethyl acetate (δ : 4.12 ppm; q), and for DFM PLP model reaction and its authentic standard is benzene (δ : 7.15 ppm; s).

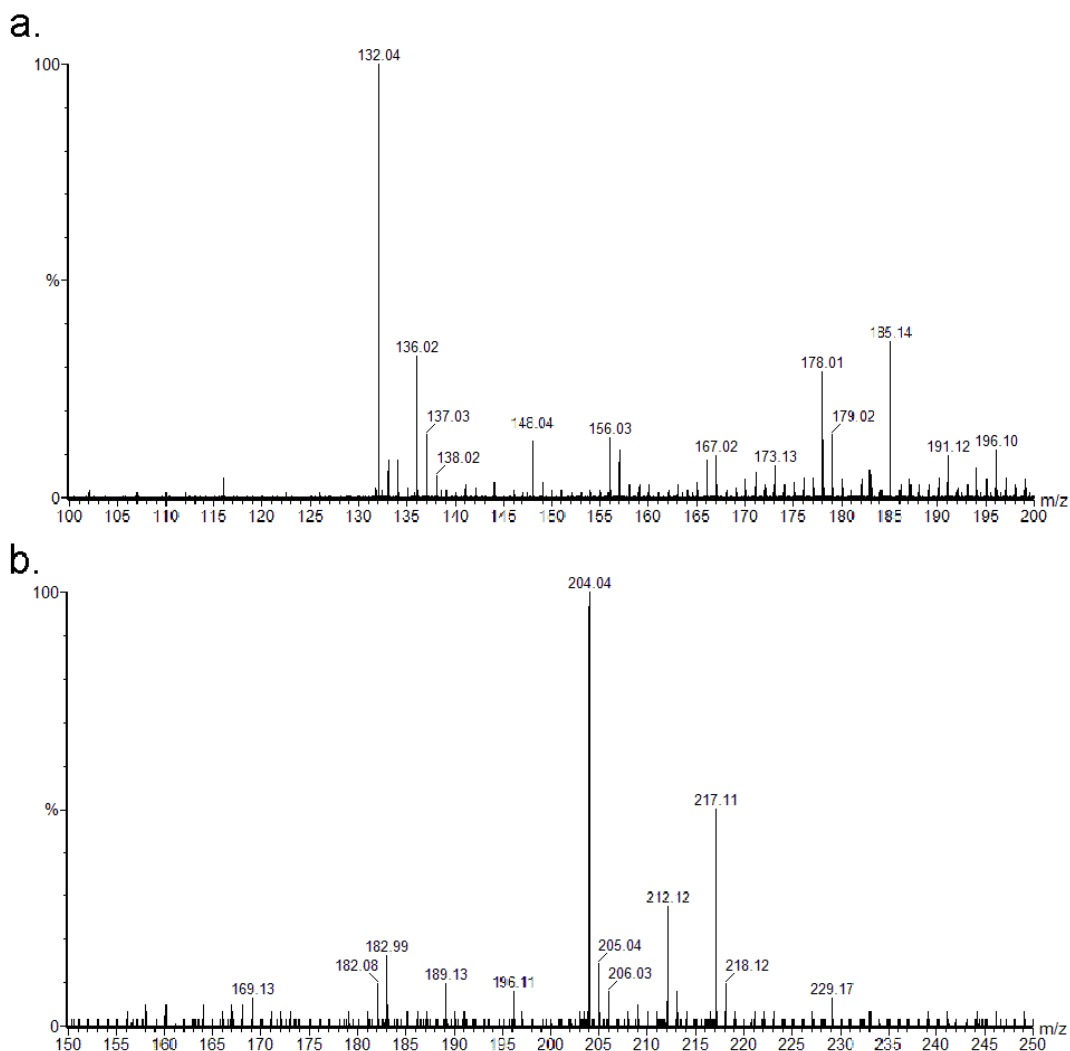


Figure 3.7. ESI-MS spectra of the extracted compounds from the TFM and DFM PLP model reaction.

The trapped compound from **a)** the DFM reaction had a mass of 132.04 Da $[M+H]^+$ that corresponded to the expected mass of 4-thioformylmorpholine, and **b)** the TFM reaction had a mass of 217.11 Da $[M+H]^+$ that corresponded to the expected mass of 4,4'-thiocarbonyldimorpholine. Samples were diluted with ACN/H₂O/formic acid (1:1:0.004). Possible impurities for the TFM reaction include *N*-methylpyridoxal (182.08 Da, $[M]^+$), *N*-methylpyridoxal monomethylacetal (196.10 Da, $[M]^+$) and trifluoromethionine (204.04 Da, $[M+H]^+$). Possible impurities for the DFM reaction include *N*-methylpyridoxal monomethylacetal (196.10 Da, $[M]^+$) and difluoromethionine (185.14, $[M+H]^+$).

3.5.2. Monitoring the Intermediates Produced from the Processing of TFM and DFM by MPAL

In the PLP model system, ^{19}F -NMR spectroscopy was used to identify the fluorine nuclei of the unstable intermediates produced from the processing of TFM and DFM by the modified cofactor, MPAL. Initially, no intermediates were detected by ^{19}F -NMR when maintaining the reaction conditions constant as previously described in the paper. The likely problems for the negative results were as follows: 1) formation of crystals as the reaction proceeded overtime and consequently a lack of a fluorine signal for fluoride anion, 2) morpholine and basic methanol may have quenched the signal of the intermediates, 3) and a low amount of catalyst to initiate the reaction. Despite fluoride anion crystallizing out of solution, the system was not supplemented with water because the thioacylating agents were predicted to undergo hydrolysis. The concentration of nucleophiles within the system was reduced to 1.0 mM KOH and 90 mM morpholine, and the mixture was subsequently diluted to 30% (v/v) with ethyl acetate. Finally, the amount of catalyst was increased to 1 mM in order for MPAL to process more DFM and TFM. During the time frame of the ^{19}F -NMR experiment, two fluorine signals with a chemical shift of +11.6 ppm and -41.4 ppm were observed for the TFM sample after 2.5 hr (Figure 3.8). The chemical shift at -41.4 ppm coincided with the authentic reference standard TMF, while +11.6 ppm coincided with the theoretically calculated and experimentally reported value of *N,N'*-dimethyl thiocarbamoyl fluoride (**3.23**) (Tyrra, 2001), and very close to the ^{19}F -NMR chemical shift calculated for the more computationally demanding morpholine adduct (**3.24**; Table 3.1). Thus, the ^{19}F -NMR

chemical shift of -41.4 ppm corresponded to TFM, while the chemical shift of +11.6 ppm likely corresponded to 4-morpholino thiocarbonyl fluoride (**3.24**), a chemical analog of *N,N*-dimethyl thiocarbamoyl fluoride (**3.23**; Table 3.1). No other fluorine signals were observed during the timeframe of the experiment for the processing of either TFM or DFM in the methanol-ethyl acetate mixture (3:7 v/v ratio). The lack of any other fluorine signal may have resulted from the extensive crystallization that occurred upon the addition of ethyl acetate, and potential nucleophiles predicted to react with the thioacylating agent.

3.5.3. Kinetic Parameters for the Enzymatic Processing of the Fluorinated Methionine

Analogs

The activity of the enzyme was initially assayed spectrophotometrically at 320 nm after incubation of the enzymatic products with the derivatizing agent, 3-methyl-2-benzothiazalone hydrazone hydrochloride (MBTH) as previously described (Soda *et al.*, 1969). However, the kinetic parameters of TvMGL1 upon processing of DFM at high concentrations (>1.2 mM) could not be accurately obtained due to extensive precipitation upon inclusion of the derivatization reagent (data not shown). To circumvent this issue, another approach was developed (see below) as we hypothesized that the derivatizing agent might not be compatible with the product, thioformyl fluoride that was generated from the enzymatic reaction.

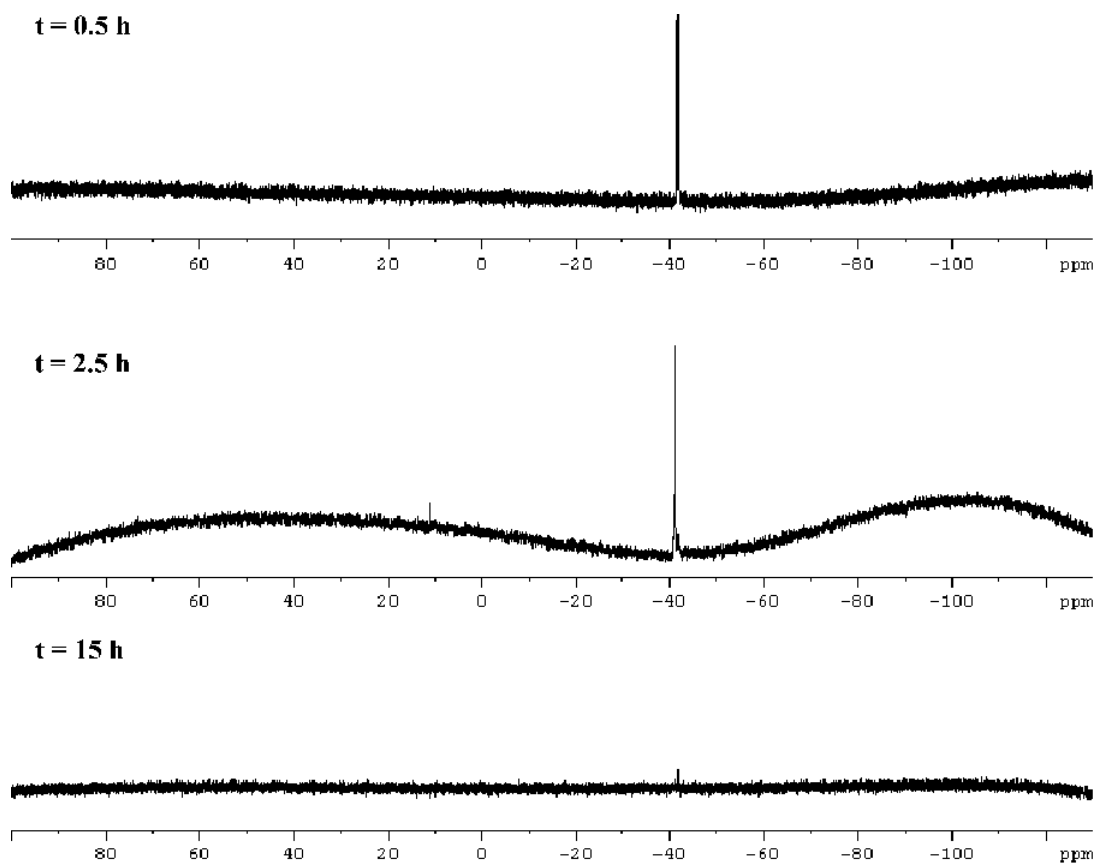


Figure 3.8. ^{19}F -NMR spectrum for the processing of TFM by MPAL in a solution of methanol-ethyl acetate (externally locked with CFCl_3).

The processing of TFM (δ : -41.4 ppm) at given time intervals and the appearance of a measurable intermediate at 2.5 hr (δ : $+11.6 \text{ ppm}$; 364 scans).

A lactate dehydrogenase (LDH) coupled assay was developed in order to obtain the kinetic parameters for the processing of methionine and its fluorinated analogs by TvMGL1, similar to the method described for the γ -lyase activity of cystathionine γ -synthase (Holbrook *et al.*, 1990). The product, α -ketobutyrate produced by the activity of TvMGL1, was coupled to the oxidation of NADH by LDH to produce 2-hydroxybutyrate, and the resulting loss in NADH was monitored spectrophotometrically at 340 nm (Figure 3.9a). The catalytic turnover rate constant (k_{cat}) for TvMGL1 was found to increase as follows: methionine < DFM < TFM; while the K_m value was found to increase as follows: DFM < TFM < methionine (Table 3.4; Figure 3.9 b and c). Analysis of the enzyme's catalytic efficiency indicated that DFM was processed more efficiently than TFM and methionine (Table 3.4).

Table 3.4. The kinetic parameters of TvMGL1 for methionine and its analogs.

Substrate	K_m mM	k_{cat} min ⁻¹	k_{cat}/K_m M ⁻¹ s ⁻¹
Methionine	0.193 ± 0.014	403 ± 12	34.8 x10 ³
DFM	0.025 ± 0.003	498 ± 5	332 x10 ³
TFM	0.130 ± 0.005	810 ± 4	104 x10 ³

The standard errors were obtained from three independent experiments.

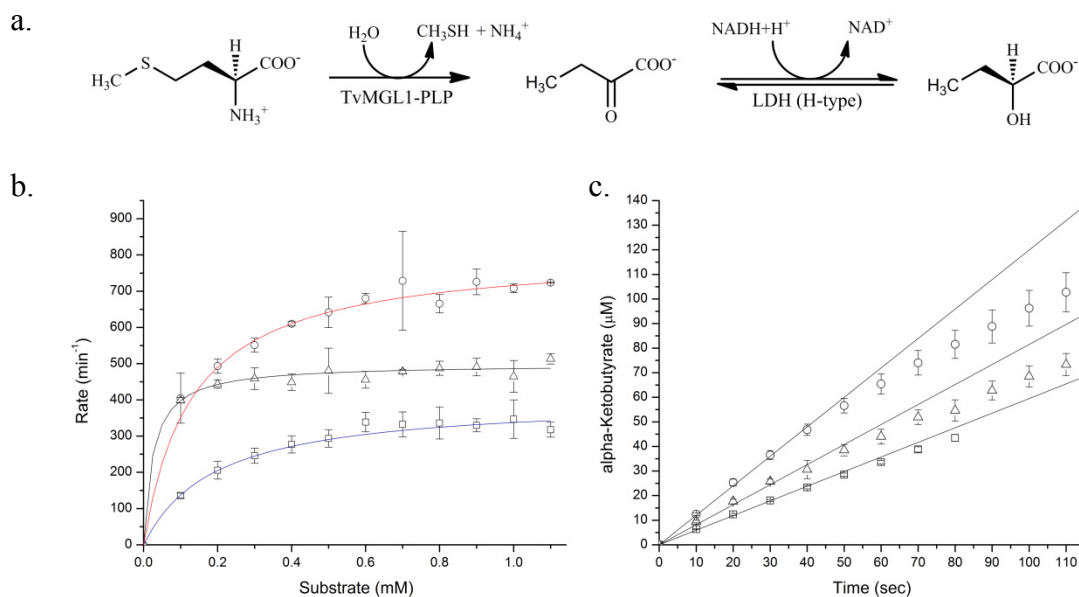


Figure 3.9. Michaelis-Menten kinetics and initial rates for the LDH coupled assay of TvMGL1 processing methionine and its fluorinated analogs.

a) The reaction overview of MGL and the LDH coupled reaction. **b)** The kinetic parameters for the turnover rate of methionine (squares), DFM (triangles) and TFM (circles) with standard errors from three independent experiments. **c)** The initial rates of the enzyme for 1.0 mM of substrate: methionine (squares), DFM (triangles) and TFM (circles) with standard error from three independent experiments.

3.5.4. Possible Modes of Inhibition of TvMGL1

The evidence presented so far suggested that the processing of fluorinated methionine analogs would generate thioacylating agents that have the potential to react with cellular nucleophiles as well as covalently modifying protein. For example, the processing of TFM by TvMGL1 would likely generate thiocarbonyl difluoride, which has the potential to thiocarbamoylate an amine or cross-link another amine on the surface of the protein (Figure 3.10a). Alternatively, the processing of DFM by TvMGL1 would generate thioformyl

fluoride, which has the potential to thioformylate only a single amine on the surface of the protein since only one fluorine atom is present (Figure 3.10b). Either one of the two scenarios might interfere with the activity of the enzyme or inactivate it. The possibility of this occurring in the LDH coupled assay was uncertain, because product inhibition might lead to the decrease in the initial rate of the enzyme after 80 sec upon processing of TFM or DFM (Figure 3.9c).

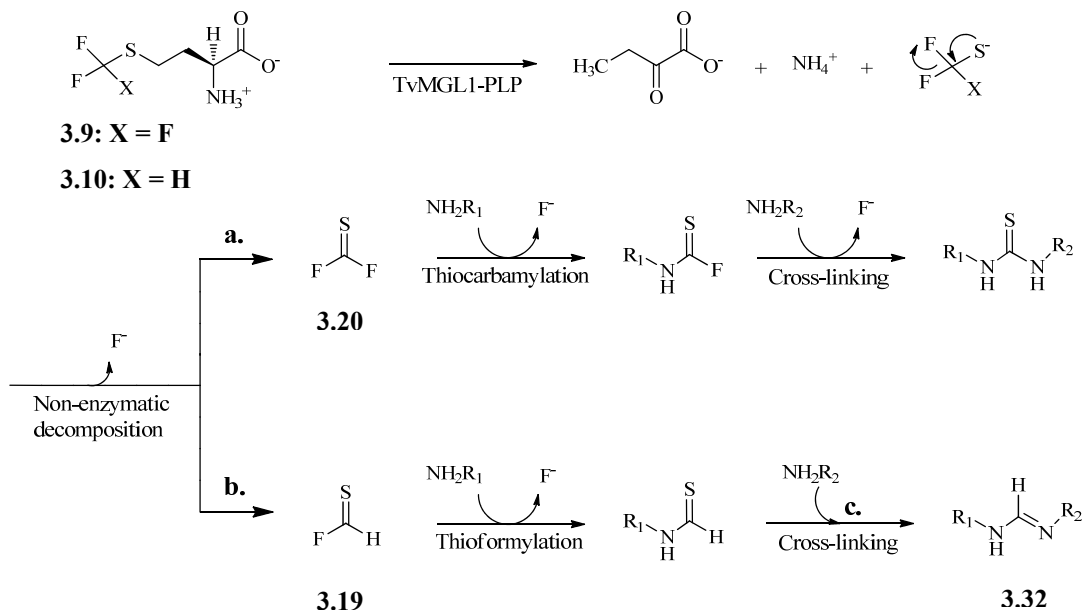


Figure 3.10. The proposed reaction scheme for the production of the thioacylating agents upon processing of the fluorinated methionine analogs by TvMGL1.

a) Thiocarbonyl difluoride (**3.20**) generated from the enzymatic processing of trifluoromethionine (**3.8**), and **b)** thioformyl fluoride (**3.19**) generated from the enzymatic processing of difluoromethionine (**3.9**), and potential chemical modification(s). **c)** The proposed cross-linking reaction for thioformyl fluoride (**3.19**) with a primary amine to afford an amidine (**3.32**).

Evidence for protein modification was examined by the extent of cross-linking of MGL, since the processing of DFM by MGL might lead to the sequential reaction of thioformyl fluoride with two primary amines. For this to occur, the sulfur atom in thioformyl fluoride would have to be eliminated as hydrogen sulfide upon reacting with two primary amines (Figure 3.10c). Precedent for this alternative reaction has indeed been observed for the decomposition of a thioformamide to an amidine (**3.32**; Figure 3.10) as a result of an excess of a primary amine (Moltzen *et al.*, 1987). To examine this possibility, an intermolecular cross-linking experiment was performed by incubating TvMGL1 with the substrate of choice (either methionine plus formaldehyde, DFM or TFM) for 30 min at 30°C. Aliquots for each of the reactions were loaded onto a SDS-polyacrylamide gel in order to visualize any changes in molecular weight of TvMGL1. The positive controls, formaldehyde and TFM (when processed by MGL) were selected for the experiment because they are known cross-linking agents (Metz *et al.*, 2004; Sato *et al.*, 2008). Incubation of TvMGL1 with formaldehyde, TFM or DFM followed by an SDS-PAGE analysis revealed the presence of higher molecular weight proteins than expected for TvMGL1 (Figure 3.11). Based on the integrated density values, the concentrations for the higher molecular weight proteins (~88 kDa) were 1.99 μ M, 199 nM and 225 nM for the samples treated with either formaldehyde, TFM and DFM, respectively. Importantly, samples containing methionine in place of the potential prodrugs resulted in no observable changes in the molecular weight of TvMGL1.

During the course of the cross-linking experiments, the appearance of a lower molecular weight band (~32 kDa) was observed for the samples treated with DFM and TFM (Figure

3.11), as reported in a cross-linking study for the processing of TFM by EhMGL (Sato *et al.*, 2008). However, further analysis of the cleavage product was not possible, as the protein fragment was either lost or failed to resolve during the subsequent chromatographic purification steps (*i.e.*, size exclusion, ion exchange and C8 chromatographic steps).

To provide further evidence that the thioacylating agents may lead to intermolecular cross-linking of the enzyme, attempts were made to reduce cross-linking by either inhibiting the enzyme or by scavenging any reactive intermediates with a nucleophilic compound included in the reaction buffer. Cysteamine was selected as a suitable candidate for this experiment because it is known to efficiently react with carbonyl groups (Miyake and Shibamoto, 1995) and with the free or bound PLP to produce a thiazolidine (De Marco and Bognolo, 1962). Therefore, protection against cross-linking might be achieved when cysteamine reacts with the electrophilic thioacylating agent or inactivates the enzyme upon sequestering PLP. Upon visualization of the SDS-polyacrylamide gel, the addition of cysteamine reduced the extent of intermolecular cross-linking for the samples treated with formaldehyde, TFM and DFM (Figure 3.11). These results strongly support the notion that the processing of TFM and DFM by TvMGL1 could produce a relatively low amount of cross-linked proteins as well, under the above experimental conditions.

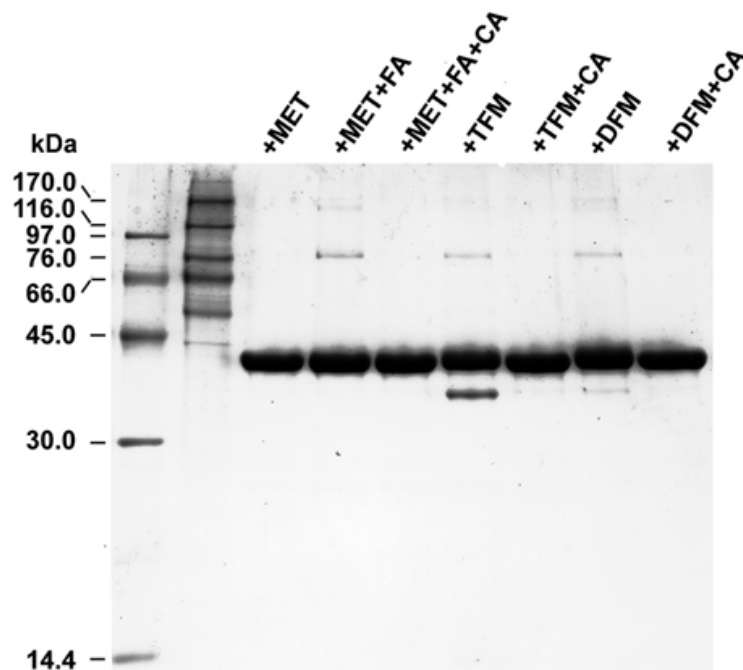


Figure 3.11. An SDS-polyacrylamide gel analysis of the intermolecular cross-linking of TvMGL1 with various compounds, and its inhibition with cysteamine *in vitro*.

The samples were loaded onto the SDS-polyacrylamide gel as follows: low molecular weight marker; high molecular weight marker; methionine (MET); methionine and formaldehyde (FA); methionine, formaldehyde and cysteamine (CA), TFM; TFM and cysteamine; DFM; and DFM and cysteamine.

3.5.5. Cellular toxicity of the Fluorinated Methionine Analogs in Organisms that Express TvMGL1

To examine the differences in the cytotoxic effects of TFM and DFM, the level of cell growth inhibition for an *E. coli* model system that expresses TvMGL1 was measured spectrophotometrically by following an earlier reported procedure (Coombs and Mottram, 2001). For this experiment, the *mg11* gene from *T. vaginalis* was cloned into an expression vector and overexpressed in *E. coli*. The transformed cells with the plasmid containing the

mgII gene were incubated with various concentrations of the fluorinated analogs, and the level of inhibition was measured relative to negative control (*i.e.*, cells untreated with the compound). The positive controls were conducted in the presence of either ampicillin and NaF as inhibitors since ampicillin is known to inhibit bacterial growth, and fluoride ion can inhibit certain enzymes such as acid phosphatase (von Hofsten, 1961a). As expected, ampicillin and an excess of NaF inhibited cell growth, while no effects were observed upon treatment with methionine (Table 3.5; Figure 3.12 b and a respectively). When the cells were treated with DFM and TFM, inhibition of cell growth was observed (an EC₅₀ value of ~20 µM for both compounds; Table 3.5; Figure 3.12 c and d respectively).

The negative control cells (lacking the *mgII* gene) were examined in order to correlate cell growth inhibition with the activation of the fluorinated methionine analogs by TvMGL1. Cell growth was inhibited when the cells were treated with either ampicillin or NaF, but not with DFM, TFM or methionine (Figure 3.12f). Overall, the fluorinated methionine analogs did not inhibit cell growth for *E. coli* cells lacking TvMGL1.

To determine if DFM was toxic to organisms that endogenously express MGL, the growth inhibitory effects of DFM (performed by our collaborators Westrop and Coombs, University Strathclyde, Glasgow, UK) was tested on *T. vaginalis*, an anaerobic pathogen that is known to contain high levels of MGL activity (Coombs and Mottram, 2001; Lockwood and Coombs, 1991). DFM was found to be active against this pathogen, approximately 20-fold less potent than the clinically approved drug, metronidazole (Table 3.5; Figure 3.12 e); and 2-fold less potent than the EC₅₀ value of DFM obtained in the *E. coli* model (Table 3.5).

Assuming that the transporter efflux between TFM and DFM in *T. vaginalis* did not significantly differ from the *E. coli* model, the growth inhibitory effects should reflect the potency of the compound between the two model organisms.

Table 3.5. The EC₅₀ values of various compounds for *E. coli* cells expressing TvMGL1 (*E. coli* model) and for *T. vaginalis*.

Species & Compounds	EC ₅₀ μM
<i>E. coli</i> model	
MET	0
TFM	21.7 ± 0.7
DFM	24.0 ± 0.9
Amp	0.498 ± 0.009
NaF	(19.3 ± 1.2) x10 ³
<i>T. vaginalis</i>	
Metronidazole	2.12 ± 6.08
DFM	40.1 ± 6.3
TFM*	ND

The standard errors for the *E. coli* model and *T. vaginalis* were obtained from three and two independent experiments, respectively. *Note, the MIC for TFM was reported to be 24.6 μM for a 24 h time period (Coombs and Mottram, 2001). ND, not determined.

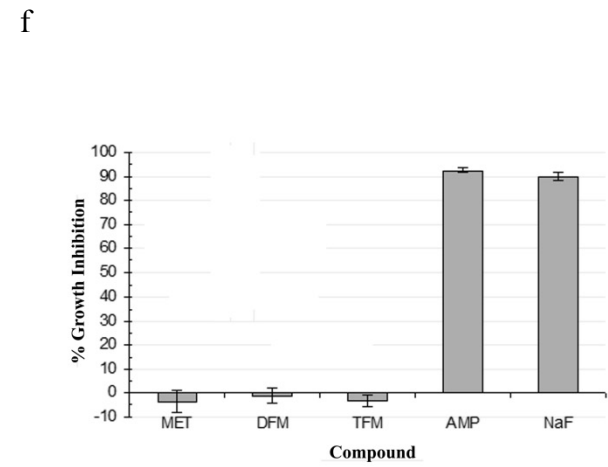
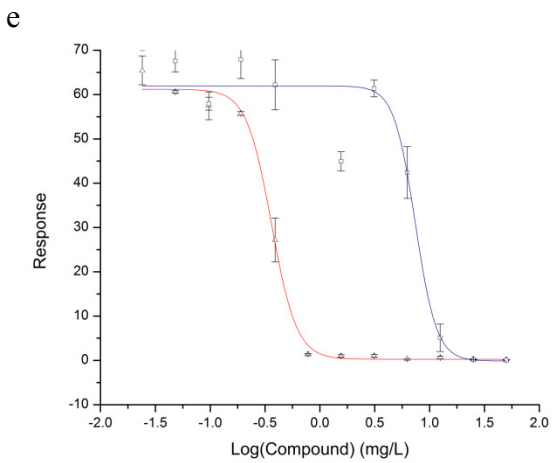
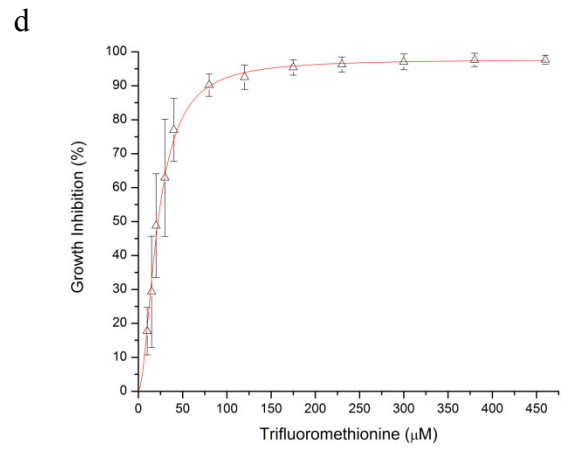
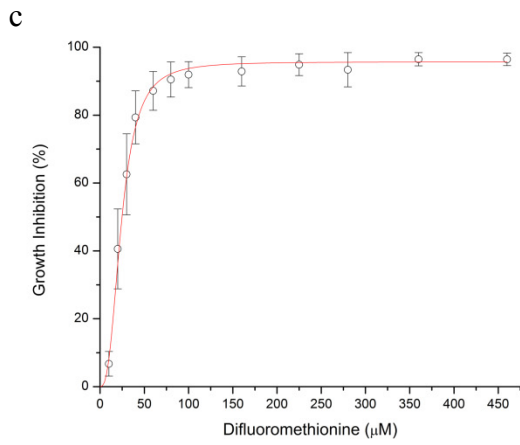
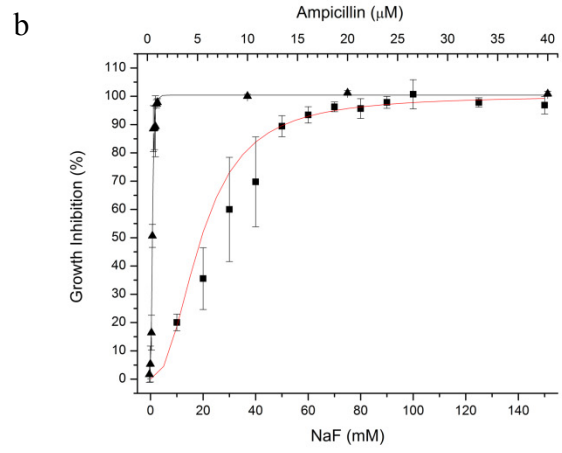
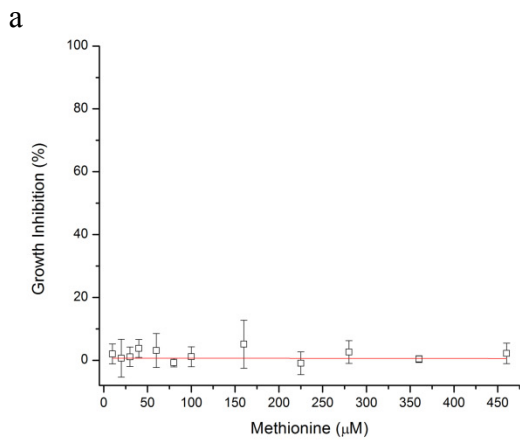


Figure 3.12. The growth inhibition of *E. coli* cells overexpressing MGL1 and control *E. coli* cells, and the growth response of *T. vaginalis*.

The *E. coli* cells overexpressing MGL1 were treated with **a)** L-methionine, **b)** ampicillin (triangles) and NaF (squares), **c)** DFM and **d)** TFM with standard error from three independent experiments. The EC₅₀ value for ampicillin was similar to the value reported for *E. coli* CCM 3988 (Jantova *et al.*, 1999). *T. vaginalis* were treated with **e)** metronidazole (triangles) and DFM (squares) with standard error from two independent experiments. The growth inhibition of *E. coli* cells that lacked TvMGL1 in the presence of the following compounds (left to right): 71 μM L-methionine, 71 μM DFM, 71 μM TFM, 2 μM ampicillin (AMP) and 52 mM NaF with standard errors from three independent experiments.

3.6. Discussion

¹⁹F-NMR studies demonstrated that TvMGL1 rapidly processed DFM as the ¹⁹F-NMR signals rapidly disappeared in the presence of enzyme (Figure 3.4d). The proposed intermediates, difluoromethanethiol and thioformyl fluoride were not observed by ¹⁹F-NMR, since the species were likely too short lived for the observable time frame of the experiments. Similar results were observed for the processing of TFM by TvMGL1, in which the fluorine nuclei signals were not observed for trifluoromethanethiol and thiocarbonyl difluoride by ¹⁹F-NMR spectrometry. In general, the processing of DFM and TFM by TvMGL1 was supported by the additional resonance that coincided with the fluorine nucleus of the fluoride ion, which was the final decomposition product.

¹⁹F-NMR studies on the PLP model system indicated a lack of a fluorine signal for the proposed fluorinated mercaptans and thioacylating agents produced from the processing of DFM and TFM by MPAL (Figure 3.8). Extending the model to the intact enzyme, the results

would suggest that the intermediates were extremely short lived and were undetectable under the basic methanol reaction conditions, and consistent with the ^{19}F -NMR results for the intact enzyme, TvMGL1 (Figure 3.6). The detection of the likely intermediate, 4-morpholino thiocarbonyl fluoride suggested that the thioacylating agent, thiocarbonyl difluoride was generated from the processing of TFM by MPAL as well as the intact enzyme, TvMGL1 (Figure 3.8).

The notion that the above reactive intermediates were too short lived to be observed was consistent with the thiols existing as thiolates based on the calculated pK_a values, and the anionic hyperconjugation and electrostatic effects that favour their decomposition to the thioacylating agents (Schneider *et al.*, 1995). The observed reactivity of the thioacylating agents supported the calculated heats of reaction (Table 3.2), in which nucleophilic attack on the thioacylating agents by water or amines is a thermodynamically favourable process. This would explain the production of fluoride ion as observed by ^{19}F -NMR (Figure 3.4), and previous reports on the instability of trifluoromethanethiolate and thiocarbonyl difluoride (Alston and Bright, 1983; Coombs *et al.*, 2004; Jellinek, 1959).

The incompatibility of the derivatizing agent, MBTH with DFM in the presence of TvMGL1 led to the development of an LDH coupled assay. For the turnover of methionine by TvMGL1, the kinetic parameters obtained from the assay were consistent with the values obtained by utilizing the MBTH assay (McKie *et al.*, 1998). For the processing of TFM, the k_{cat} for TvMGL1 was ~6-fold greater than the previously reported activity of a MGL1/MGL2 mixture from *T. vaginalis*, and with similar K_m values, which were obtained by utilizing the

MBTH assay method (Coombs and Mottram, 2001). These differences in catalytic activity were likely to have arisen from the differences in kinetic parameters between the two MGL isozymes as reported for the turnover of methionine (McKie *et al.*, 1998). Additionally, its catalytic activity was comparable to *E. histolytica* EhMGL 2 enzyme, and its K_m value was similar to EhMGL 1, both of which were obtained utilizing the MBTH method (Sato *et al.*, 2008). For the processing of DFM by an MGL enzyme, to our knowledge, this is the first report of its kinetic values.

The correlation between increasing fluorination of the compound and increasing rate of reaction (i.e., TFM > DFM > methionine) would suggest that the inductive effect and anionic hyperconjugation of the fluorinated methyl thiolates improve its leaving ability. This is consistent with the idea that the C-S bond cleavage is a rate determining step of the enzyme as reported by a $^1\text{H-NMR}$ study on MGL from *Pseudomonas putida* (Esaki *et al.*, 1977).

The activity of the enzyme does not appear to be compromised as a result of the increase in volume for each fluorine atom in the fluorinated methionine analogs (19% for the trifluoromethanethio group and 12% for the difluoromethanethio group relative to the methanethio group) (Houston *et al.*, 1997). Additionally, the enzyme appears to favour the enzyme-substrate complex for DFM over methionine as indicated by the 10-fold difference in K_m value, despite its bulky substitution. On the other hand, TFM has in a similar K_m value as methionine, which suggests that the bulkier substitution do not enhance the enzyme-substrate complex (Table 3.4). Overall, the processing of DFM by TvMGL1 is catalytically more efficient than TFM and methionine (Table 3.4).

The processing of the fluorinated methionine analogs by TvMGL1 likely inactivated some molecules of the enzyme as a result of covalent modification. This was supported by a similar finding for the processing of TFM by MGL from *E. histolytica* (EhMGL) (Sato *et al.*, 2008), intermolecular cross-linking of TvMGL1 (Figure 3.11), the thioacylating agent reacting with a restrained secondary amine in the PLP model system (Figure 3.6 and Figure 3.7), and the thermodynamically favourable process of the thioacylating agent reacting with nucleophiles such as the side chains of lysine residues on the surface of the protein or water (Table 3.2). It is tempting to extrapolate the data for the amount of cross-linked dimers to explain the apparent decrease in the initial rate for the LDH coupled assay after 60 sec, i.e., 6.6 nM and 7.5 nM of cross-linked homodimeric enzymes for the enzymatic processing of TFM and DFM, respectively (Figure 3.9c). However, caution should be exercised when applying quantitative values to other experiments such as the LDH coupled assay and the cell inhibition assay, because of differences in protein concentration, quantities of cross-linking agent and potential side reactions. More importantly, the rate of protein cross-linking is expected to be influenced by a variety of factors such as proximity effects, number of collisions, amount of cross-linking agent and competing side reactions (*e.g.*, dimer or monomer form of MGL, concentration of macromolecules and the amount of competing water molecules for the cross-linking agent). Therefore, cross-linking is expected to be higher within the crowded cellular cytoplasm such as the cell inhibition assay (an estimated concentration of 300-400 g/l of protein and RNA inside *E. coli*) (Ellis, 2001). On the other hand, cross-linking is expected to be lower in dilute solutions such as the LDH coupled assay

(4.4×10^{-3} g/l of TvMGL1 and 0.15 g/l of LDH) and the cross-linking experiment (0.88 g/l of TvMGL1).

In the PLP model system, analysis of the results suggests that the processing of DFM and TFM by MPAL leads to the production of thioformyl fluoride and thiocarbonyl difluoride, respectively. Therefore, it was very likely that these intermediates were generated during the course of the enzymatic reaction, since MPAL is known to follow the same γ -elimination reaction steps as MGL in the turnover of methionine (Johnston *et al.*, 1981; Karube and Matsushima, 1977). Thus, thioformyl fluoride has the potential to thioformylate an amine, while thiocarbonyl difluoride has the potential to sequentially thiocarbamoylate two amines.

The model proposed above did not rule out the possibility that thioformyl fluoride might sequentially react with two amines to produce an amidine with the elimination of the sulfur atom as hydrogen sulfide (Figure 3.10c). Evidence for the latter proposal is supported by the intermolecular cross-linking of TvMGL1 for the enzymatic processing of DFM (Figure 3.11). The results suggest that upon processing of DFM by TvMGL1, the enzyme (~44 kDa) is cross-linked to an adjacent subunit to form a covalently linked dimer (~88 kDa), which is similar to the cross-linking pattern observed for the two positive controls (formaldehyde and TFM). The enzymatic processing of DFM leads to two faint, higher molecular proteins on the gel that correspond to cross-linked trimers (~132 kDa) and tetramers (~176 kDa), which is consistent with the cross-linking pattern for the positive control (formaldehyde). The intermolecular cross-linking results were unexpected since the release of thioformyl fluoride was expected to react with only a single lysine. Overall, the additional finding remained

consistent with the idea that basic side chain residues on the surface of the enzyme are susceptible to covalent modification following the processing of the fluorinated methionine analogs by MGL. The different modes of covalent modification described in this paper suggest that there are likely a variety of cytotoxic and/or inhibitory events taking place within the organism expressing MGL.

In the *E. coli* model system, the quantity of the fluorinated methionine analog required to inhibit 50% of cell growth was two-fold greater than the values obtained for the intact parasites, *T. vaginalis* in a 24 hr time period (reported here; Table 3.5) and *E. histolytica* 72 hr time period (Tokoro *et al.*, 2003). This might indicate that there were some limitations to using the *E. coli* model when compared to intact parasite studies, such as the differences in their metabolism (see below). Overall, the model system provides a facile and safer screening method for testing potential compounds before further evaluating the compound on MGL-containing organisms, such as *T. vaginalis*, *E. histolytica* and *Porphyromonas gingivalis*.

For the processing of the fluorinated methionine analogs by MGL, the reaction of the thioacylating agent with cellular macromolecules was likely the mode of cellular toxicity, given the evidence supporting its existence in this study. In the *E. coli* model, it was unlikely that cellular toxicity arisen from the release of the fluoride ion upon hydrolysis from the thioacylating agent; since a high concentration of NaF was required to inhibit *E. coli* growth (Table 3.5), which was consistent with a previous study (von Hofsten, 1961a). In a similar study, cell growth is not inhibited when intracellular fluoride is released upon induction of β -galactosidase by fluoro β -D-galactoside (which is known to hydrolyze intracellularly to

fluoride ion) does not inhibit cell growth in *E. coli* (von Hofsten, 1961b). In *T. vaginalis*, the release of toxic H₂S upon hydrolysis of thiocarbonyl difluoride as reported by Careless *et al.* (1973) is not likely to inhibit cell growth; since the anaerobic parasitic protozoa lacks the cellular target, cytochrome oxidase (Muller, 1988); and MGL is implicated in generating H₂S from homocysteine for cysteine biosynthesis (Sato *et al.*, 2008; Westrop *et al.*, 2006). On the other hand, H₂S may inhibit the growth in *E. coli* since the organism contains cytochrome oxidase (Savage, 1977).

In summary, a detailed investigation of the enzymatic processing of fluorinated methionines was undertaken, providing insight into the mechanistic aspects of substrate and inhibitor turnover by this key protozoan enzyme. Trapping of the resulting reactive compounds (the thioacylating agents) provides, for the first time, chemical knowledge of the structure and reactivity of these compounds. The toxicity of these compounds were further studied in intact *E. coli* and *T. vaginalis*, and provide further impetus to the exploration of these fluorinated structural types to other areas of cellular biochemistry.

3.7. Materials and Methods

3.7.1. Materials

Biological reagents and chemicals were purchased from Bioshop and Sigma Chemicals respectively, unless otherwise stated. The cell line, M15pREP4 *E. coli* that contains the gene

encoding *mgl1* from *Trichomonas vaginalis* was a gift from Dr. G. Coombs (University Strathclyde, Glasgow, UK).

3.7.2. Protein Purification

The recombinant enzyme, TvMGL1 was purified from M15pREP4 *E. coli* as described by McKie *et al.* (1998) with some minor changes. Following the purification of the enzyme from the Ni²⁺-NTA superflow resin (Qiagen), the enzyme (1 mL) was dialyzed (4 x 1 L) against buffer (100 mM sodium phosphate buffer at pH 7.8, 10 mM EDTA, 0.2 M NaCl, 4 mM DTT and 100 μ M PLP), over a period of 15 hr at 4°C. The samples were concentrated to 25 mg mL⁻¹ with a 10k MWCO centrifuge tube (Sartorius Stedim Biotech & Corning), flash frozen in liquid nitrogen and stored at -80°C for future use (stable for more than a month). Total amount of enzyme obtained from 1 L culture was 15 mg.

ESI-MS calculated for TvMGL1 was 43 960.47, observed 43 957.5 \pm 4.4.

3.7.3. MBTH Assay Method for Detecting α -Ketobutyrate

The activity of MGL was initially monitored by utilizing the MBTH assay as previously reported (Soda, 1968) . The reaction mixture (50 μ L) consisted of 60 mM HEPES-NaOH, pH 8.0, 20 μ M PLP, 2 mM DTT, 0.1 to 4.0 mM substrate, and 0.5 μ M TvMGL1. All other procedures were followed as described in section 2.6.7.

3.7.4. Michaelis-Menten Kinetics

In the LDH coupled assay, the reaction mixture (300 μ L) consisted of 60 mM HEPES-NaOH, pH 8.0, 5.0 Units LDH porcine heart (Calbiochem; Cat# 427211), 400 μ M NADH (Sigma-Aldrich; extinction coefficient of 6.22 $\text{mM}^{-1} \text{cm}^{-1}$) (Dawson, 1985), 0.1 μ M TvMGL1, 10 μ M PLP, and 0.1-1.2 mM substrate. The reaction was incubated for 2 min at 37°C on a 96 well plate (Greiner Bio One) and initiated with the addition of TvMGL1. The data was collected with a Spectramax M5 plate reader (Molecular Devices Corporation, Sunnyvale, CA), and the kinetic values were determined with Microcal™ Origin® v6.0 (Microcal Software, Northampton, MA) using the Michaelis-Menten equation. In the presence of pyruvate, 1 Unit of LDH will oxidize 1 μ mole NADH per min at 25°C, pH 7.4, as reported by the manufacturer (Calbiochem). In the presence of α -ketobutyrate, 0.1 Unit of LDH will oxidize >0.02 μ mole NADH per min at 37°C, pH 8.0.

3.7.5. ^{19}F -NMR Experiments

The processing of TFM and DFM were detected by ^{19}F -NMR and ^1H -decoupled ^{19}F NMR, respectively using a 600 MHz NMR (Bruker) spectrometer. The reaction mixture consisted of 20 μ M PLP, 30 mM HEPES-NaOH, pH 7.2, 4.2 mM substrate and 10% (v/v) D_2O . The reactions were performed at 25°C and initiated with the addition of 0.50 μ M TvMGL1. The ^{19}F -NMR data (externally locked with CFCl_3) δ : -93.3 ppm for DFM, -41.4 ppm for TFM and -119.8 ppm for fluoride anion.

3.7.6. Theoretical Calculation of the ^{19}F -NMR Chemical Shifts

The ^{19}F NMR shielding constants were calculated at the Hartree-Fock level (HF/6-311+G(d,p)//B3LYP/6-31G(d)) gauge-invariant atomic orbitals (GIAO), Møller-Plesset theory (MP2/6-311++G(2d,p)//B3LYP/6-311++G(2d,p)) GIAO, and the density functional theory (DFT/B3LYP/6-31+G(df,p)//B3LYP/6-31+G(df,p)) GIAO levels (Ditchfield, 1974). An IR frequency check was performed in order to ensure the lowest ground state structures were utilized, and the theoretical chemical shifts were referenced to CFCl_3 . Spartan '08 and Gaussian '03 were utilized for these calculations (Frisch *et al.*, 2003b; Shao *et al.*, 2006)

3.7.7. Theoretical Calculations of the Heats of Formation

The G3(MP2) theory, based on MP2(full)/6-31G(d) geometries using all electrons, has an overall average absolute deviation of 1.02 kcal/mol for a set of 299 organic molecules (Curtiss *et al.*, 1999). The reference energy is calculated with accurate quadratic configuration interaction (QCISD(T)/6-31G(d)), and is then modified by a series of corrections to obtain a total energy, E_0

$$E_0[\text{G3(MP2)}] = \text{QCISD(T)/6-31}(d) + \Delta E_{\text{MP2}} + \Delta E(\text{SO}) + E(\text{HLC}) + E(\text{ZPE}) \quad (1)$$

$$\text{Where } \Delta E_{\text{MP2}} = [E(\text{MP2/G3MP2large})] - [E(\text{MP2/6-31G(d)})] \quad (2)$$

The energy corrections in Eq. (1) consist of an equilibrium geometry correction (ΔE_{MP2}), spin-orbit corrections ($\Delta E(\text{SO})$) for atomic species only, zero-point corrections ($E(\text{ZPE})$) are

obtained from scaling harmonic frequencies by 0.8929, “higher level correction” (HLC) for open shell molecules and for atoms (Curtiss *et al.*, 1998; Curtiss *et al.*, 1999).

The T1 recipe is similar to the G3(MP2) recipe, except that the geometry optimization with MP2/6-31G* basis set is replaced by the use of a HF/6-31G* basis set, the MP2/G3MP2large energy is approximated with the dual basis set RI-MP2 techniques, and QCISD(T) calculations and zero-point corrections are removed from the recipe (Ohlinger *et al.*, 2009). The T1 procedure reduces the computation time by 2-3 orders of magnitude when compared to the G3(MP2) recipe. The heats of formation are reported to reproduce the values with a mean absolute error of 8.5 kJ/mol for a set of 1805 diverse organic molecules (Ohlinger *et al.*, 2009).

3.7.8. Theoretical Calculation of the pK_a Values for the Thiol Compounds

The pK_a values for the thiols were calculated using the Jaguar v4.1 pK_a module (Schrödinger Inc), which involved geometry optimization for the protonated and deprotonated species at the HF/B3LYP/6-31G* level of theory, accurate single point energies for the species at the DFT/cc-pVTZ(+) level of theory, and the computation of the solvation free energy of the gas phase geometry optimized species. The theoretical pK_a values for the reference compounds CH₃SH (10.6), CH₃CH₂SH (10.6) were similar to the reported literature values (10.3 and 10.6 respectively); and HOCH₂CH₂SH (10.2) and HSCH₂CH₂SH (10.2) where ~1 pK_a greater than the literature pK_a values (9.4 and 9.1 respectively).

3.7.9. Cross-linking of MGL Protein Upon Processing of Fluorinated Analogs

For the MGL intermolecular cross-linking experiments, the reaction mixture (50 μ L) consisted of 100 mM HEPES-NaOH, pH 8.0, 5.0 mM EDTA-NaOH at pH 8.0, 4.2 mM of the fluorinated methionine analog (or 4.2 mM methionine in the presence or absence of 40 mM formaldehyde), and 20 μ M TvMGL1. The reactions were quenched by the addition of 2-fold loading buffer [100 mM Tris, pH 6.8, 2% (v/v) β -mercaptoethanol, 4% (v/v) SDS, 0.2% (w/v) bromophenol blue, 20% (v/v) glycerol], and 10 μ L aliquots from the reaction mixture were resolved on a 13% (w/v) SDS-polyacrylamide gel at 200 volts. For the inhibition of cross-linking of MGL, a final concentration of 50 mM cysteamine at pH 8.0 was added to the reaction mixture. The integrated density value for the stained protein bands were calculated with AlphaEase[®]FC software v6.0 (Alpha Innotech Corporation; San Leandro, CA, USA).

3.7.10. Model Processing of Fluorinated Analogs

For the PLP model system, 1.0 mM of the fluorinated methionine analog and 0.10 mM MPAL were incubated in a 2.0 mM KOH/methanol solution for 1 hr at 21°C. Afterwards, a final concentration of 0.10 mM Al(NO₃)₃ and 900 mM morpholine were added sequentially to the reaction mixture, and incubated for 15 hr at 21°C. The product of the TFM reaction was extracted with ethyl acetate and dried under vacuum, while the DFM reaction was extracted with CHCl₃. The extracted products for the DFM and TFM were developed by TLC with CH₂Cl₂ and ethyl acetate/ethanol (4:1 ratio), respectively, visualized at 320 nm and

with iodine stain, and compared to the authentic standards. The yields for 4,4'-thiocarbonyldimorpholine and fluoride based on NMR spectroscopy were 50% and 82%, respectively for the processing of TFM (Table 3.3). The yields for 4-thioformylmorpholine and fluoride, based on NMR spectroscopy, were 16% and 83%, respectively for the processing of DFM (Table 3.3).

3.7.11. Syntheses

The synthesis of the fluorinated methionine analogs was adapted from previously reported procedures (Houston and Honek, 1989; Tsushima *et al.*, 1990). In a 3-neck round bottom flask fitted with a dry ice/acetone condenser, L-homocystine (3.8 mmol, 1.0 g) was stirred in liquid ammonia (50 mL) at -75°C, and the disulfide bonds were reduced with a slight excess of sodium metal (until a purple color remained for 20 min). The reaction was carefully quenched by the addition of ammonium chloride until the sodium metal was completely reduced, and liquid ammonia was evaporated off. Potassium *t*-butoxide solution (17.8 mmol, 2.00 g) in deoxygenated ethanol (15 mL) was added dropwise to the mixture over a period of 30 min. Chlorodifluoromethane or iodotrifluoromethane (under UV-light) was bubbled into the solution for 2 hr to yield DFM or TFM, respectively. The reaction was allowed to stand at 21°C for 15 hr, and quenched with concentrated HCl to a pH of 7. The white solid was suspended in methanol (30 mL) and the inorganic salts were removed by filtration. The fluorinated methionine analogs were purified with a RediSep C₁₈ reverse phase column

(Teledyne Isco, Lincoln, NE; water/acetonitrile, 10:1). The spectroscopic properties were in complete agreement with those previously published (Houston and Honek, 1989).

The synthesis of 4,4'-thiocarbonyldimorpholine was performed as described by Beerheide *et al.* (2000). Briefly, morpholine (1.0 mmol, 90 μ L) and triethylamine (0.50 mmol, 70 μ L) were added to a solution of 1,1'-thiocarbonyldiimidazole (0.50 mmol, 89 mg) in CH_2Cl_2 (1 mL) at 4°C with stirring. The reaction was warmed up to 21°C, which turned pale orange after 3 hr, and quenched with brine (4 mL) after 4 hr. The organic layer was combined, dried over magnesium sulphate, filtered, and purified by silica gel chromatography.

4,4'-Thiocarbonyldimorpholine was obtained as an oil (54 mg, 50%). R_f (ethyl acetate/hexane, 1:1) 0.39. $^1\text{H-NMR}$ (CDCl_3) δ : 3.59 (t, $J = 4.9$ Hz, 8H), 3.72 (t, $J = 4.9$ Hz, 8H). MS-ESI calculated for $\text{C}_9\text{H}_{17}\text{N}_2\text{O}_2\text{S}^+$ $[\text{M}+\text{H}]^+$ 217.10121 found 217.0899.

The synthesis of 4-thioformylmorpholine was performed as described by Mills (1986). Briefly, a mixture of *N,N'*-dimethyl thioformamide (1.50 mmol, 150 mg) and morpholine (1.50 mmol, 130 μ L) in toluene (5 mL) was contained in a three-neck, 25 mL round bottom flask with an Ar inlet tube, water-cooled condenser, magnetic stirring bar, and refluxed at 115°C for 15 hr. The sample was concentrated *in vacuo* and purified by silica gel chromatography.

4-Thioformylmorpholine was obtained as a light brown solid (118 mg, 60%): mp 67-67.5°C (lit. 67-68°C) (Mills, 1986). R_f (ethyl acetate/ CH_2Cl_2 , 1:4) 0.34. $^1\text{H-NMR}$ (C_6D_6) δ : 2.33 (t, $J = 4.9$ Hz, 2H), 2.80 (t, $J = 4.9$ Hz, 2H), 3.03 (t, $J = 4.9$ Hz, 2H), 3.61 (t, $J = 4.9$ Hz, 2H), 8.76 (s, 1H). MS-ESI calculated for $\text{C}_5\text{H}_{10}\text{NOS}^+$ $[\text{M}+\text{H}]^+$ 132.04840 found 132.0432.

The synthesis of MPAL was adapted from procedure previously reported (Heyl *et al.*, 1951; Johnston *et al.*, 1981). Briefly, pyridoxal hydrochloride (4.9 mmol, 1.0 g) was dissolved in anhydrous methanol (6.25 mL), which was contained in a three-neck, 500 mL round bottom flask with a water-cooled condenser, magnetic stirring bar, and refluxed at 60°C for 15 min. The solution was cooled and sodium bicarbonate (5.0 mmol, 0.42 g) was added to the mixture, and refluxed for an additional 1.5 hr. The sodium chloride precipitate from the cooled solution was filtered and washed with anhydrous methanol (4 mL). Benzene (200 mL) and methyl iodide (240 mmol, 15.0 mL, very toxic) were added sequentially to the methanol solution, which was contained in a three-neck, 500 mL round bottom flask with a water-cooled condenser, magnetic stirring bar, and refluxed in the dark at 60°C for 15 hr. The solution was distilled to dryness as a yellow residue in a water bath *in vacuo*, and crystallized from methanol-ether to afford pyridoxal monomethylacetal iodide (950 mg, 60%). Pyridoxal monomethylacetal iodide (1.4 mmol, 0.45 g) was dissolved in water (7 mL), and silver chloride (1.70 mmol, 250 mg) was added with stirring for 2 hr in the dark at 21°C. The mixture was filtered, titrated to pH 2.0 with 1N HCl, evaporated to dryness *in vacuo*, and crystallized from water-acetone.

N-Methyl pyridoxal chloride was obtained as white crystals (107 mg, 35%): decomp. 120°C (lit. 120°C) (Heyl *et al.*, 1951). ¹H-NMR (D₂O) δ: 2.60 (s, 3H), 4.16 (s, 3H), 5.19 (dd, J = 47.0, 13.8 Hz, 2H), 6.66 (s, 1H), 8.13 (s, 1H). MS-ESI calculated for C₉H₁₂NO₃⁺ [M]⁺ 182.08176 found 182.0847.

3.7.12. Cloning of *mgll* into the pET28b Vector and Cell Inhibition Assay

The *mgll* gene from the pMGL4100 plasmid was cloned into the pET28b vector (Novagen, Madison, WI) at the *NcoI* and *XhoI* sites with the appropriate restriction enzymes (NEB). The gene was amplified by overlap extension PCR with Pwo SuperYield DNA polymerase (Roche Applied Science, Indianapolis, IN), which replaced an internal *XhoI* site with a non-degenerate codon, and introduced a linker sequence at the C-terminus of the sequence. The primer pair (Invitrogen, Burlington, ON) termed “MGL1 forNcoI” (5’-GATATACCATGG-CGCACGAGAGAATGAC-3’) and “MGL1 revC222G” (5’-TTCTGTTTTCTCCAG-GAAGGCGATCTTGC-3’) generated the N-terminal fragment, which introduced the *NcoI* restriction site (underlined) and non-degenerate codon (lower case letter), respectively. The primer pair termed “MGL1 forC222G” (5’-ATCGCCTTCCTgGAGAAAACAGAAAGC-ATG-3’) and “MGL1 rev1aTHB” (5’-cacgtggcaccagacctAAAA-GAGCGTCAAG-3’) generated the C-terminal fragment, which introduced the non-degenerate codon (lowercase letters) and linker region (lower case lettering and underlined), respectively. The N-terminal fragment and C-terminal fragment were combined and amplified with the primer pair termed “MGL1 forNcoI” and “MGL1 rev1bXhoI” (5’-GTAAATCTCGAGgctaccacgtggcaccagac-3’), which introduced the *XhoI* site (uppercase lettering and underlined) and the linker region (lowercase letters and underlined); and thereby, generating the ORF of *mgll*. Amplification of the PCR products was carried out under the following conditions: denatured at 95°C, 1’; 18 cycles (95°C, 1’; 63°C, 1’; 72°C, 1’45”); and 11 cycles (95°C, 1’; 63°C, 1’; 72°C, 1’ 35”) and 72°C, 5’. The PCR products were recovered using a Silica Bead DNA Gel Extraction Kit

(Fermentas, Hanover, MD). The PCR products and the pET28b vector were double digested with *NcoI* and *XhoI* restriction enzymes (NEB, Ipswich, MA), purified using the Silica Bead DNA Gel Extraction kit, and ligated with T4 DNA ligase (NEB). The ligation mixture was transformed into electrocompetent XL-1 Blue cells (Stratagene, La Jolla, CA) and selected on Luria Bertani (LB)-agar media with 35 mg/L KAN. The plasmids with the insert were purified from the transformed cells using a QIAGEN miniprep kit (QIAGEN, Valencia, CA), and then transformed into electrocompetent BL21 (DE3) cells (Stratagene). The gene sequence for the MGL1 construct was verified by DNA sequencing (DNA Sequencing Facility, Department of Biology, University Waterloo, Waterloo, ON).

In the cell growth inhibition assay, the BL21 (DE3) cells (Stratagene) containing the recombinant MGL (as described above) were grown overnight at 37°C in the presence of 35 mg/L KAN, inoculated into 10 mL LB media (2×10^6 cells/ml) containing, 35 mg/L KAN and induced with 0.1 mM IPTG for 30 min at 37°C with shaking. The cells were diluted two-fold in a 96 well plate (Falcon), which contained 35 mg/L KAN, 0.1 mM IPTG and the compound of interest. The plate was sealed with a gas permeable tape, the cells were grown at 37°C, and the readings were taken at 600 nm when the negative control cells (in the absence of the compound) reached an optical density of 0.15 to 0.16. The percent growth inhibition for each compound was normalized to the uninhibited growth of the negative control cells. The EC₅₀ values of the compounds were determined with Microcal™ Origin® v6.0 using the Hill equation.

In the growth inhibition of *T. vaginalis*, the procedures were followed as described by McMillan et al (2009). Briefly, the cells were diluted by two-fold in a 96 well plate (to a final concentration of 10^5 cells/ml) in Modified Diamond's medium with 10% (v/v) heat inactivated horse serum and the compound of interest. The plates were sealed with a gas permeable tape and incubated for 18 to 22 hrs at 37°C in a humidified box. Aliquots were transferred to a black, 96-well luminometer plate and luminescence was measured with Cell Titer-Glo[®] Assay (Promega). The EC₅₀ values were determined with Microcal™ Origin[®] v6.0 using the standard dose-response equation

$$y = A_1 + \frac{A_2 - A_1}{1 + 10^{\log(EC_{50} - x)n}}$$

Where A_1 is the lowest value, A_2 is the highest value, x is the concentration of compound and n is the Hill slope.

CHAPTER 4

SYNTHETIC ROUTES TO 3,3-DIFLUORO-O-METHYL-L-HOMOSERINE

4.1. Authors' Contributions

Dr. G. Coombs provided the *mgll* gene from *Trichomonas vaginalis* G3. Dr. R. Smith obtained the ESI-MS data for the enzyme and reported compounds. C. Myers obtained the ESI-MS data for *O*-methyl-L-homoserine. Q. Bhatti synthesized compound **4.45**, and performed the fluorination of the model β -ketoester with Xtalfluor E and compound **4.35a** under the guidance of I. Moya. Q. Bhatti and I. Moya synthesized compounds **4.35a** and **4.35b**. All other work reported here was performed by I. Moya. Dr. J. Honek conceived the project.

4.2. Introduction

A C(sp³)-F bond has an average energy of approximately 105 to 116 kcal mol⁻¹, which makes it one of the strongest covalent bonds available in organic chemistry (Berkowitz *et al.*, 2008). In combination with fluorine's low polarizability, these properties are ideal for protecting labile sites within a compound against metabolic processes (O'Hagan, 2008). These properties stem from the fact that fluorine is the most electronegative element in the periodic table; and therefore, has the greatest propensity to attract electron density (O'Hagan, 2008). Thus, introducing a C-F bond alters the physical and chemical properties of an organic

compound, which is useful for the development of biologically active compounds (Berkowitz *et al.*, 2008).

Another application of a C-F bond is in nuclear medicine, where radioactive isotope fluorine-18 is incorporated into a cell specific marker in order to serve as an imaging agent in the diagnosis of diseases (Vallabhajosula, 2007). The naturally stable isotope fluorine-19 has been applied to substrate binding and/or changes in enzyme conformation by ^{19}F -NMR as a result of the sensitivity of fluorine's nuclei to small changes in the microenvironment of the protein (Danielson and Falke, 1996). The method is also useful in monitoring the activity of an enzyme, and to obtain accurate IC50 values for drug candidates (Papeo *et al.*, 2007). In a similar ^{19}F -NMR study, fluorinated L-amino acids have been incorporated into enzymes in order to correlate the chemical shifts of the fluorine nuclei to the conformational changes of the enzyme alone and upon binding of the ligand, such as the reported studies of trifluoromethionine and difluoromethionine incorporation into lambda lysozyme, and 5-fluoroleucine incorporation into dihydrofolate reductase (Dewel *et al.*, 1997; Dewel *et al.*, 2001; Feeney *et al.*, 1996; Vaughan *et al.*, 1999). Thus, ^{19}F -NMR is a sensitive tool to monitor the chemical shifts of the fluorine nuclei upon perturbation of the protein's microenvironment, which may serve as a probe to study structure and dynamics of enzymes.

4.3. Chemical Properties of the Fluorine Atom

Even though fluorine has a similar size as a hydroxyl group (a van der Waals radii of 1.47 Å and 1.57 Å, respectively), the two atoms nevertheless possess important differences (O'Hagan and Rzepa, 1997). In comparison to the hydroxyl group, the electrostatic influence of fluorine is weaker because of its very high polarizability volume (units of Å³ atom⁻¹) and electronegativity (Nagle, 1990). Based on high level theoretical calculations at the MP2 level of theory, there is a reduction in strength for hydrogen bonding of the fluorine atom to water (O'Hagan and Rzepa, 1997). For example, the F···H hydrogen bond between fluoromethane (CH₃F) and a water molecule has a calculated strength of 2.38 kcal mol⁻¹ (a distance of 1.9 Å); while an O···HO hydrogen bond for a methanol-water interaction has a strength of 4.48 kcal mol⁻¹ (a distance of 1.942 Å), and an O···HO hydrogen bond for a water-methanol interaction has a strength of 5.15 kcal mol⁻¹ (a distance of 1.90 Å; Figure 4.1) (Fileti *et al.*, 2004; Howard *et al.*, 1996). Thus, fluorine acts as a poor hydrogen bond acceptor when compared to the hydroxyl group; and in most cases, such a substitution reduces the binding affinity and/or turnover of the analog by the target enzyme (Howard *et al.*, 1996).

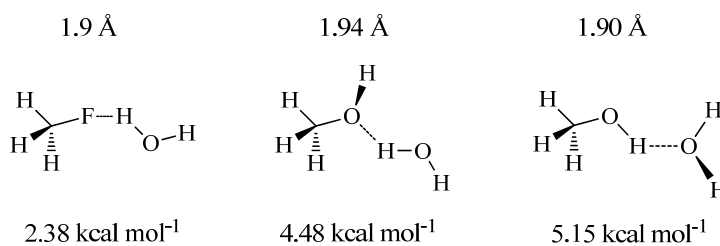


Figure 4.1. Hydrogen bonding interactions between water and C(sp³)-X groups.

The figure was adapted from Howard *et al.* (1996) and Fileti *et al.* (2004).

4.4. Conformational Preference of Fluorinated Molecules

Before examining the effects of C-F bond on the conformational preference of a molecule, various models to explain these preferences will be presented. The Pauli repulsion model will be discussed in greater detail because of its ability to explain the conformational preference adopted by fluorinated molecules. However, by no means does this quantum mechanical model give a complete and accurate picture.

4.4.1. Models for the Preferred Conformation of Molecules

The anomeric effect is a classical example of an electronegative atom influencing the stereochemistry of a molecule (O'Hagan, 2008). For example, an electronegative substituent that is attached to the C1 atom of a pyranoid ring has a tendency to adopt the axial rather than equatorial orientation (Figure 4.2a). Visualizing the effect with a Newman projection from the C1-O bond on-end, the antiperiplanar position for the fluorine atom (torsion angle $\pm 150^\circ$ to 180°) is favoured over the gauche position (torsion angle $\pm 60^\circ$) as a result of steric repulsion and a reduction in dipole-dipole repulsion (Figure 4.2a) (Mo, 2010; Trapp *et al.*, 2006; Vila *et al.*, 2011). An alternative model to describe the antiperiplanar position for electronegative atom in the axial preference is hyperconjugation, which involves electron delocalization of lone pair electrons to an anti-parallel, empty antibonding orbital (termed $n \rightarrow \sigma^*$ interaction; Figure 4.2b) (O'Hagan and Rzepa, 1997). However, the model cannot explain why this process is reversed, *i.e.*, a shift from an axial to an equatorial conformation

in the pyranoid ring, when a less electronegative atom at the C1 position such as nitrogen or a more polar solvent such as water is used (Juaristi *et al.*, 1986; Lemieux *et al.*, 1969).

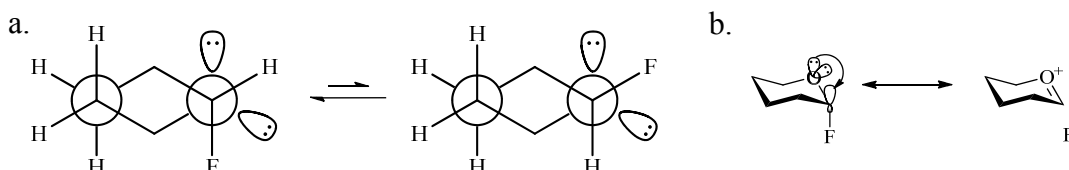


Figure 4.2. Stereochemistry of a carbohydrate and stabilizing hyper-conjugation effects.

a) The stereochemistry of a fluorine atom in the antiperiplanar conformation (left) and the gauche conformation (right). **b)** The antiperiplanar conformation which is suitable for $n \rightarrow \sigma^*$ interaction (neutral hyperconjugation). The figure was adapted from O'Hagan and Rzepa (1997).

The contribution of hyperconjugation, on the conformational preference of carbohydrates, is reported to be negligible when examined by the block localized wavefunction method, which calculates the extent of electron delocalization for an O-C-X bond that contains an electronegative substituent at position X (Mo, 2010). The model suggests that steric effects caused by Pauli repulsion and electrostatic interactions will contribute to the stereochemical preference of fluorinated carbohydrates (and possibly fluorinated molecules in general) (Mo, 2010; Ren, 2006). These results are consistent with several lines of studies, such as perturbation theory, minimization of dipole-dipole interactions at the axial position in the gas-phase and non-polar solvents, and stabilization of dipole-dipole interactions at the equatorial position in polar solvents as a result of changes in the distribution of electron

density within the carbohydrate (Bingham, 1976; Gillespie, 1967; Mo, 2010; Vila *et al.*, 2011).

As a side note, the Pauli repulsion model describes the nature of two electrons of different coordinates (spin and spatial) to exist in the same orbital provided that their wavefunctions are antisymmetric. On the other hand, electrons of the same coordinate (spin and spatial) will not exist because the wavefunction is non-existent (*i.e.* the electrons are mutually repulsive). The rule establishes where an electron pair will be arranged in a molecule, and the probable molecular shape of the molecule (Gillespie, 1967). Therefore, the electron pair in a given molecular orbital maximizes its distance or delocalize its electrons away from the neighbouring orbital in order to reduce the electrostatic repulsion (as defined by $F = 1/r^2$) (Gillespie, 1967).

The effects of electrostatic repulsion are observed in the bond angles of monofluoromethane (relative to methane), the F-C-H bond angles decrease and adjacent H-C-H bond angles increase, as a result of an increase in s character for the hybridization orbital of the F-C bond and a corresponding decrease in s character (a corresponding increase in p character) for the hybridization orbital of the C-H bond (Figure 4.3a) (Gillespie, 1967; Wiberg and Murcko, 1988). In other words, the hybridization orbital of the F-C bond is smaller in size than the C-H bonds. This is reflected by alterations in the ideal VSEPR bond angles of adjacent atoms due to changes in electrostatic repulsion between the different sizes of hybridization orbitals.

Consequences of an increased bond angle in a molecule may lead to an increase in entropy (O'Hagan and Rzepa, 1997), as reported for lipids that contain a CF_2 substitution (McDonough *et al.*, 1983). Normally, the carbon chain of the lipid will adopt a trans conformer, but a CF_2 substitution reduces the energy of the gauche conformer and is reflected by an increase in distance between the two 1,4 hydrogen atoms due to a wider bond angle (Figure 4.3b)(O'Hagan and Rzepa, 1997; Sturtevant *et al.*, 1979). Additionally crystallographic and theoretical evidence supports a widening of C-CX₂-C angle from a sp³ tetrahedral angle (109.5°) in hydrocarbons to 115-119° in CF_2 methylene systems (Chambers *et al.*, 1990; Durig *et al.*, 1981).

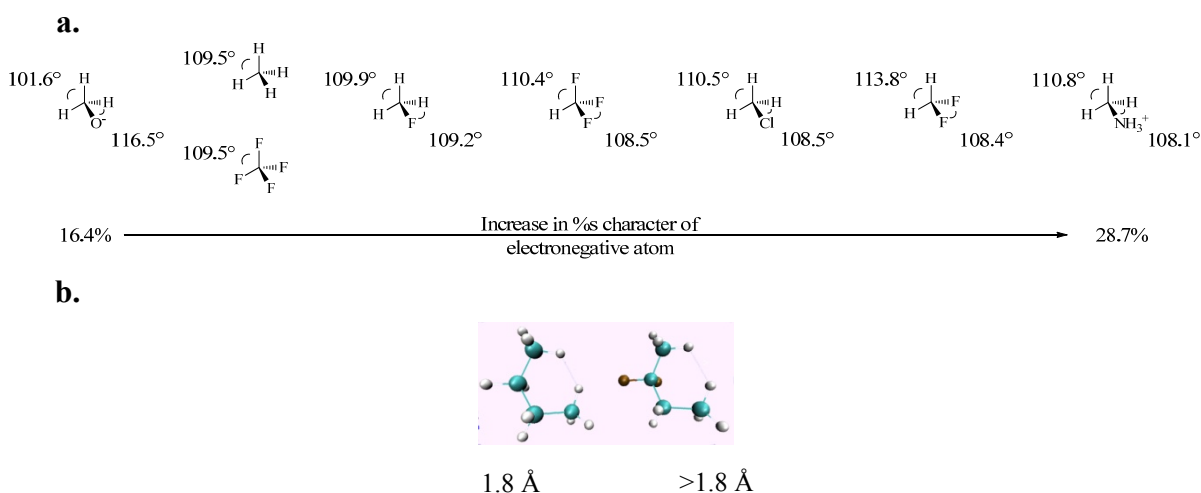


Figure 4.3. The relationship between bond angles of a molecule and percent bonding character of substituted electronegative atoms.

a) An increase in percentage of s character (*i.e.*, decrease in p character) for the C-X bond coincides with a decrease in bond angle for the electronegative atom (A-C-X).
b) An increase in bond angles from X-CH₂-X (left) to X-CF₂-X (right) for butane leads to an increase in the bond distance of 1,4-hydrogen interactions in the gauche conformer. Geometry optimization and wave functions of the molecules were

obtained with HFT/6-31G*/HFT/6-31++G** basis sets, and the figure was adapted from O'Hagan (2007) and Wiberg and Murcko (1988).

The extent of electrostatic interactions for the gauche preference of 1,2-difluoropropane and 1-fluoropropane has yet to be determined; however, MP2 level calculations suggest that hyperconjugation may be the dominant effect (Bitencourt *et al.*, 2007; Goodman and Sauers, 2005). Perturbation theory is an alternative explanation for the preferred gauche conformer of fluorinated alkanes, which explains the optimal conformer in terms of maximizing overlapping orbitals while minimizing Pauli repulsion energies (Bingham, 1976). The theory states that delocalized electrons of non-bonding (or bonding) orbitals will adopt a trans conformer when the antibonding orbital of the neighbouring atom is empty. The trans conformer reduces the extent of electron repulsion within a molecule by minimizing the energy gap for electron delocalization to occur (*e.g.*, the s-trans conformer of 1,3-butadiene are favoured over the s-cis conformer) (Squillacote *et al.*, 1979). On the other hand, delocalized electrons are unfavourable when occupied non-bonding (or bonding) orbital encounters an occupied antibonding orbital. The molecule will adopt a gauche conformer in order to reduce the electrostatic repulsion associated with filled orbitals, which is dependent on the electronegativity of the donor atom (Bingham, 1976). Thus, a gauche conformer is favoured when the donor atom is more electronegative, which increases the energy gap between the two filled molecular orbitals (*e.g.*, fluorinated carbon; Figure 4.4) (Bitencourt *et al.*, 2007; Durig *et al.*, 2005). Overall, the perturbation theory is a useful model in explaining the conformational preference of molecules that contain electronegative substitutions.

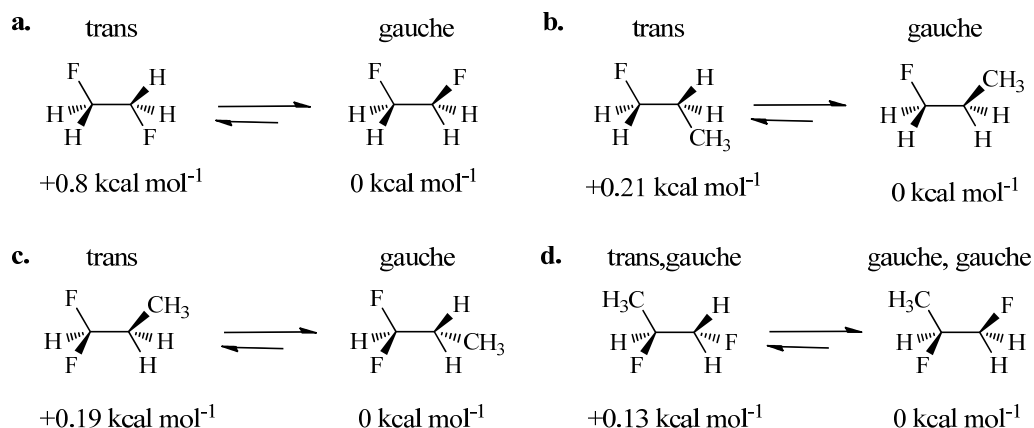


Figure 4.4. Energy difference between trans and gauche conformers.

The energy difference between trans and gauche conformers for **a**) 1,2-difluoroethane, **b**) 1-fluoropropane, **c**) 1,1-difluoropropane (methyl group relative to the lone hydrogen atom) and **d**) 1,2-difluoropropane. The energy minimum for each rotamer was optimized at the MP2 level of theory with either 6-31+G* (for 1,2-difluoroethane and 1-fluoropropane), augmented correlation-consistent polarized valence-only triple-zeta (aug-cc-pVTZ level; for 1,2-difluoropropane), or 6-31G(d) (for 2,2-difluoropropane). The figure was adapted from Rablen *et al.* (1999), Durig *et al.* (2005) and Bitencourt *et al.* (2007).

4.5. Fluorination Reagents and Applications

Deoxyfluorination using nucleophilic-type fluorinating reagents was first employed with SF₄ (**4.1**) in the transformation of hydroxyl groups to fluorides, carbonyl groups to difluoromethylene, and carboxylic acid groups to trifluoromethylene functionalities (Figure 4.5 a and d) (Hasek *et al.*, 1960). The fluorination reagent **4.1** is a gaseous substance, extremely toxic and corrosive. It also requires extensive safety measures, high temperatures (100°C) and specialized equipment. On the other hand, the organic fluorinating reagent, diethylaminosulfur trifluoride (DAST, **4.2**) became widely popular in fluorine chemistry (Figure 4.5) because of its wide spectrum of applicability, exists as a liquid, utilizes lower

temperatures, and produces fewer side products (Middleton, 1975b). The only concern when handling DAST is its potential to explode upon heating above 90°C. This led to further improvements in its heat stability with the modified fluorinating reagent, diethylaminodifluoro-sulfinium tetrafluoroborate (XtalFluor-E; **4.3**; Figure 4.5) in conjunction with an HF amine salt such as Et₃N*3HF, while maintaining the same deoxyfluorination selectivity as DAST (L'Heureux *et al.*, 2010).

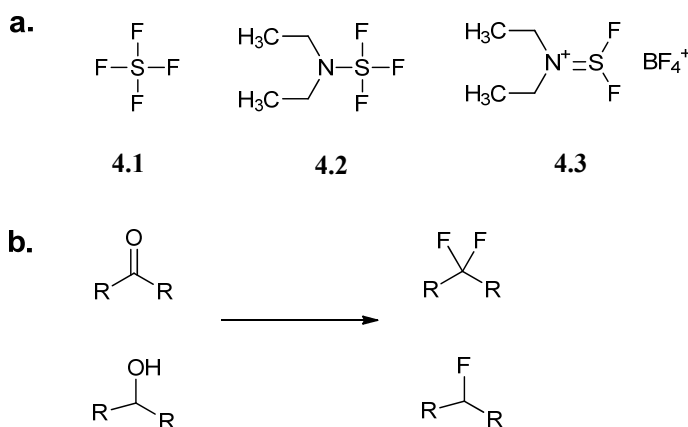


Figure 4.5. Fluorination reagents and deoxyfluorination of molecules.

a) Fluorination reagents: sulfur tetrafluoride (**4.1**), diethylaminosulfur trifluoride (**4.2**), and diethylamino-difluorosulfinium tetrafluoroborate (**4.3**). Deoxyfluorination of **d)** carbonyl and hydroxyl groups to their corresponding fluorocarbons. The figure was adapted from L'Heureux *et al.* (2010).

In the literature, there is a lack of evidence to suggest that DAST will fluorinate β-keto esters (**4.4**) to produce 3,3-difluoroesters (**4.5**). There is only one successful report by Buss *et al.* (1986) where 3,3-difluoroesters (**4.5**) are generated with DAST in a non-polar, non-basic solvent with a 76% yield (Figure 4.6a). All other reports with β-ketoester starting materials

afford α -fluoro- β -ketoesters **4.6** and vicinal difluoro-olefin side products **4.7** when treated with one and two equivalents of DAST, respectively (Figure 4.6b) (Asato and Liu 1986, Bildstein *et al.* 1995, and Singh 2002). In the fluorination of carbonyl groups, DAST has the potential to favour carbonium ion-type rearrangements in non-basic polar (*e.g.*, methylene chloride) and basic polar solvents (*e.g.*, tetrahydrofuran) (Middleton, 1975a). A classic example of such a case is the fluorination of the acid sensitive pivaldehyde (**4.8**) in a non-polar non-basic solvent (*e.g.*, pentane), which affords 1,1-difluoro-2,2-dimethyl-propane (**4.9**). However, fluorination in a non-basic polar solvent affords 2-methyl-2,3-difluorobutane (**4.10**), and fluorination in basic polar solvents affords 3-fluoro-2-methyl-but-1-ene (**4.11**) as a result of rearrangement of the carbocation (Figure 4.6c) (Middleton, 1975a).

The complication of fluorinating β -ketoesters with DAST likely arises from its inherent chemical properties. For example, electrostatic repulsion between carbonyl groups is reduced in polar solvents when the β -dicarbonyl exists as the keto form, and consequently enhances its solvation energy (Emsley and Freeman, 1987; Rogers and Burdett, 1965a). On the other hand, in non-polar solvents, the polarity of β -dicarbonyls is reduced in the enol form than the keto form (Emsley and Freeman, 1987; Rogers and Burdett, 1965a). Higher temperatures may be employed in order to reduce the extent of the enol form in β -dicarbonyls, because of the disruption in intramolecular H-bonding of the *cis*-enol (Rogers and Burdett, 1965b). Thus, changes in concentration, solvent and temperature may alter the equilibrium of the keto-enol tautomers for β -dicarbonyl compounds.

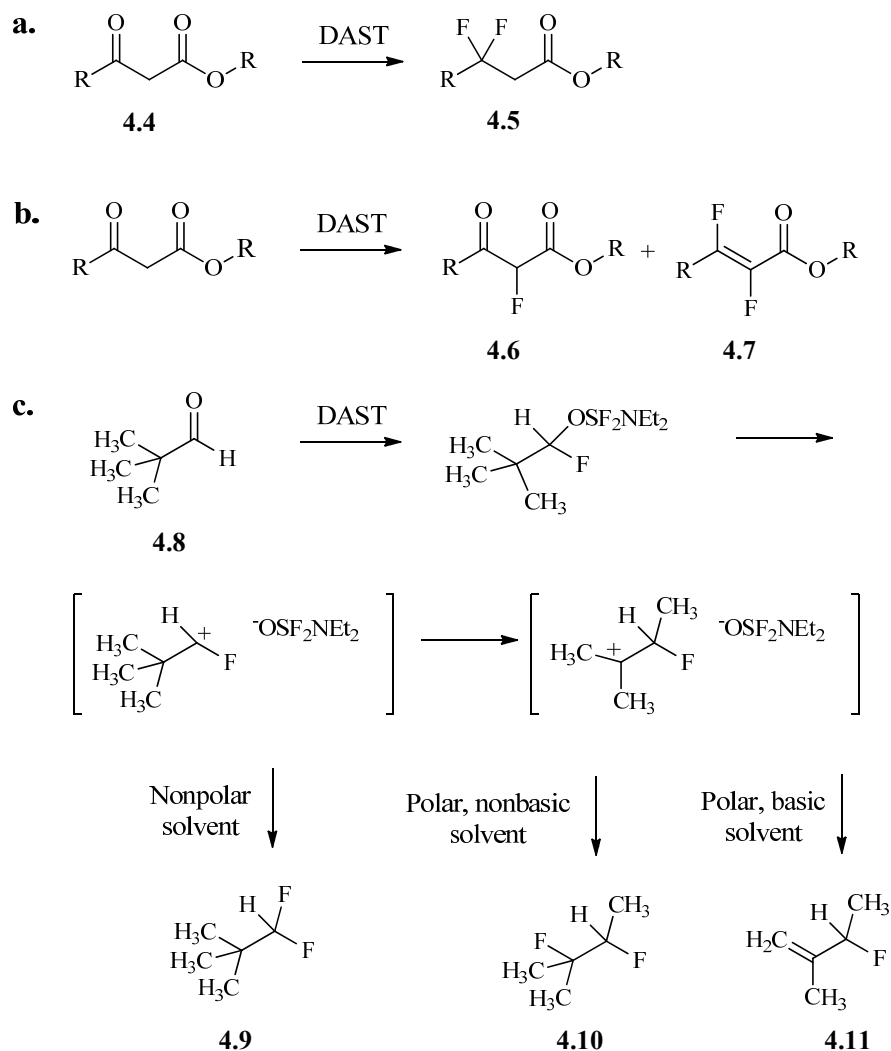


Figure 4.6. Fluorination of β -ketoesters and carbonium ion type rearrangement of pivaldehyde during deoxyfluorination.

Fluorination of pivaldehyde (**4.8**) with DAST may lead to either 1,1-difluoro-2,2-dimethyl-propane (**4.9**; nonpolar solvent), methyl-2,3-difluorobutane (**4.10**; polar, nonbasic solvent), or 3-fluoro-2-methyl-but-1-ene (**4.11**; polar basic solvent). Where R = Alkyl group. The figure was adapted from Middleton (1975a).

4.6. Mechanism Based Inhibitors

Mechanism-based inhibitors of enzymes, also referred to as suicide inhibitors, are compounds that require binding to the enzyme, and conversion to a reactive species as a result of the catalytic capabilities of the active site (Abeles and Maycock, 1976). For example, propargylglycine (L-2-amino-4-pentynoic acid, **4.12**) acts as a general mechanistic inhibitor of PLP-dependent enzymes (Figure 4.7a) (Abeles and Walsh, 1973). The steps leading to inhibition involve formation of an aldimine linkage between **4.12** and the enzyme-bound PLP, followed by labilization of the α -hydrogen atom to afford an imino- γ -alkyne, a shift of electrons to afford β,γ -diene **4.14**, and the active site base forming a covalent linkage to the C_γ atom of the diene *via* a Michael addition (**4.15**) (Abeles and Walsh, 1973; Silverman and Abeles, 1976).

For β -eliminating PLP-dependent enzymes, suicide inhibition is not observed for an α -alkene compounds, since it is hypothesized that the C_β atom is not sufficiently electronegative for nucleophilic attack (Silverman and Abeles, 1976). To improve its electrophilicity, halogens are introduced at the C_β atom to yield compounds such as 3,3-dichloroalanine (**4.18**) and 3,3,3-trifluoroalanine (**4.19**) (Silverman and Abeles, 1976). These halogenated compounds are found to inactivate several PLP-dependent enzymes, as a result of a covalent linkage between the catalytic base of the enzyme and the C_β atom (Figure 4.7c).

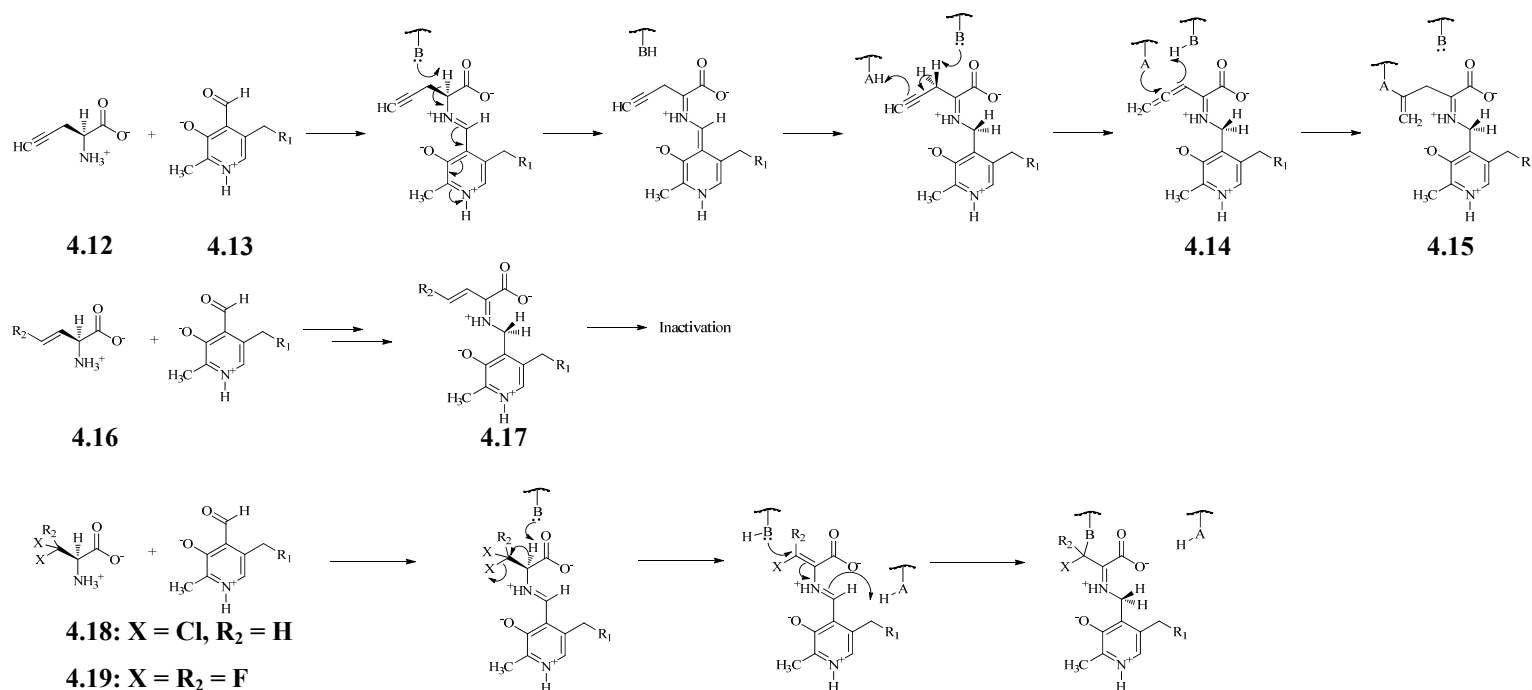


Figure 4.7. Suicide inhibition mechanism of β - and γ -eliminating PLP-dependent enzymes.

a) Inactivation by propargylglycine (L-2-amino-4-pentynoic acid, **4.12**): formation of an aldimine linkage between **4.12** and PLP (**4.13**), formation of an imino- β,γ -diene intermediate (**4.14**), and inactivation of the PLP-dependent enzyme at the γ -carbon atom (**4.15**). **b)** Inactivation by β -unsaturated L-amino acids (**4.16**): formation of an aldimine linkage between **4.16** and PLP, formation of a β -unsaturated imine intermediate (**4.17**), and inactivation of the PLP-dependent enzyme. **c)** Suicide inhibition of a β -eliminating enzyme with either L-dichloroalanine (where X = Cl and R₂ = H; **4.18**) or L-trifluoroalanine (where X = F and R₂ = F; **4.19**). Formation of an aldimine linkage between the suicide inhibitor and PLP, formation of a imino-acrylate (**4.20**), and inactivation of the PLP-dependent enzyme at the β -carbon atom (**4.21**) Where R₁ = OPO₃²⁻; the figure was adapted from Silvermann and Abeles (1976).

The goal of this study was to investigate the role of the catalytic residues of MGL with a fluorine probe, 3,3-difluoro-*O*-methyl-L-homoserine (**4.23**), an oxo derivative of L-methionine analog (**4.24**; Figure 4.9). Keqiang *et al.*(1998) reported the synthesis of 3,3-difluoro-L-methionine; however, the synthetic route was laborious (19 steps) and an overall yield of 0.4% (Figure 4.8). We were unable to obtain the sulfur compound from Dr. Liu for our study since it was disposed of upon his move to the University of Texas (personal communication, J. Honek). Thus, an approach for a simplified synthetic route was undertaken.

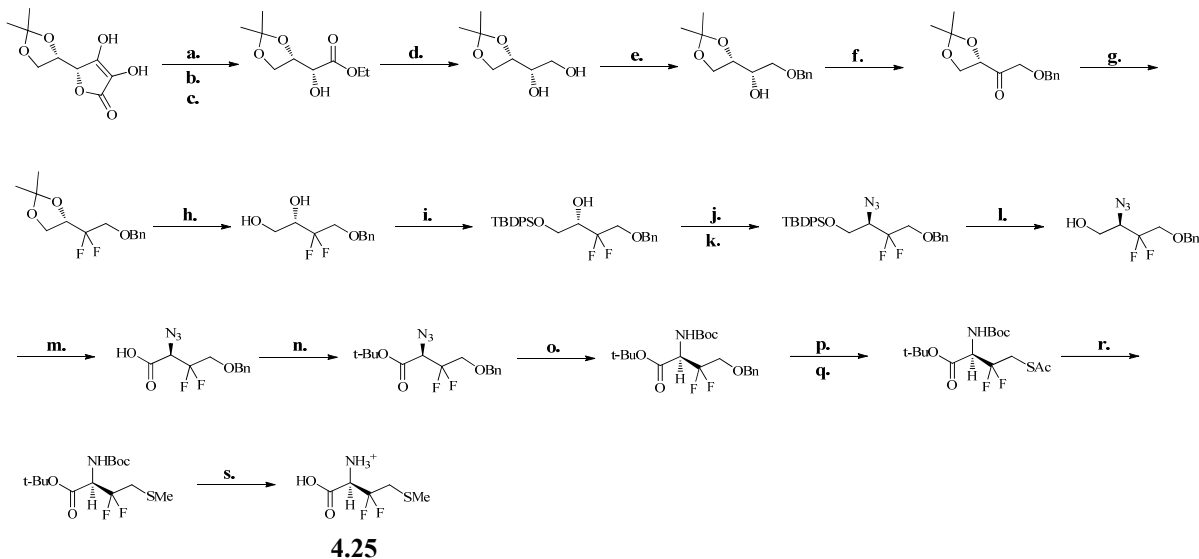


Figure 4.8. The synthetic route of 3,3-difluoro-L-methionine (**4.25**) from the precursor L-ascorbic acid.

a) Acetone, CuSO₄; **b)** K₂CO₃, H₂O₂; **c)** KI, MeCN; **d)** LiAlH₄, THF; **e)** NaH, BnBr; **f)** (COCl)₂, DMSO, Et₃N; **g)** Diethylaminosulfur trifluoride (DAST), CH₂Cl₂, -78°C; **h)** Dowex 50 (H⁺), MeOH; **i)** *t*-butyldiphenylsilyl chloride (TBDPSCI), imidazole; **j)** Tf₂O, pyridine; **k)** NaN₃, DMF; **l)** *t*-Bu₄NF, THF; **m)** CrO₃, H₂SO₄; **n)** Cl₃CC(NH)O-*t*-Bu, BF₃ Et₂O; **o)** Boc₂O, H₂, Pd/C; **p)** Tf₂O, pyridine; **q)** KSac; **r)** 0.2 N NaOH, MeI; **s)** trifluoroacetic acid (TFA)/CH₂Cl₂, 0°C. The reaction scheme was adapted from Keqiang *et al.* (1998).

The sulfur analog of the compound was not synthesized in order to avoid the odiferous synthetic reagents and compounds containing sulfur, and in consideration that a simplified synthetic scheme had not been established. The synthetic routes to the oxo derivative of the fluorinated methionine analog, 3,3-difluoro-L-methionine (**4.25**) are presented. The oxo derivative of methionine was hypothesized to act as a suitable substrate for the enzyme; and therefore, *O*-methyl-L-homoserine (**4.22**) was examined as a potential substrate for TvMGL1. Future studies of the proposed fluorinated compound may extend into characterizing the catalytic role of C113 in TvMGL1 as well as an investigation of its incorporation into proteins as an unnatural amino acid, provided that a synthetic route to the compound is found.

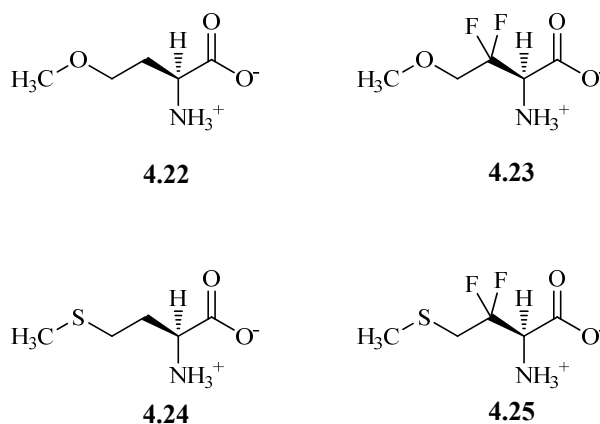


Figure 4.9. L-Homocysteine (**4.22**), L-methionine (**4.24**) and their fluorine derivatives.

4.7. Results and Discussion

4.7.1. Synthetic Approaches to 3,3-Difluoro-L-Methionine Analogs

The potential inhibitor, 3,3-difluoro-*O*-methyl- L-homoserine is expected to bind within the active site of TvMGL1. The methoxy group is not expected to interfere with the binding of the substrate since PpMGL and *Citrobacter freundii* (Cf)MGL are reported to process *O*-ester-containing L-homoserine substrates (such as acetyl and succinyl moieties) (Esaki *et al.*, 1985; Manukhov *et al.*, 2006). On the other hand, Lockwood and Coombs (1991) report that L-homoserine breakdown is not catalyzed by TvMGL and in fact acts as a weak inhibitor. Introducing a 3,3-difluoro moiety into the amino acid should not significantly impair binding of the suicide inhibitor, since a wide variety of fold type I family of PLP-dependent enzymes are capable of activating such compounds, as reported for 3,3,3-trifluoroalanine and 3,3-dichloroalanine suicide inhibitors (Silverman and Abeles, 1975). Thus, the processing of this 3,3-difluoro-*O*-methyl-L-homoserine by TvMGL1 has not been investigated, nor is it known whether the compound would be accepted as a substrate.

O-Methyl-L-homoserine (OMHser) was used as a model substrate for TvMGL in order to test the possibility that the methoxy moiety of 3,3-difluoro-*O*-methyl-L-homoserine may be accommodated in the active-site of TvMGL1. The results indicated that the substrate specificity of the enzyme for *O*-methyl-L-homoserine is greater than L-methionine; a 3.5 fold increase in turnover rate (and no significant differences in K_m values when compared to L-methionine). Thus, the compound was turned over more rapidly than L-methionine, even

though the methoxide group of the compound should act as a poorer leaving group relative to the methanethiolate group of L-methionine during the γ -elimination step. Enhanced orientation of *O*-methyl-L-homoserine within the active site of the enzyme may have contributed to the faster turnover rate when compared to L-methionine, as a result of differences in hydrogen bonding acceptor strength and angle of the hydrogen bonding acceptor to donor molecule. Evidence to support this hypothesis is based on theoretical calculations at the B3LYP level of theory, where the sulfur atom of dimethyl sulfide-water complex, compared to the dimethyl ether equivalent, is reported to be a weaker hydrogen bonding acceptor as a result of its intermediate electronegativity and have a reduced O-H-X bond angle (where X = sulfur or oxygen) (Rablen *et al.*, 1998).

Table 4.1. The kinetic parameters of TvMGL1 for L-methionine and *O*-methyl-L-homoserine (OMHSer).

Substrate	K_m mM	k_{cat} min ⁻¹	k_{cat}/K_m M ⁻¹ s ⁻¹
Methionine	0.22 ± 0.05	416 ± 15	32 × 10 ³
OMHSer	0.44 ± 0.11	1470 ± 119	56 × 10 ³

The standard errors were obtained from three independent experiments.

The initial synthetic route to synthesize 3,3-difluoro-*O*-methyl- L-homoserine (**4.25**) was proposed as follows: 1) methoxyacetyl chloride (**4.26**) condenses with 1,2-dimethyl imidazole to form an activated acyl ammonium intermediate (**4.27**), 2) *Ti-crossed*-Claisen condensation of the activated acyl ammonium intermediate (**4.27**) with a protected glycine

(**4.28**) to yield the α -amido- β -ketoester **4.29**, 3) fluorination of α -amido- β -ketoester **4.29** with DAST to afford 3,3-difluoro-*O*-methyl-D,L-homoserine (**4.30**), 4) saponification of the ester group, and 5) enzymatic resolution of the L-enantiomer with pig liver acylase (Figure 4.10). Precedent for the first reaction was recently described by Misaki *et al.* (2005), where a variety of β -ketoesters and α -amido- β -ketoesters are reported to be synthesized, including the compound of interest *N*-acetyl methylmethioinine. In the second step, fluorination of α -

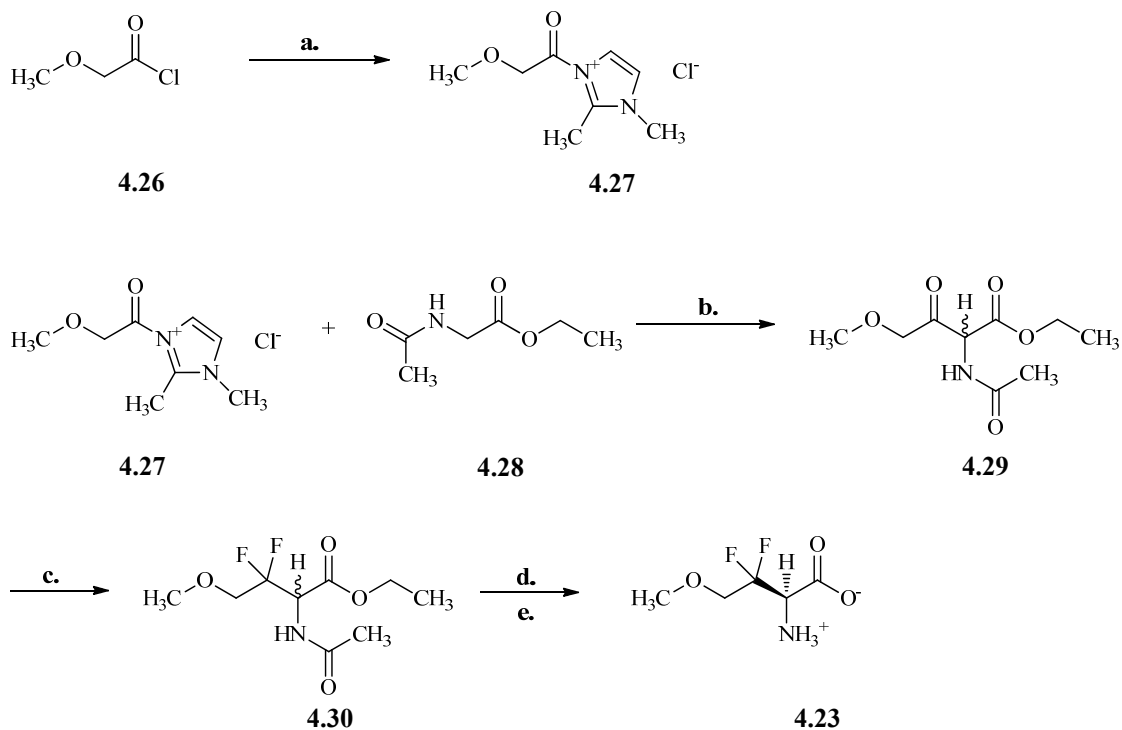


Figure 4.10. Proposed synthetic route to 3,3-difluoro-*O*-methyl-L-homoserine (4.23**).**

a) 1,2-Dimethyl imidazole, methylene chloride, 10 min, -45°C ; **b)** titanium tetrachloride, triethylamine, methylene chloride, -45°C , 30 min; **c)** DAST, methylene chloride, -78°C to 21°C , 2 hr; **d)** 1.1 equiv. NaOH, 4°C , 30 min; **e)** porcine kidney acylase, 37°C , 15 hr.

amido- β -ketoesters with DAST has not been reported in the literature. Pig liver acylase has been previously utilized to resolve racemic mixtures of D, L-amino acids by hydrolyzing the acyl group from L-amino acids (Jones *et al.*, 1991).

Several attempts at the Ti-*crossed*-Claisen condensation reaction afforded the crude α -amido- β -ketoester **4.29** with an estimated yield between 5 to 20%. Variations in the synthesis included the use of tributylamine as a base for the deprotonation of the α -carbon atom, anhydrous triethylamine, sequential addition of TiCl₄ and triethylamine, and extraction of product with ethyl acetate. Due to the limited success of the reaction as a result of complexity in purification and low yields, an alternative synthetic route was examined.

The condensation reaction with lithium diisopropylamide was employed to synthesize the α -amido- β -ketoester **4.35**, in order to reduce the complexity of the synthesis (Figure 4.11), and since the procedure was successful in synthesizing a previously reported compound (**4.32**) (Nicolaou *et al.*, 2008). Upon following the procedure, the methoxyacetyl chloride was found to react with the nitrogen of the *N*-acetylamido group of the protected glycine to afford compound **4.33**, as opposed to the α -carbanion in order to afford compound **4.32** (Figure 4.11). After several attempts at manipulating the reaction conditions, another synthetic step was pursued.

The synthesis of an α -amido- β -ketoester, 2-*N*-acetylamido-3-oxo-ethylbutanoate (**4.35a**) is reported by Thrift *et al.* (1967) in a one pot reaction, which involves the oximation of the β -ketoester **4.34a** at the α -carbon and subsequent reduction with zinc in acetic anhydride (Figure 4.11 d and e respectively). The reaction was found to be facile and the product was

easily purified by column chromatography with an overall yield of 40% and 60% for the α -amido- β -ketoester **4.35b** and **4.35a**, respectively (Figure 4.11).

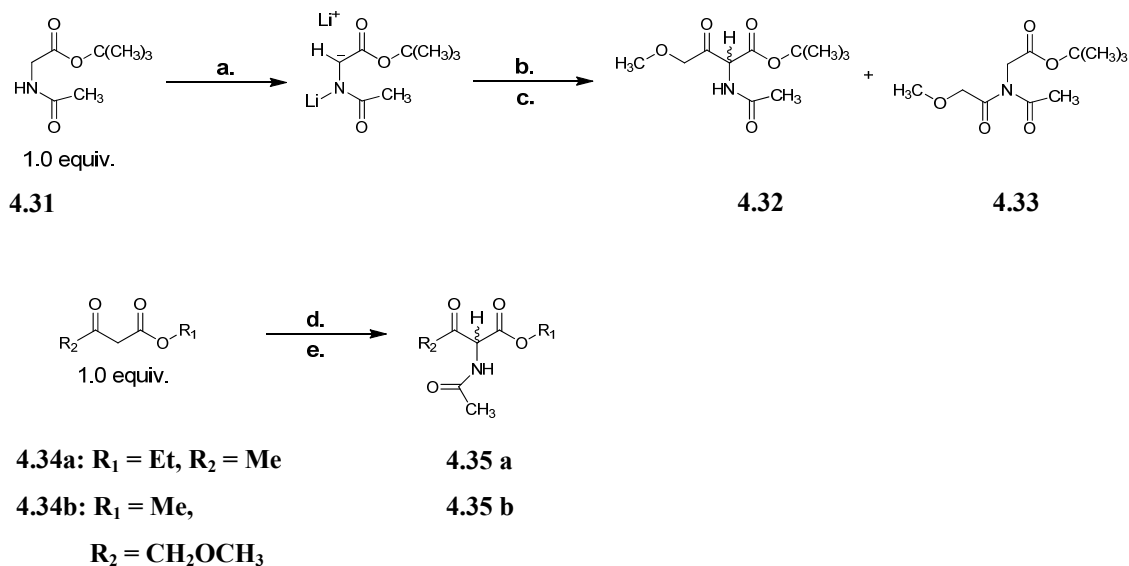


Figure 4.11. Synthetic routes toward α -amido- β -ketoester.

Lithium diisopropylamide (LDA) condensation reaction (top): **a**) 2.5 equiv. LDA, THF, -70°C , 1 hr; **b**) 1.2 equiv. methoxyacetyl chloride, -70°C to 21°C , 15 min; **c**) 1.2 equiv. dilute acetic acid, 4°C . Oximation of β -ketoester **4.34** (bottom): **d**) 1.1 equiv. sodium nitrite, acetate, 10°C to 21°C and **e**) 3 equiv. acetic anhydride, 3 equiv. zinc dust, 21°C , 1.5 hr.

To synthesize the 3,3-difluoro compound from the α -amido- β -ketoester, DAST and Xtalfluor-E fluorination reagents were utilized under a variety of experimental conditions. Initial attempts with one equivalent of fluorinating reagent led to very little or no product, while two equivalents of the fluorinating reagent led to a complex mixture that decomposed upon purification. Based on the ^1H -NMR spectrum for a partially purified product, compound **4.40** was produced from the α -amido- β -ketoester **4.35a** starting material (Figure 4.12). To validate the observation, two equivalents of DAST were tested on the β -ketoester **4.34a** starting material (Figure 4.12). The reaction afforded compound **4.39** based on ^1H -NMR and ^{19}F -NMR, and is consistent with previous reports (Asato and Liu, 1986; Bildstein *et al.*, 1995), despite several fractions that underwent decomposition upon purification on a silica gel column, (Figure 4.12). Alterations to the reaction conditions were also examined; however, the reaction did not afford the 3,3-difluoro compound of interest (see materials and methods). Thus, a lack of a reported procedure for fluorinating β -ketoesters with DAST may indicate that the tautomerization between the enol and keto forms of β -ketoester (Figure 4.12a) impairs fluorination at the 3-oxo position, or the proper conditions have yet to be determined.

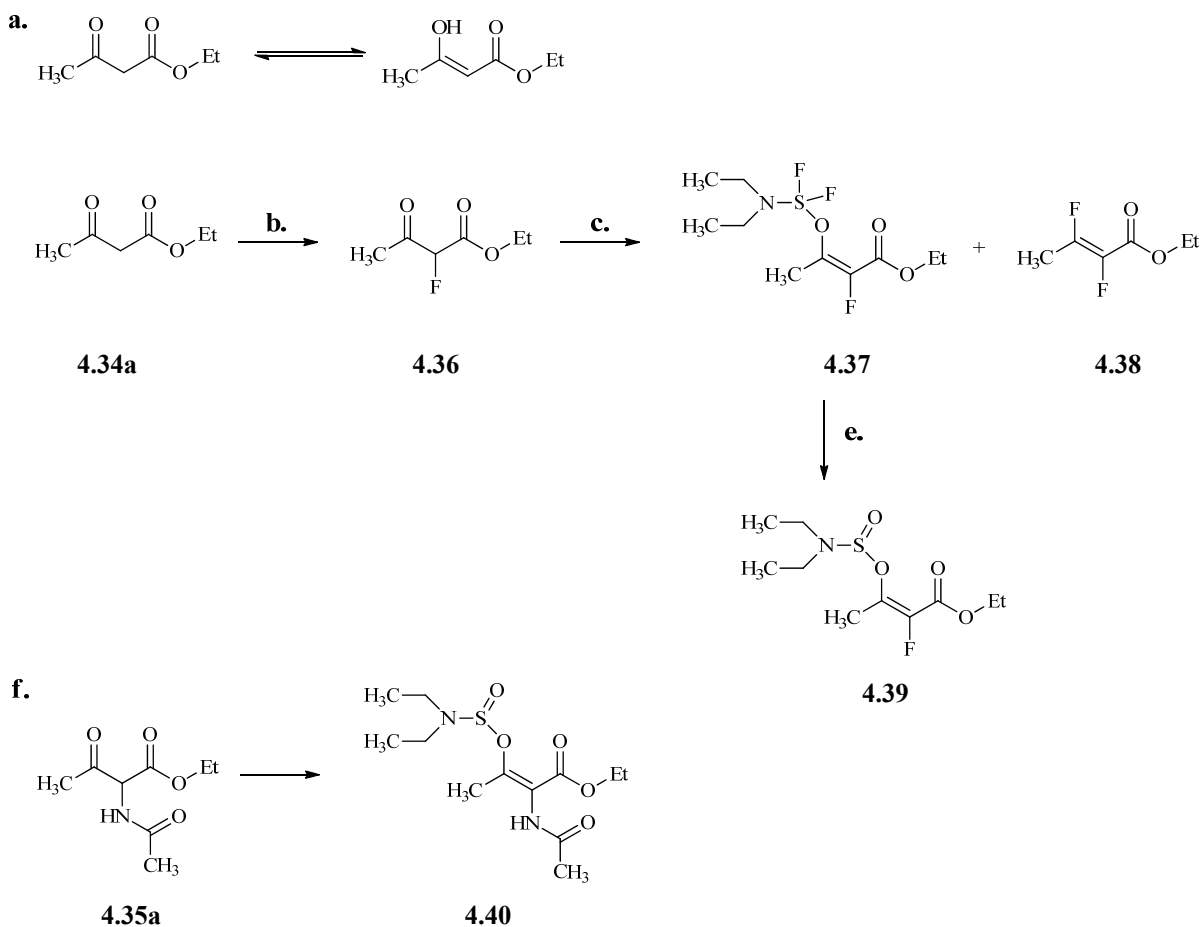
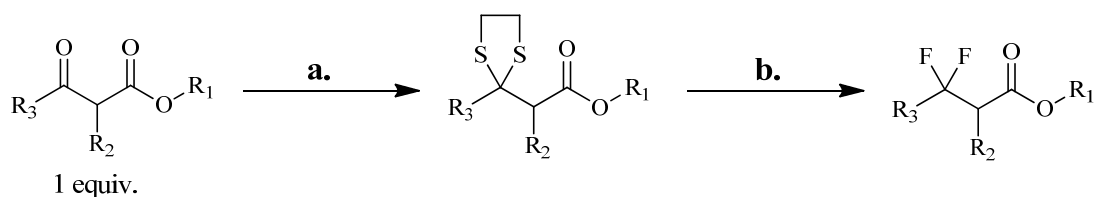


Figure 4.12. Side products reported for the deoxyfluorination of β -ketoesters.

a) The enol and keto tautomers of a β -ketoester. Fluorination of the β -ketoester **4.34a** with **b)** one equivalence of DAST affords α -fluoro- β -ketoester **4.36**, and **c)** the second equivalence of DAST affords compound **4.37** and difluoro-olefine **4.38**, **e)** extraction from brine affords compound **4.39** (Bildstein *et al.*, 1995). **f)** α -amido- β -ketoester **4.35a** with two equivalence of DAST affords the proposed compound **4.40**.

Problems when fluorinating β -ketoesters with DAST have also been reported by Bosch *et al.* (1996), which yields the undesired side product similar to compound **4.39** reported here. To avoid this problem, the carbonyl group of the β -ketoester **4.35c** is replaced with 1,2-ethanedithiol to afford the dithiolane **4.41c**, and then treated in a mixture containing pyridine hydrogen fluoride and *N*-bromosuccinimide (NBS) to afford the 3,3-difluoro-ester **4.42c** (Figure 4.13) (Bosch *et al.*, 1996). We also followed this synthetic route, in which the first step afforded 1,3-dithiolane in 95% yield from the β -ketoester **4.35d** starting material. In the second step, the fluorination procedure resulted in several fluorinated side products with inconsistent results as indicated by ^{19}F -NMR analysis. Synthesizing the dithiolane **4.41b** with α -amido- β -ketoester **4.35b** as the starting material was more problematic due to poor yields and problems resolving the compound by silica gel chromatography. In the second step, fluorination of the crude dithiolane **4.41b** did not afford a fluorinated product as indicated by ^{19}F -NMR spectroscopy. Thus, the reaction was abandoned because the methoxy group in compound **4.35b** was likely incompatible with the Lewis acid reagent used in the dithioketal protection and fluorination procedures, and this limitation has been previously reported by Hart *et al.* (1978a).



4.35b: $R_1 = \text{Me}$, $R_2 = \text{NH}(\text{CO})\text{CH}_3$,

4.41b-d

4.43c

$R_3 = \text{CH}_2\text{OCH}_3$

4.35c: $R_1 = \text{H}$, $R_2 = \text{H}$, $R_3 = \text{Alkyl}$

4.35d: $R_1 = \text{H}$, $R_2 = \text{H}$, $R_3 = \text{Me}$

Figure 4.13. Synthesis of 3,3-difluoro-ester (4.43) from 1,3-dithiolane (4.41).

Synthesis of 3,3-difluoro-ester (**4.43**): **a**) 1.5 equiv. boron trifluoride etherate, methylene chloride, 21°C, 24 hr; **b**) 2 equiv. *N*-bromosuccinimide, 20 equiv. pyridinium hydrofluoride, methylene chloride, -78°C, 30 min.

An alternative synthetic route to 3,3-difluoro-D, L-amino acids is reported by the ring opening of azirines (**4.46**) with pyridinium hydrogen fluoride (Figure 4.14d), in synthesis of compounds such as 3,3-difluoro-2-D,L-amino-butanoate (**4.47**) (Wade and Kheribet, 1980). To synthesize the azirine ring **4.46**, the starting material, β -ketoester **4.34** undergoes oximation to produce the ketoxime **4.43**, which is immediately protected with a tosylate group to afford the oxime tosylate **4.45** in order to avoid the competing formation of isoxazolone (**4.44**; Figure 4.14) (Verstappen *et al.*, 1996). The desired azirine **4.46** is synthesized by treating the oxime tosylate **4.45** with a base, such as triethylamine (Figure 4.14c). Our first attempt at synthesizing the oxime tosylate **4.45a** worked well (undertaken by a Chem 494 student, Qasim Bhatti), but synthesis of the azirine **4.46** compound was likel

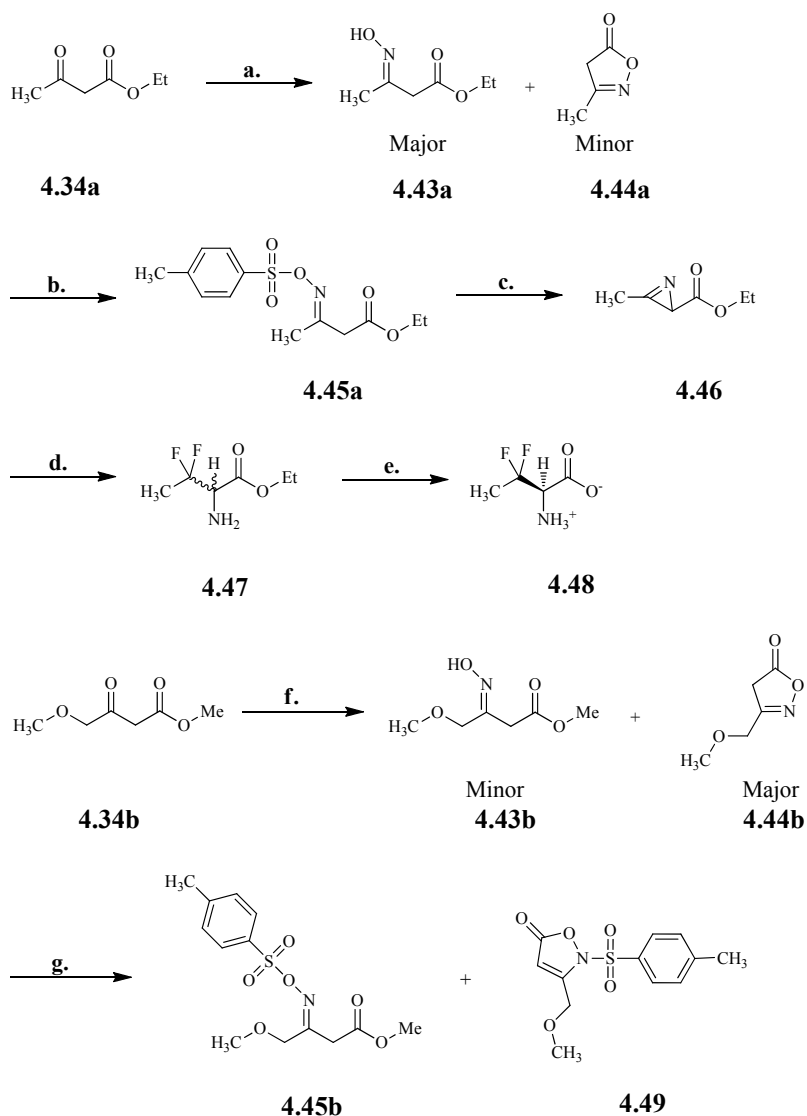


Figure 4.14. Synthesis of 3,3-difluoro-L-amino acid (4.48) via the Neber reaction.

a) 1.1 equiv. hydroxylamine-HCl, 1.1 equiv. sodium hydroxide, methanol, 22°C, 30 min; **b)** 1.1 equiv. *p*-toluenesulfonyl chloride, methylene chloride, pyridine, 22°C, 3 hr; **c)** 1.1 equiv. triethylamine, toluene, 4°C to 21°C, 24 hr; **d)** neat pyridinium hydrofluoride, benzene, 5°C, 10 min; **e)** lipase, water, 40°C, 24 hr. Adapted from Bosch *et al.* (1996), Verstappen *et al.* (1996), and Wade and Kheribet (1980). **f)** 1.1 equiv. hydroxylamine-HCl, 1.1 equiv. sodium hydroxide, methanol or water, 22°C, 30 min; **g)** 1.1 equiv. *p*-toluenesulfonyl chloride, methylene chloride, pyridine, 21°C, 3 hr.

lost upon removal of solvent *in vacuo*. On the other hand, oximation of the starting material **4.34b** (the methoxy derivative) afforded the undesired the isoxazolone tosylate **4.49** side product, instead of a protected the oxime tosylate **4.45b**. Similar problems have been reported by Sakai *et al.* (2005) and Alves *et al.* (2005), and in one case is alleviated by utilizing a *t*-butyl ester protecting group. Substituting methanol with water (step f) afforded the oxime tosylate **4.45b** in low yields (Figure 4.14). Thus, synthesis of the was problematic because of intramolecular cyclization of β -oximinoester **4.43b** to afford the undesired isoxazolone tosylate **4.49**. Methods to reduce the intramolecular cyclization of the oxime might require maintaining the temperature of the water bath below 40°C when removing methanol *in vacuo*, or by introducing a *t*-butyl ester protecting group into the compound.

4.8. Conclusions and Future Work

The methoxy moiety for the proposed compound 3,3-difluoro-*O*-methyl-L-homoserine is expected to bind to TvMGL1, considering that the enzyme is able to catalyze the electronegative substituent of *O*-methyl L-homoserine with a 3.5-fold greater turnover rate than L-methionine and with no significant differences in K_m values. Work by Silverman and Ables suggests that orthologous PLP-dependent MGLs, such as cystathione- γ -lyase and cystathionine- γ -synthase, are capable of accommodating fluorine substitutions at the C_β atom of L-amino acids, and consequently result in the inhibition of the enzyme (Silverman and

Abeles, 1976). Therefore, the fluorine atoms in the proposed compound, 3,3-difluoro-*O*-methyl-L-homoserine should inhibit the activity of TvMGL1.

The underlying reason(s) for TvMGL1 exhibiting a greater substrate specificity for *O*-methyl L-homoserine than L-methionine is unknown. One possible explanation is an improved orientation of the compound within the active site when compared to L-methionine. Thus, future biophysical and structural data are required in order to investigate this possibility.

A general synthetic strategy for synthesizing 3,3-difluoro-*O*-methyl-L-homoserine has yet to be determined. Fluorination of β -ketoesters was unsuccessful when utilizing DAST and similar fluorinating reagents reported in this study, which led to a side product (**4.39**) that is consistent with literature reports (Asato and Liu, 1986; Bildstein *et al.*, 1995; Bosch *et al.*, 1996). The use of a dithiolane protecting group and a Lewis acid to fluorinate the C β atom did not appear to be feasible for the β -ketoester **4.35b** starting material because the methoxy moiety might be labile to nucleophilic attack as reported for the synthesis of (\pm)-Cherylline (Hart *et al.*, 1978b). The most promising synthetic route was the Neber reaction, which has been successfully applied in the synthesis of 3,3-difluoro phenylalanine and 3,3-difluoro-2-aminobutyric acid (Verstappen *et al.*, 1996; Wade and Kheribet, 1980). However, upon following the procedures, the undesired isoxazolone side product was obtained, which is consistent with reports from two independent groups (Alves *et al.*, 2005; Sakai *et al.*, 2005). The Neber reaction is a likely route to synthesizing 3,3-difluoro-*O*-methyl-L-homoserine; however, a strategy to prevent the undesired isoxazolone side product will have to be

addressed. Thus, the potential inhibitor, 3,3-difluoro-*O*-methyl-L-homoserine has yet to be synthesized and tested on TvMGL1.

4.9. Materials and Methods

4.9.1. General Experimental

Anhydrous solvents and reagents were obtained by standing over a drying reagent (15 to 24 hr) as previously reported (Burfield and Smithers, 1978). The appropriate drying reagent for removing trace water from the solvents was selected based on drying agent compatibility charts (Merck KGaA, Darmstadt, Germany). Briefly, ethyl acetate was dried over anhydrous KHCO_3 , and alkylamines (triethylamine, tributylamine and pyridine) were dried over potassium hydroxide. The following anhydrous solvents and reagents in Sure-Seal protected containers were obtained from Aldrich Chemicals (Milwaukee, WI): methylene chloride, THF, neat TiCl_4 , methoxyacetyl chloride, lithium diisopropylamide in THF. For water sensitive reactions, all glassware and syringes were dried in a 110°C oven before use and assembled under an argon atmosphere while supplying heat by way of using a heating gun. During workup, drying of organic solutions was accomplished over anhydrous sodium sulfate or anhydrous magnesium sulfate.

Reagent grade solvents were used throughout the experiments and were purchased from Aldrich Chemicals unless otherwise stated.

Solvent evaporation was carried out under reduced pressure (Wheaton water aspirator) with a bath temperature of 20 to 40°C.

Thin layer chromatography was carried out on aluminum-backed sheets, precoated with Kieselgel 60 F₂₅₄, 0.2 m thick (EMD Chemicals Inc., Darmstadt, Germany). Prepacked flash silica gel chromatography columns were obtained commercially (Biotage; Charlotte, NC), and samples were purified utilizing Isolera One Flash Purification System (Biotage).

NMR spectra were recorded on a Bruker 300 MHz NMR, operating at 300.13 MHz for ¹H-NMR and 282.40 Hz for ¹⁹F-NMR. The chemical shifts (δ ppm) for ¹H-NMR were reported downfield from the internal reference standard TMS (0 ppm). The chemical shifts (δ ppm) for ¹⁹F NMR were recorded upfield from the external reference standard trifluoroacetic acid (-76.53 ppm). Mass spectra were recorded using electrospray ionization (ESI), electron ionization (EI) or chemical ionization (CI; NH₃ as the reactant gas), which were obtained by Dr. R. W. Smith (University of Waterloo, Waterloo, ON).

4.9.2. MBTH Assay Method for Detecting α-Ketobutyrate

The activity of MGL was monitored by utilizing the MBTH assay as previously described (Soda, 1968). Briefly, the 50 μL reaction mixture for the turnover of L-methionine consisted of 60 mM HEPES-NaOH, pH 8.0, 10 μM PLP, 0.05 to 3.0 mM substrate, and 0.1 μM TvMGL1. The reaction mixture for the turnover of *O*-methyl-L-homoserine was the same as

above except 0.5 to 4 mM substrate and 0.05 μM TvMGL1 were used. All other procedures were followed as described in section 2.6.7.

4.9.3. O-Methyl-L-Homoserine Physical Data

O-Methyl-L-homoserine was purchased from CBL (Patras, Greece), purity not available. White solid: decomp. 224°C (lit. 224-225°C) (McCoy *et al.*, 1935).

$^1\text{H-NMR}$ (D_2O) δ : 2.16 (m, 2H, C_βH_2), 3.38 (s, 3H, OCH_3), 3.69 (m, 2H, $\text{C}_\gamma\text{H}_2$), 3.87 (dd, 1H, $\text{C}_\alpha\text{H}_A$, $J_{ab} = 4.3$ Hz, $J_{bx} = 7.2$ Hz). Lit. $^1\text{H-NMR}$ (D_2O): 2.02-2.26 (m, 2H), 3.36 (s, 3H); 3.57-3.79 (m, 2H); 3.85 (dd, 1H, $J = 7.4$ Hz) (Seebach *et al.*, 1987). ESI-MS calculated for $\text{C}_5\text{H}_{12}\text{NO}_3^+$ ($\text{M}+\text{H}$) $^+$ 134.08176, found 134.0727.

4.9.4. Titanium-Claisen Condensation Reaction

The synthesis was adapted from Misaki *et al.* (2005) and Carlson *et al.* (1992). The reaction was contained in a three-neck 25 mL round bottom flask, a water-cooled condenser, under argon, and a magnetic stirring bar was added. Methoxy acetyl chloride (1.50 mmol, 137 μL) was added dropwise over 10 min to a solution of 1,2 dimethyl imidazole (1.50 mmol, 150 mg) in methylene chloride (2 mL) at -45°C . Within 10 min of stirring, a white precipitate formed, and the mixture was purged with argon gas. Ethyl acetamidoacetate (1.00 mmol, 145 mg) and neat TiCl_4 (3.00 mmol, 330 μL) were sequentially added to the mixture and stirred for 10 min at -45°C , which completely dissolved the white precipitate and resulted in a

yellow homogenous solution. Anhydrous Et₃N (3.30 mmol, 460 μL) was added dropwise to the mixture (resulting in the solution turning dark red and then black), and warmed up to 4°C for 30 min. The mixture was cooled with ice, then quenched with brine (10 mL) and aqueous NaHCO₃ (8.4 mmol, 0.71 g). The product was extracted with ethyl acetate (3 x 25 mL), dried with sodium sulphate, and concentrated *in vacuo* to yield a colourless oil. Attempts to purify the crude product by silica column chromatography or oiling out the product with methylene chloride/hexane were unsuccessful.

Crude α-amido-β-ketoester **4.28** product in 10 to 20% yield. R_f (ethyl acetate/THF, 2:1) 0.5. ¹H-NMR data not available. EI-MS calculated for C₉H₁₆NO₅⁺ [M+H]⁺ 218.10288, found 218.12.

4.9.5. Neber Reaction

4.9.5.1. Synthesis of Tosylates

The procedure was adapted from Wade (1980) and Vestappen (1996). 4-Methoxy methyl acetoacetate (compound **4.34b**; 2.00 mmol, 258 μL) was added to a solution containing hydroxylamine-HCl (2.10 mmol, 153 mg) and NaOH (2.1 mmol, 88 mg) in aqueous methanol (10 mL) 22°C. After 30 min the solvent was removed under reduced pressure (temperature 40°C), and extracted with ethyl acetate (2 x 10 mL). The combined organic fractions were dried with anhydrous magnesium sulphate, and concentrated *in vacuo*. The crude oxime was immediately dissolved in dry dichloromethane (15 mL), and *p*-

toluenesulfonyl chloride (2.00 mmol, 381 mg dissolved in 1 mL CH₂Cl₂) and pyridine (2.00 mmol, 161 μL) were added sequentially at 22°C. The reaction was stirred for 3 hr, quenched with saturated aqueous ammonium chloride solution (10 mL), and extracted with ethyl acetate (3 x 10 mL). The combined organic layers were washed with brine (2 x 10 mL) and dried over magnesium sulphate. The major product, isoxazolone was purified by silica gel flash chromatography and concentrated *in vacuo*. The oxime tosylate **4.45a** was synthesized in a similar manner, but with ethyl acetoacetate (compound **4.34a**; 2.00 mmol, 225 μL) as a starting material, and the product was resolved by silica gel flash chromatography.

The isoxazolone tosylate **4.49** was isolated as an oil (184 mg, 70%). R_f (hexane/ethyl acetate, 7:1) 0.17. ¹H-NMR (CDCl₃) δ: 2.48 (s, 3H, CH₃), 3.37 (s, 3H, CH₃), 4.42 (s, 2H, CH₂), (s, 1H, C_αH₂), 5.93 (s, 1H, CH₁), 7.39 (d, 2H, aromatic, *J* = 8.3 Hz), 7.85 (d, 2H, aromatic, *J* = 8.3 Hz). ESI-MS calculated C₁₂H₁₄NO₅S⁺ [M+H]⁺ 284.05932, observed 284.0415.

The oxime tosylate **4.45a** was isolated as a yellow oil (479 mg, 80%). R_f (hexane/ethyl acetate, 4:1) 0.75. ¹H-NMR (CDCl₃) mixture of isomers δ: 1.24 (m, 3H, CH₂CH₃), 2.04 (d, 3H, C_γH₃, *J* = 4.9 Hz), 2.44 (s, 3H, ArCH₃), isomer 3.25 (s, 1H, C_αH₂), isomer 3.43 (s, 1H, C_αH₂), 4.14 (m, 2H, COCH₂), 7.33 (d, 2H, aromatic H, *J* = 8.3 Hz), 7.85 (d, 2H, aromatic H, *J* = 8.3 Hz). ESI-MS not available.

Aqueous NaOH (2.1 mmol, 88 mg, in 1 mL H₂O) was added to 4-methoxy methyl acetoacetate (compound **4.34b**; 2.00 mmol, 258 μL, in 3 mL H₂O) at 22°C. After 30 min the solvent was removed under reduced pressure (temperature 30°C), and extracted with CH₂Cl₂ (3 x 5 mL). The combined organic fractions were dried with anhydrous magnesium sulphate.

The crude oxime was immediately added to *p*-toluenesulfonyl chloride (2.00 mmol, 381 mg dissolved in 1 mL CH₂Cl₂), followed by the addition pyridine (2.00 mmol, 161 μL) at 22°C. The reaction was stirred for 3 hr, quenched with saturated aqueous ammonium chloride solution (10 mL), and extracted with ethyl acetate (3 x 10 mL). The combined organic layers were washed with brine (2 x 10 mL) and dried over magnesium sulphate. The crude product, tosyl oxime was purified by silica gel flash chromatography and concentrated *in vacuo*.

Oxime sulfonate **4.45b** was isolated as a light yellow oil (32 mg, 5%). R_f (CHCl₃/CH₂Cl₂, 3:1) 0.14. ¹H-NMR (CDCl₃) δ: 2.45 (s, 3H, ArCH₃), 3.31 (s, 3H, CH₃), 3.34 (s, 2H, CH₂), 3.67 (s, 3H, CH₃), 4.33 (s, 2H, CH₂), 7.34 (d, 2H, aromatic H, *J* = 8.1 Hz), 7.84 (d, 2H, aromatic H, *J* = 8.1 Hz). ESI-MS not available.

4.9.5.2. Synthesis of Azirine Ester

The oxime tosylate **4.45a** (2.00 mmol, 470 mg) was added dropwise (over a period of 15 min) to a stirred solution containing dry toluene (15 mL) and Et₃N (2.00 mmol, 279 μL) at 0°C. After stirring the reaction for 24 hr, it was quenched with aqueous HCl (50.0 mM, 110 mL), and the compound was extracted with diethyl ether (3 x 20 mL). The combined organic layers were washed with brine, dried over anhydrous magnesium sulphate and concentrated *in vacuo*, but the crude (±) azirine ester **4.46** was likely lost during this process. ¹H-NMR (CDCl₃) mixture of isomers δ: 1.28 (t, 3H, CH₂CH₃, *J* = 7.1 Hz), isomer 2.45 (s, 2.6H, NCH₃), isomer 2.53 (s, 0.8H, NCH₃), 4.15-4.23 (m, 2H, COCH₂). ESI-MS not available.

4.9.6. Lithium Diisopropylamide-cross Claisen Condensation Reaction

The procedure was adapted from Nicolaou *et al.* (2008). Lithium diisopropylamide (3.45 mmol, 2.30 mL) was added to tetrahydrofuran (5 mL) at -78°C under argon. *t*-Butyl acetoamidoacetate (compound **4.31**; 1.38 mmol, 204 µL diluted in 1 mL of anhydrous THF) was added drop wise over a period of 15 min, and the solution was stirred vigorously for 1 hr. (Incubation time for lithium diisopropylamide may require more time and higher temperature in order to deprotonated the α -carbon atom). Methoxyacetyl chloride (1.65 mmol, 151 µL) was added to the mixture dropwise over a period of 15 min, which led to the appearance of white precipitate. The temperature was maintained at -78°C for 1 hr, and afterwards warmed up to 22°C for 15 hr. The reaction was quenched with acetic acid (5.00 mmol, 286 µL) and brine (5 mL) at -10°C. The aqueous solution was extracted with diethyl ether (3 x 25 mL), and the organic layers were combined and dried with anhydrous sodium sulphate. Sample was resolved on a silica gel column by flash chromatography.

Compound **4.33** was isolated as an oil (210 mg, 60%). R_f (hexane/ethyl acetate, 2:1) 0.5. $^1\text{H-NMR}$ (CDCl_3) δ : 1.51 (s, 9H, $\text{C}(\text{CH}_3)_3$), 3.47 (s, 3H, CH_3), 3.74 (s, 3H, CH_3), 4.47 (s, 2H, CH_2), 4.60 (s, 2H, CH_2). MS-ESI data not available.

4.9.7. Oximation of β -Ketoesters

Synthetic procedures were adapted from Nudelman and Nudelman (1999) and Girard *et al.* (1996). In a round bottom flask, β -ketoester (10.3 mmol; 1.33 mL of compound **4.34a**; 2.63

mL of compound **4.34b**) was dissolved in acetic acid (4 mL). NaNO₂ (11.0 mmol, 770 mg) was added over a period of 20 min, and the temperature of the exothermic reaction was maintained below 12°C in an ice-water bath. The mixture was warmed up to 22°C and proceeded for 3.5 hr with stirring, and the solution changed from yellow to an orange colour. Acetic anhydride (30.0 mmol, 2.82 mL) was added to the mixture, followed by zinc powder (30.0 mmol, 1.96 g) over a period of 1 hr. The mixture was topped up by the addition of acetic acid (3 mL) in order to dissolve any crystals formed, and stirred for a total of 2 hr at 22°C. The mixture was filtered and the cake was washed with ethyl acetate (60 mL). Samples were dried *in vacuo* and purified on a silica column by flash chromatography.

α -Amido- β -ketoester **4.35a** was isolated as a colourless oil (1.16 g, 60%). R_f (hexane/ethyl acetate, 2:1) 0.22. ¹H-NMR (CDCl₃) δ : 1.30 (t, 3H, CH₂CH₃, *J* = 7.2 Hz), 2.06 (d, 3H, CH₃, *J* = 4.9 Hz), 2.38 (s, 3H, C _{γ} H₃), 4.27 (t, 2H, OCH₂CH₃, *J* = 7.2 Hz), 5.24 (d, 1H, C _{α} H, *J* = 7.2 Hz). ESI-MS calculated for C₈H₁₄NO₄⁺ [M+H]⁺ 188.09232, found 188.0845.

α -Amido- β -ketoester **4.35b** was isolated as a colourless oil (837 mg, 40%). R_f (methylene chloride/ethyl acetate, 2:1) 0.22. ¹H-NMR (CDCl₃) δ : 2.07 (s, 3H, CH₃), δ : 3.45 (s, 3H, OCH₃), δ : 4.36 (d, 2H, CH₂, *J* = 6.1 Hz), δ : 5.40 (d, 1H, C _{α} H, *J* = 6.6 Hz). ESI-MS calculated for C₈H₁₄NO₅⁺ [M+H]⁺ 204.08722, found 204.0766.

4.9.8. Fluorination of β -Ketoesters with Tetrafluoride Analog Reagents

4.9.8.1. Diethylaminosulfur Trifluoride Reagent

A solution of β -ketoester (0.53 mmol; either 67 μ L compound **4.34a**, 99 mg compound **4.35a**, or 108 mg compound **4.35b**) in methylene chloride (2 mL) contained in a three-neck, 25 mL round bottom flask, under argon, a rubber septum and magnetic stirring bar was cooled to -78°C . Neat DAST (1.06 mmol, 140 μ L) was added to the solution dropwise over a period of 15 min, and warmed up to 21°C for 2 hr. The reaction was quenched with NaHCO_3 (2.5 mL). The products were extracted with methylene chloride (3 x 2 mL), the organic phase was dried with sodium sulphate, filtered and evaporated *in vacuo*, and purified on a silica column by flash chromatography. Alternative variations to the reaction include addition of either ZnI_2 (0.50% mmol, 1.6 mg), BF_3 diethyletherate (2.12 mmol, 2.7 mL; 1.1 mmol, 1.3 mL; or 0.69 mmol, 0.87 mL), or triethylamine trihydrofluoride (1.20 mmol, 195 μ L; or 0.60 mmol, 98 μ L) before the addition of DAST. No products were observed when using 1:1 ratio of starting material and DAST as indicated by $^1\text{H-NMR}$ spectroscopy.

Compound **4.39** was isolated as a colourless oil (24 mg, 15%). R_f (hexane/ethyl acetate, 10:1) 0.51. $^1\text{H-NMR}$ (CDCl_3) δ : 1.11 (t, 6H, $(\text{CH}_2\text{CH}_3)_2$, $J = 7.3$ Hz), 1.33 (t, 3H, CH_2CH_3 , $J = 7.3$ Hz), δ : 2.39 (d, 3H, $\text{C}_\gamma\text{H}_3$, $J = 3.9$ Hz), δ : 3.04 (q, 4H, $(\text{CH}_2\text{CH}_3)_2$, $J = 6.9$ Hz), δ : 4.29 (m, 2H, CH_3CH_2). $^{19}\text{F NMR}$ (CDCl_3 ; externally locked with CFCl_3) δ : -143 (s). No mass detected by ESI-MS for the expected $[\text{M}^+ + \text{H}]^+$ product.

4.9.8.2. Reaction of XtalFluor-E Reagent with a Model β -Ketoester

A solution of XtalFluor-E (0.0530 mmol, 12.1 mg; Sigma Aldrich) and triethylamine trihydrofluoride (0.11 mmol, 17 μ L) in anhydrous methylene chloride (0.2 mL) were contained in a 3 mL conical vial with a water-cooled condenser, under argon, magnetic stirring bar, and cooled to -78°C . The model β -ketoester (0.0530 mmol, 11.5 mg dissolved in 0.1 mL of anhydrous methylene chloride; 2-ethoxyamido-3-oxo-ethylbutyrate) was added dropwise to the mixture over a period of 10 min. The mixture was warmed up to 22°C and stirred for 2 hr. The reaction was quenched with NaHCO_3 (1 mL), and the products were extracted into methylene chloride (3 x 1 mL), dried with sodium sulphate, filtered and evaporated *in vacuo*. The mixture had several side products based on TLC analysis, and no success was obtained by silica gel column chromatography.

4.9.9. Dithiolane Esters

4.9.9.1. Synthesis of Dithiolane Ester

A solution of β -ketoester (0.53 mmol; either 67 μ L compound **4.35d** or 108 mg compound **4.35b**) and 1,2 ethanedithiol (1.06 mmol 124 μ L) in anhydrous methylene chloride (2 mL) were contained in a three-neck, 25 mL round bottom flask, under argon, a rubber septum and magnetic stirring bar at 22°C . After 10 min, $\text{BF}_3\text{-Et}_2\text{O}$ (0.689 mmol, 87.0 μ L) was added dropwise to the mixture and stirred at 22°C for 15 hr. For dithiolane **4.41d** afforded from β -ketoester **4.35d** starting material, the mixture was diluted with hexane (3 mL) and washed

with brine (3 x 3 mL). For dithiolane **4.41b** afforded from β -ketoester **4.35b** starting material, the mixture was diluted with ethyl acetate (3 mL) and washed with brine (3 x 3 mL). The organic extracts were dried with sodium sulphate, concentrated *in vacuo* as colourless oils, and purified by flash silica gel chromatography.

1,2-Dithiolane-3-ethylbutanoate (**4.41d**) was isolated as a colourless oil (104 mg, 95%). R_f (hexane/ethyl acetate, 7:1) 0.57. $^1\text{H-NMR}$ (CDCl_3) δ : 1.25 (t, 3H, CH_2CH_3 , $J = 7.1$ Hz), 1.89 (s, 3H, CH_3), δ : 2.99 (s, 2H, CH_2), δ : 3.32 (s, 4H, CH_2CH_2), δ : 4.14 (q, 2H, CH_2CH_3 , $J = 7.1$ Hz). No mass detected by ESI-MS and ESI-GC/MS for the expected $[\text{M}^+ + \text{H}]^+$ product.

The complex reaction mixture for 1,2-dithiolane-3-methoxy-3-methylbutanoate (**4.41b**) precluded its isolation by flash silica gel chromatography. ESI-MS calculated for $\text{C}_{10}\text{H}_{18}\text{NO}_4\text{S}_2^+$ $[\text{M} + \text{H}]^+$ 280.06784, found 280.0550.

4.9.9.2. Fluorination of 3,3-Dithioester

A solution of *N*-bromosuccinimide (2.00 mmol, 362 mg) and pyridinium hydrofluoride (3 mmol, 351 μL) in methylene chloride (2 mL) at -78°C with stirring were contained in a 25 mL round bottom polypropylene flask, under argon, a rubber septum and magnetic stirring bar. Compound **4.41d** (0.500 mmol, 105 mg) was added dropwise over 15 min and stirred for 60 min at -78°C . The mixture was diluted with methylene chloride (10 mL). The bottom layer of the organic solution was applied to neutral alumina resin and the flow through was collected. The crude mixture was partially dried by a stream of argon gas before examination by $^{19}\text{F-NMR}$.

^{19}F -NMR (externally locked with CFCl_3) δ : -67.6, -73.4, -86.2, -90.7. No mass detected by ESI-MS and ESI-GC/MS for the expected $[\text{M}^+ + \text{H}]^+$ product.

CHAPTER 5

SUMMARY AND FUTURE WORK

The thioacylating agents generated from the processing of fluorinated methionine analogs by L-methionine γ -lyase from *T. vaginalis* (TvMGL1) were identified and their chemistry was characterized. Thiocarbonyl difluoride generated from the processing of TFM (5.1) by TvMGL1 was found to sequentially thiocarbamoylate two primary amines. On the other hand, thioformyl fluoride generated from the processing of DFM (5.2) by TvMGL1 was found to thioformylate a single primary amine, but had the potential to form an amidine upon reacting with a second primary amine. Based on theoretical calculations using high level of theory, the theoretical pK_a values for the mercaptans, generated from the enzymatic processing of the fluorinated compounds by TvMGL1, suggests that the compounds are likely to collapse as a result of elimination. The theoretical calculated heats of formation for thiocarbonylation and thioformylation suggests that the reactions are extremely thermodynamically favourable. For model organisms expressing MGL, these results suggest that the generation of the thioacylating agents, upon processing the fluorinated methionine analogs by TvMGL1, likely contributed to the observed cellular cytotoxicity in the cell growth inhibition assay. Thus, the generation of the thioacylating agents likely results in cellular toxicity as a result of thioacylation of primary amines, and may not require cross-linking as previously proposed by Alston and Bright (1983). Knowledge of the chemistry for the thioacylating agents may be applied to other areas of cellular biochemistry, and in

designing a second generation of fluorinated methionine analogs by replacing the hydrogen in the difluoromethylthio group with other moieties (**5.3**; Figure 5.1).

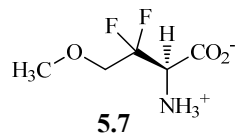
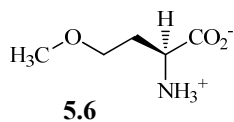
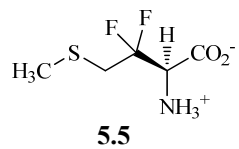
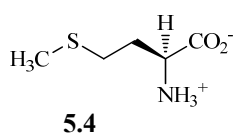
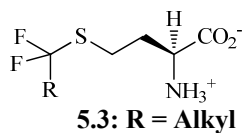
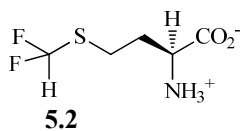
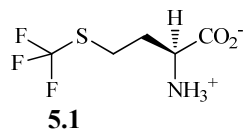


Figure 5.1. L-Methionine (5.4), L-homocysteine (5.6) and their fluorine derivatives.

The enzymatic processing of TFM and DFM by TvMGL1 reveals that the γ -elimination step is rate determining. The bulky fluorine atoms in the compound were found to enhance the turnover rate of the enzyme, and did not interfere with the Michaelis-Menten complex. The results suggest that the enzyme may handle large side chain substitutions. Mutation of the active site residue, C113 in TvMGL1, suggests that the residue plays an important role in catalysis. A definitive understanding into the exact role of C113 side chain, such as its implicated role in substrate specificity, will require structural and biophysical data in order to substantiate the kinetic values, which has not been reported for MGL enzymes as studied to date. Future application of TvMGL1 C113S mutant may extend to verifying its catalytic role by using fluorinated methionine analogs.

A synthetic route to 3,3-difluoro-*O*-methyl- L-homoserine (**5.7**), an oxo derivative of L-methionine was not obtained. A promising route might involve the Neber reaction, if one is able to avoid the undesired side product, isoxazole. The only reported synthetic route to the sulfur derivative, 3,3-difluoro-L-methionine (**5.5**), involves 19 steps with an overall yield of 0.4% (Keqiang *et al.*, 1998). Thus, there is a need to find an alternative synthetic route to the oxo derivative, 3,3-difluoro-*O*-methyl- L-homoserine (**5.7**). Future studies with the fluorinated compound may involve characterization of the catalytic role of C113 in TvMGL1, and its incorporation into proteins as an unnatural amino acid for biophysical studies.

Enzymatic processing of *O*-methyl-L-homoserine (**5.6**) by TvMGL1 is 3.5-fold greater than the turnover rate of L-methionine and no significant differences in its K_m value when compared to L-methionine. The results suggest that the proposed oxo moiety in 3,3-difluoro-*O*-methyl-L-homoserine (**5.7**) will not interfere with the processing of the compound. These

results are unexpected because the oxo moiety is a poorer leaving group than sulfur. Reasons for the enhanced turnover are unclear, but it may have resulted from an improved orientation within the active site of the enzyme. Thus, future biophysical and structural data are required to further elucidate these differences.

REFERENCES

- Abeles, R.H., and Maycock, A.L. (1976). Suicide enzyme inactivators. *Acc. Chem. Res.* *9*, 313-19.
- Abeles, R.H., and Walsh, C.T. (1973). Acetylenic enzyme inactivators. Inactivation of gamma-cystathionase, *in vitro* and *in vivo* by propargylglycine. *J. Am. Chem. Soc.* *95*, 6124-25.
- Ackers, J.P., Clark, C.G., Diamond, L.S., Cantellano, M.E., Jackson, T.F.H.G., Martínez-Palomo, A., Mirelman, D., Hernández, O.M., Tamayo, R.P., William A. Petri, J., Reed, S.L., Palacios, G.M.R., Samuelson, J.C., Preciado, J.I.S., Tannich, E., Takeuchi, T., and García, C.X. (1997). Amoebiasis. *WHO Wkly. Epidemiol. Rec.* *72*, 97-100.
- Adams, D.J., Tavener, S.J., and Clark, J.H. (1998). Reactions of silver(I) trifluoromethanethiolate with halotrimethylsilanes: in situ generation of trimethylsilyl trifluoromethyl sulfide. *J. Fluorine Chem.* *90*, 87-91.
- Agren, D., Schnell, R., Oehlmann, W., Singh, M., and Schneider, G. (2008). Cysteine synthase (CysM) of *Mycobacterium tuberculosis* is an O-phosphoserine sulfhydrylase: evidence for an alternative cysteine biosynthesis pathway in mycobacteria. *J. Biol. Chem.* *283*, 31567-74.
- Aguilera, P., Barry, T., and Tovar, J. (2008). *Entamoeba histolytica* mitochondria: organelles in search of a function. *Exp. Parasitol.* *118*, 10-16.
- Ali, V., and Nozaki, T. (2007). Current therapeutics, their problems, and sulfur-containing-amino-acid metabolism as a novel target against infections by "amitochondriate" protozoan parasites. *Clin. Microbiol. Rev.* *20*, 164-87.
- Alston, T.A., and Bright, H.J. (1983). Conversion of trifluoromethionine to a cross-linking agent by gamma-cystathionase. *Biochem. Pharmacol.* *32*, 947-50.
- Alves, M.J., Fortes, A.G., Lemos, A., and Martins, C. (2005). Ethyl 3-(2-Pyridyl)-2H-azirine-2-carboxylate: Synthesis and Reaction with Dienes. *Synthesis*, 555-58.
- Anderson, I.J., and Loftus, B.J. (2005). *Entamoeba histolytica*: observations on metabolism based on the genome sequence. *Exp Parasitol* *110*, 173-7.

- Andersson, J., Hirt, R., Foster, P., and Roger, A. (2006). Evolution of four gene families with patchy phylogenetic distributions: influx of genes into protist genomes. *BMC Evol. Biol.* *6*, 27-45.
- Appelman, E.H., Mendelsohn, M.H., and Kim, H. (1985). Isolation and characterization of acetyl hypofluorite. *J. Am. Chem. Soc.* *107*, 6515-18.
- Asato, A.E., and Liu, R.S.H. (1986). The preparation of vicinal difluoroolefinic carbonyl compounds and their application to the synthesis of difluororetinol analogs. *Tetrahedron Lett.* *27*, 3337-40.
- Bartlett, J.G., Chang, T.W., Gurwith, M., Gorbach, S.L., and Onderdonk, A.B. (1978). Antibiotic-associated pseudomembranous colitis due to toxin-producing clostridia. *N. Engl. J. Med.* *298*, 531-4.
- Beerheide, W., Sim, M.M., Tan, Y.-J., Bernard, H.-U., and Ting, A.E. (2000). Inactivation of the human papillomavirus-16 E6 oncoprotein by organic disulfides. *Bioorg. Med. Chem.* *8*, 2549-60.
- Berkowitz, D.B., Karukurichi, K.R., de la Salud-Bea, R., Nelson, D.L., and McCune, C.D. (2008). Use of Fluorinated Functionality in Enzyme Inhibitor Development: Mechanistic and Analytical Advantages. *J. Fluor. Chem.* *129*, 731-42.
- Bildstein, S., Ducep, J.-B., Jacobi, D., and Zimmermann, P. (1995). Synthesis of tetrasubstituted vicinal difluoroolefines. *Tetrahedron Lett.* *36*, 5007-10.
- Bingham, R.C. (1976). The stereochemical consequences of electron delocalization in extended π systems. An interpretation of the cis effect exhibited by 1,2-disubstituted ethylenes and related phenomena. *J. Am. Chem. Soc.* *98*, 535-40.
- Bitencourt, M., Freitas, M.P., and Rittner, R. (2007). Conformational and stereoelectronic investigation in 1,2-difluoropropane: The gauche effect. *J. Mol. Struct.* *840*, 133-36.
- Bock, E., Iwacha, D., Hutton, H., and Queen, A. (1968). Electric moments and conformation of substituted fluoroformates in benzene solutions. *Can. J. Chem.* *46*, 1645-8.

- Bosch, M.P., Pérez, R., Lahuerta, G., Hernanz, D., Camps, F., and Guerrero, A. (1996). Difluoropalmitic acids as potential inhibitors of the biosynthesis of the sex pheromone of the Egyptian armyworm *Spodoptera littoralis*--IV. *Bioorg. Med. Chem.* *4*, 467-72.
- Bradford, M.M. (1976). A rapid and sensitive method for the quantitation of microgram quantities of protein utilizing the principle of protein-dye binding. *Anal. Biochem.* *72*, 248-54.
- Brown, D.M., Upcroft, J.A., Dodd, H.N., Chen, N., and Upcroft, P. (1999). Alternative 2-keto acid oxidoreductase activities in *Trichomonas vaginalis*. *Mol. Biochem. Parasitol.* *98*, 203-14.
- Bruchhaus, I., Richter, S., and Tannich, E. (1998). Recombinant expression and biochemical characterization of an NADPH:flavin oxidoreductase from *Entamoeba histolytica*. *Biochem. J.* *330*, 1217-21.
- Burfield, D.R., and Smithers, R.H. (1978). Desiccant efficiency in solvent drying. 3. Dipolar aprotic solvents. *J. Org. Chem.* *43*, 3966-68.
- Burk, P., Koppel, I.A., Rummel, A., and Trummel, A. (2000). Can O-H Acid be More Acidic Than Its S-H Analog? A G2 Study of Fluoromethanols and Fluoromethanethiols. *J. Phys. Chem. A* *104*, 1602-07.
- Burns, K.E., Baumgart, S., Dorrestein, P.C., Zhai, H., McLafferty, F.W., and Begley, T.P. (2005). Reconstitution of a new cysteine biosynthetic pathway in *Mycobacterium tuberculosis*. *J Am Chem Soc* *127*, 11602-3.
- Buss, C.W., Coe, P.L., and Tatlow, J.C. (1986). 3,3-Difluorochlorambucil. *J. Fluor. Chem.* *34*, 83-104.
- Careless, A.J., Kroto, H.W., and Landsberg, B.M. (1973). The microwave spectrum, structure and dipole moment of thiocarbonyl fluoride, F₂CS. *Chem. Phys.* *1*, 371-75.
- Carlson, R., Larsson, U., and Hansson, L. (1992). Efficient Synthesis of Imines by a Modified Titanium Tetrachloride Procedure. *Acta. Chem. Scand.* *24*, 1211-14.
- Carlton, J.M., Hirt, R.P., Silva, J.C., Delcher, A.L., Schatz, M., Zhao, Q., Wortman, J.R., Bidwell, S.L., Alsmark, U.C., Besteiro, S., Sicheritz-Ponten, T., Noel, C.J., Dacks, J.B.,

- Foster, P.G., Simillion, C., Van de Peer, Y., Miranda-Saavedra, D., Barton, G.J., Westrop, G.D., Muller, S., Dessi, D., Fiori, P.L., Ren, Q., Paulsen, I., Zhang, H., Bastida-Corcuera, F.D., Simoes-Barbosa, A., Brown, M.T., Hayes, R.D., Mukherjee, M., Okumura, C.Y., Schneider, R., Smith, A.J., Vanacova, S., Villalvazo, M., Haas, B.J., Perteu, M., Feldblyum, T.V., Utterback, T.R., Shu, C.L., Osoegawa, K., de Jong, P.J., Hrady, I., Horvathova, L., Zubacova, Z., Dolezal, P., Malik, S.B., Logsdon, J.M., Jr., Henze, K., Gupta, A., Wang, C.C., Dunne, R.L., Upcroft, J.A., Upcroft, P., White, O., Salzberg, S.L., Tang, P., Chiu, C.H., Lee, Y.S., Embley, T.M., Coombs, G.H., Mottram, J.C., Tachezy, J., Fraser-Liggett, C.M., and Johnson, P.J. (2007). Draft genome sequence of the sexually transmitted pathogen *Trichomonas vaginalis*. *Science* 315, 207-12.
- Cellarier, E., Durando, X., Vasson, M.P., Farges, M.C., Demiden, A., Maurizis, J.C., Madelmont, J.C., and Chollet, P. (2003). Methionine dependency and cancer treatment. *Cancer Treat. Rev.* 29, 489-99.
- Chambers, R.D., O'Hagan, D., Lamont, R.B., and Jaina, S.C. (1990). The difluoromethylenephosphonate moiety as a phosphate mimic: X-ray structure of 2-amino-1,1-difluoroethylphosphonic acid. *J. Chem. Soc., Chem. Commun.*, 1053-54.
- Chaudiere, J., Courtin, O., and Leclaire, J. (1992). Glutathione oxidase activity of selenocystamine: a mechanistic study. *Arch. Biochem. Biophys.* 296, 328-36.
- Christen, P., Kasper, P., Gehring, H., and Sterk, M. (1996). Stereochemical constraint in the evolution of pyridoxal-5'-phosphate-DApenDant enzymes. A hypothesis. *FEBS Lett.* 389, 12-14.
- Christen, P., and Mehta, P.K. (2001). From cofactor to enzymes. The molecular evolution of pyridoxal-5'-phosphate-dependent enzymes. *Chem Rec* 1, 436-47.
- Clark, L.C., Combs, G.F., Jr., Turnbull, B.W., Slate, E.H., Chalker, D.K., Chow, J., Davis, L.S., Glover, R.A., Graham, G.F., Gross, E.G., Krongrad, A., Leshner, J.L., Jr., Park, H.K., Sanders, B.B., Jr., Smith, C.L., and Taylor, J.R. (1996). Effects of selenium supplementation for cancer prevention in patients with carcinoma of the skin. A

- randomized controlled trial. Nutritional Prevention of Cancer Study Group. *JAMA* 276, 1957-63.
- Coalson, D.W., Mechem, J.O., Stern, P.H., and Hoffman, R.M. (1982). Reduced availability of endogenously synthesized methionine for S-adenosylmethionine formation in methionine-dependent cancer cells. *Proc. Natl. Acad. Sci. USA* 79, 4248-51.
- Coombs, G.H., and Mottram, J.C. (2001). Trifluoromethionine, a prodrug designed against methionine gamma-lyase-containing pathogens, has efficacy in vitro and in vivo against *Trichomonas vaginalis*. *Antimicrob. Agents Chemother.* 45, 1743-5.
- Coombs, G.H., Westrop, G.D., Suchan, P., Puzova, G., Hirt, R.P., Embley, T.M., Mottram, J.C., and Muller, S. (2004). The amitochondriate eukaryote *Trichomonas vaginalis* contains a divergent thioredoxin-linked peroxiredoxin antioxidant system. *J. Biol. Chem.* 279, 5249-56.
- Crossnoe, C.R., Germanas, J.P., LeMagueres, P., Mustata, G., and Krause, K.L. (2002). The crystal structure of *Trichomonas vaginalis* ferredoxin provides insight into metronidazole activation. *J Mol Biol* 318, 503-18.
- Cudmore, S.L., Delgaty, K.L., Hayward-McClelland, S.F., Petrin, D.P., and Garber, G.E. (2004). Treatment of infections caused by metronidazole-resistant *Trichomonas vaginalis*. *Clin. Microbiol. Rev.* 17, 783-93.
- Curtiss, L.A., Raghavachari, K., Redfern, P.C., Rassolov, V., and Pople, J.A. (1998). Gaussian-3 (G3) theory for molecules containing first and second-row atoms. *J. Chem. Phys.* 109, 7764-76.
- Curtiss, L.A., Redfern, P.C., Raghavachari, K., Rassolov, V., and Pople, J.A. (1999). Gaussian-3 theory using reduced Møller-Plesset order. *J. Chem. Phys.* 110, 4703-09.
- Danielson, M.A., and Falke, J.J. (1996). Use of ¹⁹F NMR to probe protein structure and conformational changes. *Annu Rev Biophys Biomol Struct* 25, 163-95.
- Dawson, R.B. (1985). *Data for biochemical research* (Oxford, Clarendon Press).
- De Marco, C., and Bognolo, D. (1962). The reaction between cysteamine and pyridoxal phosphate. *Arch. Biochem. Biophys.* 98, 526-27.

- de Rege, P.J.F., Gladysz, J.A., and Horvath, I.T. (1997). Spectroscopic Observation of the Formyl Cation in a Condensed Phase. *Science* 276, 776-79.
- Degani, Y., Neumann, H., and Patchornik, A. (1970). Selective cyanilation of sulfhydryl groups. *J. Am. Chem. Soc.* 92, 6969-71.
- Demidkina, T.V., Anston, A.A., Faleev, N.G., Phillips, R.S., and Zakomyrdina, L.N. (2009). Spatial structure and mechanism of tyrosine phenol-lyase and tryptophan indole-lyase. *Mol. Biol.* 43, 295-308.
- Dias, B., and Weimer, B. (1998). Purification and characterization of L-methionine gamma-lyase from *brevibacterium linens* BL2. *Appl Environ Microbiol* 64, 3327-31.
- Ditchfield, R. (1974). Self-consistent perturbation theory of diamagnetism -- I. A gauge-invariant LCAO method for N.M.R. chemical shifts. *Mol. Phys.* 27, 789 - 807.
- Downs, A.J. (1962). Thiocarbonyl fluoride. *J. Chem. Soc.*, 4361-6.
- Dubnovitsky, A.P., Ravelli, R.B., Popov, A.N., and Papageorgiou, A.C. (2005). Strain relief at the active site of phosphoserine aminotransferase induced by radiation damage. *Protein Sci.* 14, 1498-507.
- Duewel, H., Daub, E., Robinson, V., and Honek, J.F. (1997). Incorporation of trifluoromethionine into a phage lysozyme: implications and a new marker for use in protein 19F NMR. *Biochemistry* 36, 3404-16.
- Duewel, H.S., Daub, E., Robinson, V., and Honek, J.F. (2001). Elucidation of Solvent Exposure, Side-Chain Reactivity, and Steric Demands of the Trifluoromethionine Residue in a Recombinant Protein . *Biochemistry* 40, 13167-76.
- Dunne, R.L., Dunn, L.A., Upcroft, P., O'Donoghue, P.J., and Upcroft, J.A. (2003). Drug resistance in the sexually transmitted protozoan *Trichomonas vaginalis*. *Cell Res* 13, 239-49.
- Durig, J.R., Guirgis, G.A., and Li, Y.S. (1981). Microwave, Raman, and far infrared spectra, barrier to internal rotation, and dipole moment of 2,2-difluoropropane. *J. Chem. Phys.* 74, 5946.

- Durig, J.R., Zheng, C., Guirgis, G.A., and Nanaie, H. (2005). Microwave spectrum, r_0 structure, barriers to internal rotation and ab initio calculations of gauche-1,1-difluoropropane. *J. Mol. Struct.* *742*, 191-98.
- Edwards, D.I. (1980). Mechanisms of selective toxicity of metronidazole and other nitroimidazole drugs. *Br. J. Vener. Dis.* *56*, 285-90.
- Eliot, A.C., and Kirsch, J.F. (2004). Pyridoxal phosphate enzymes: mechanistic, structural, and evolutionary considerations. *Annu Rev Biochem* *73*, 383-415.
- Ellis, J.E., Yarlett, N., Cole, D., Humphreys, M.J., and Lloyd, D. (1994). Antioxidant defences in the microaerophilic protozoan *Trichomonas vaginalis*: comparison of metronidazole-resistant and sensitive strains. *Microbiology* *140 (Pt 9)*, 2489-94.
- Ellis, R.J. (2001). Macromolecular crowding: an important but neglected aspect of the intracellular environment. *Curr Opin Struct Biol* *11*, 114-9.
- Emsley, J., and Freeman, N.J. (1987). [beta]-diketone interactions : Part 5. Solvent effects on the keto-enol equilibrium. *J. Mol. Struct.*, 193-204.
- Esaki, N., Nakayama, T., Sawada, S., Tanaka, H., and Soda, K. (1985). ¹H NMR studies of substrate hydrogen exchange reactions catalyzed by L-methionine gamma-lyase. *Biochemistry* *24*, 3857-62.
- Esaki, N., Suzuki, T., Tanaka, H., Soda, K., and Rando, R.R. (1977). Deamination and gamma-addition reactions of vinylglycine by L-methionine gamma-lyase. *FEBS Lett.* *84*, 309-12.
- Faleev, N.G., Alferov, K.V., Tsvetikova, M.A., Morozova, E.A., Revtovich, S.V., Khurs, E.N., Vorob'ev, M.M., Phillips, R.S., Demidkina, T.V., and Khomutov, R.M. (2009). Methionine gamma-lyase: mechanistic deductions from the kinetic pH-effects. The role of the ionic state of a substrate in the enzymatic activity. *Biochim. Biophys. Acta* *1794*, 1414-20.
- Feeney, J., McCormick, J.E., Bauer, C.J., Birdsall, B., Moody, C.M., Starkmann, B.A., Young, D.W., Francis, P., Havlin, R.H., Arnold, W.D., and Oldfield, E. (1996). ¹⁹F Nuclear Magnetic Resonance Chemical Shifts of Fluorine Containing Aliphatic Amino

- Acids in Proteins: Studies on *Lactobacillus casei* Dihydrofolate Reductase Containing (2S,4S)-5-Fluoroleucine. *J. Am. Chem. Soc.* *118*, 8700-06.
- Fileti, E.E., Chaudhuri, P., and Canuto, S. (2004). Relative strength of hydrogen bond interaction in alcohol-water complexes. *Chem. Phys. Lett.* *400*, 494-99.
- Ford, G.C., Eichele, G., and Jansonius, J.N. (1980). Three-dimensional structure of a pyridoxal-phosphate-dependent enzyme, mitochondrial aspartate aminotransferase. *Proc. Natl. Acad. Sci. USA* *77*, 2559-63.
- Frisch, A.E., Dennington, R.D., Keith, T.A., Neilsen, A.B., and Holder, A.J. (2003a). GaussView, revision 3.0.9 (Pittsburgh PA, Gaussian, Inc.).
- Frisch, M.J., Trucks, G.W., Schlegel, H.B., Scuseria, G.E., Robb, M.A., Cheeseman, J.R., Montgomery, J.A., Jr., Vreven, T., Kudin, K.N., Burant, J.C., Millam, J.M., Iyengar, S.S., Tomasi, J., Barone, V., Mennucci, B., Cossi, M., Scalmani, G., Rega, N., Petersson, G.A., Nakatsuji, H., Hada, M., Ehara, M., Toyota, K., Fukuda, R., Hasegawa, J., Ishida, M., Nakajima, T., Honda, Y., Kitao, O., Nakai, H., Klene, M., Li, X., Knox, J.E., Hratchian, H.P., Cross, J.B., Bakken, V., Adamo, C., Jaramillo, J., Gomperts, R., Stratmann, R.E., Yazyev, O., Austin, A.J., Cammi, R., Pomelli, C., Ochterski, J.W., Ayala, P.Y., Morokuma, K., Voth, G.A., Salvador, P., Dannenberg, J.J., Zakrzewski, V.G., Dapprich, S., Daniels, A.D., Strain, M.C., Farkas, O., Malick, D.K., Rabuck, A.D., Raghavachari, K., Foresman, J.B., Ortiz, J.V.C., Q., Baboul, A.G., Clifford, S., Cioslowski, J., Stefanov, B.B., Liu, G., Liashenko, A., Piskorz, P., Komaromi, I., Martin, R.L., Fox, D.J., Keith, T., Al-Laham, M.A., Peng, C.Y., Nanayakkara, A., Challacombe, M., Gill, P.M.W., Johnson, B.; Chen, W., Wong, M.W., Gonzalez, C., and Pople, J.A. (2003b). Gaussian 03, revision A.9 (Pittsburgh, PA, Gaussian, Inc.).
- Gerken, M., Boatz, J.A., Kornath, A., Haiges, R., Schneider, S., Schroer, T., and Christe, K.O. (2002). The ¹⁹F NMR shifts are not a measure for the nakedness of the fluoride anion. *J. Fluorine Chem.* *116*, 49-58.
- Gillespie, R.J. (1967). Electron-Pair Repulsions and Molecular Shape. *Angew. Chem. Inter. Edit.* *6*, 819-30.

- Girard, A., Greck, C., Ferroud, D., and Genêt, J.P. (1996). Syntheses of the syn and anti [alpha]-amino-[beta]-hydroxy acids of vancomycin: (2S, 3R) and (2R, 3R) p-chloro-3-hydroxytyrosines. *Tetrahedron Lett.* *37*, 7967-70.
- Gorrell, T., Yarlett, N., and Müller, M. (1984). Isolation and characterization of *Trichomonas vaginalis* ferredoxin. *Carlsberg. Res. Commun.*, 259-68.
- Grishin, N.V., Phillips, M.A., and Goldsmith, E.J. (1995). Modeling of the spatial structure of eukaryotic ornithine decarboxylases. *Protein Sci* *4*, 1291-304.
- Guggenheim, S., and Flavin, M. (1969). Cystathionine gamma-synthase from *Salmonella*. Beta elimination and replacement reactions and inhibition by O-succinylserine. *J. Biol. Chem.* *244*, 3722-7.
- Guo, H., Lishko, V.K., Herrera, H., Groce, A., Kubota, T., and Hoffman, R.M. (1993). Therapeutic tumor-specific cell cycle block induced by methionine starvation *in vivo*. *Cancer Res.*, 5676-79.
- Haas, A., and Wanzke, W. (1987). Thiocarbonyl fluorides in the hydrogen fluoride solvent system. Preparation and reactions of halogenated thiocarbenium ions. *Chem. Ber.* *120*, 429-33.
- Hart, D.J., Cain, P.A., and Evans, D.A. (1978a). Approaches to the synthesis of masked p-quinone methides. Applications to the total synthesis of (+-)-cherylline. *J. Am. Chem. Soc.* *100*, 1548-57.
- Hart, D.J., Cain, P.A., and Evans, D.A. (1978b). Approaches to the synthesis of masked p-quinone methides. Applications to the total synthesis of (+-)-cherylline. *J. Am. Chem. Soc.* *100*, 1548-57.
- Hasek, W.R., Smith, W.C., and Engelhardt, V.A. (1960). The Chemistry of Sulfur Tetrafluoride. II. The Fluorination of Organic Carbonyl Compounds¹. *J. Am. Chem. Soc.* *82*, 543-51.
- Hayashi, H., Mizuguchi, H., and Kagamiyama, H. (1998). The imine-pyridine torsion of the pyridoxal 5'-phosphate Schiff base of aspartate aminotransferase lowers its pKa in the

- unliganded enzyme and is crucial for the successive increase in the pKa during catalysis. *Biochemistry* 37, 15076-85.
- Hayashi, H., Mizuguchi, H., Miyahara, I., Nakajima, Y., Hirotsu, K., and Kagamiyama, H. (2003). Conformational Change in Aspartate Aminotransferase on Substrate Binding Induces Strain in the Catalytic Group and Enhances Catalysis. *J. Biol. Chem.* 278, 9481-88.
- Heyl, D., Luz, E., Harris, S.A., and Folkers, K. (1951). Phosphates of the Vitamin B6 Group. I. The Structure of Codecarboxylase. *J. Am. Chem. Soc.* 73, 3430-33.
- Higgins, W., and Miles, E.W. (1978). Affinity labeling of the pyridoxal phosphate binding site of the beta2 subunit of Escherichia coli tryptophan synthase. *J. Biol. Chem.* 253, 4648-52.
- Hoffman, R.M., and Jacobsen, S.J. (1980). Reversible growth arrest in simian virus 40-transformed human fibroblasts. *Proc Natl Acad Sci USA*, 7306-10.
- Holbrook, E.L., Greene, R.C., and Krueger, J.H. (1990). Purification and properties of cystathionine gamma-synthase from overproducing strains of Escherichia coli. *Biochemistry* 29, 435-42.
- Holm, L., and Park, J. (2000). DaliLite workbench for protein structure comparison. *Bioinformatics* 16, 566-7.
- Honda, T., and Tokushige, M. (1986). Effects of temperature and monovalent cations on activity and quaternary structure of tryptophanase. *J. Biochem.* 100, 679-85.
- Houston, M.E., Harvath, L., and Honek, J.F. (1997). Syntheses of and chemotactic responses elicited by fMet-Leu-Phe analogs containing difluoro- and trifluoromethionine. *Bioorg. Med. Chem. Lett.* 7, 3007-12.
- Houston, M.E., and Honek, J.F. (1989). Facile synthesis of fluorinated methionines. *J. Chem. Soc., Chem. Commun.*, 761-62.
- Howard, J.A.K., Hoy, V.J., O'Hagan, D., and Smith, G.T. (1996). How good is fluorine as a hydrogen bond acceptor? *Tetrahedron* 52, 12613-22.

- Hu, J., and Cheung, N.K. (2009). Methionine depletion with recombinant methioninase: in vitro and in vivo efficacy against neuroblastoma and its synergism with chemotherapeutic drugs. *Int J Cancer* *124*, 1700-6.
- Huang, H., Weintraub, A., Fang, H., and Nord, C.E. (2009). Antimicrobial resistance in *Clostridium difficile*. *Int J Antimicrob Agents* *34*, 516-22.
- Humphrey, W., Dalke, A., and Schulten, K. (1996). VMD: Visual molecular dynamics. *J. Mol. Graphics* *14*, 33-38.
- Inoue, H., Inagaki, K., Adachi, N., Tamura, T., Esaki, N., Soda, K., and Tanaka, H. (2000). Role of tyrosine 114 of L-methionine gamma-lyase from *Pseudomonas putida*. *Biosci Biotechnol Biochem* *64*, 2336-43.
- Ishijima, J., Nakai, T., Kawaguchi, S., Hirotsu, K., and Kuramitsu, S. (2000). Free energy requirement for domain movement of an enzyme. *J. Biol. Chem.* *275*, 18939-45.
- Jantova, S., Spirkova, K., Stankovsky, S., and Duchonova, P. (1999). Antibacterial effect of some substituted tricyclic quinazolines and their synthetic precursors. *Folia Microbiol. (Praha)* *44*, 187-90.
- Jellinek, F. (1959). Existence of the trifluoromethylmercaptide ion. *Proc. Chem. Soc., London*, 319-20.
- Johnston, M., Marcotte, P., Donovan, J., and Walsh, C. (1979). Mechanistic studies with vinylglycine and .beta.-haloaminobutyrate as substrates for cystathionine .gamma.-synthetase from *Salmonella typhimurium*. *Biochemistry* *18*, 1729-38.
- Johnston, M., Raines, R., Chang, M., Esaki, N., Soda, K., and Walsh, C. (1981). Mechanistic studies on reactions of bacterial methionine gamma-lyase with olefinic amino acids. *Biochemistry* *20*, 4325-33.
- Johnston, M., Raines, R., Walsh, C., and Firestone, R.A. (1980). Mechanism-based enzyme inactivation using an allyl sulfoxide-allyl sulfenate ester rearrangement. *J. Am. Chem. Soc.* *102*, 4241-50.
- Jones, W.M., Scaloni, A., Bossa, F., Popowicz, A.M., Schneewind, O., and Manning, J.M. (1991). Genetic relationship between acylpeptide hydrolase and acylase, two hydrolytic

- enzymes with similar binding but different catalytic specificities. *Proc. Natl. Acad. Sci. USA*, 2194-98.
- Juaristi, E., Tapia, J., and Mendez, R. (1986). Study of the anomeric effect in 2-substituted 1,3-dithianes. *Tetrahedron* 42, 1253-64.
- Kalyankar, G.D., and Snell, E.E. (1962). Pyridoxal-Catalyzed Decarboxylation of Amino Acids. *Biochemistry*, 594-600.
- Karpeisky, M.Y., and Ivanov, V.I. (1966). A Molecular Mechanism for Enzymatic Transamination. *Nature* 210, 493-96.
- Karube, Y., and Matsushima, Y. (1977). A model for an intermediate in pyridoxal catalyzed .gamma.-elimination and .gamma.-replacement reactions of amino acids. *J. Am. Chem. Soc.* 99, 7356-58.
- Keqiang, L., Leriche, C., and Liu, H.-w. (1998). Synthesis of [beta]-difluorine-containing amino acids. *Bioorg. Med. Chem.* 8, 1097-100.
- Kirij, N.V., Pasenok, S.V., Yagupolskii, Y.L., Tyrra, W., and Naumann, D. (2000). Bi(CF₃)₃/Cu(OCOCH₃)₂ -- a new system for the synthesis of 2-trifluoromethylcycloalkan-1-ones, trifluoromethylanilines and phenyl(trifluoromethyl)sulfane. *J. Fluorine Chem.* 106, 217-21.
- Klicic, J.J., Friesner, R.A., Liu, S.-Y., and Guida, W.C. (2002). Accurate Prediction of Acidity Constants in Aqueous Solution via Density Functional Theory and Self-Consistent Reaction Field Methods. *J. Phys. Chem. A* 106, 1327-35.
- Kokkinakis, D.M., Hoffman, R.M., Frenkel, E.P., Wick, J.B., Han, Q., Xu, M., Tan, Y., and Schold, S.C. (2001). Synergy between methionine stress and chemotherapy in the treatment of brain tumor xenografts in athymic mice. *Cancer Res* 61, 4017-23.
- Kudou, D., Misaki, S., Yamashita, M., Tamura, T., Esaki, N., and Inagaki, K. (2008). The Role of Cysteine 116 in the Active Site of the Antitumor Enzyme L-Methionine gamma-Lyase from *Pseudomonas putida*. *Biosci. Biotechnol. Biochem.* 72, 1722-30.
- Kudou, D., Misaki, S., Yamashita, M., Tamura, T., Takakura, T., Yoshioka, T., Yagi, S., Hoffman, R.M., Takimoto, A., Esaki, N., and Inagaki, K. (2007). Structure of the

- antitumour enzyme L-methionine gamma-lyase from *Pseudomonas putida* at 1.8 Å resolution. *J. Biochem.* *141*, 535-44.
- Kulda, J. (1999). Trichomonads, hydrogenosomes and drug resistance. *Int J Parasitol* *29*, 199-212.
- Kulda, J., Tachezy, J., and Cerkasovova, A. (1993). *In vitro* induced anaerobic resistance to metronidazole in *Trichomonas vaginalis*. *J. Eukaryot. Microbiol.* *40*, 262-69.
- Kumagai, H., Yamada, H., Matsui, H., Ohkishi, H., and Ogata, K. (1970). Tyrosine Phenol Lyase. *J. Biol. Chem.* *245*, 1773-77.
- L'Heureux, A., Beaulieu, F., Bennett, C., Bill, D.R., Clayton, S., LaFlamme, F.o., Mirmehrabi, M., Tadayon, S., Tovell, D., and Couturier, M. (2010). Aminodifluorosulfonium Salts: Selective Fluorination Reagents with Enhanced Thermal Stability and Ease of Handling. *J. Org. Chem.* *75*, 3401-11.
- Lange, H.G., and Shreeve, J.M. (1985). On the reactions of dimethylsulfoxide with acyl fluorides - pummerer rearrangements and formation of monofluoromethyl esters. *J. Fluorine Chem.* *28*, 219-27.
- Leitsch, D., Kolarich, D., Binder, M., Stadlmann, J., Altmann, F., and Duchene, M. (2009). *Trichomonas vaginalis*: metronidazole and other nitroimidazole drugs are reduced by the flavin enzyme thioredoxin reductase and disrupt the cellular redox system. Implications for nitroimidazole toxicity and resistance. *Mol. Microbiol.* *72*, 518-36.
- Leitsch, D., Kolarich, D., and Duchêne, M. (2010). The flavin inhibitor diphenyliodonium renders *Trichomonas vaginalis* resistant to metronidazole, inhibits thioredoxin reductase and flavin reductase, and shuts off hydrogenosomal enzymatic pathways. *Mol. Biochem. Parasitol.* *171*, 17-24.
- Leitsch, D., Kolarich, D., Wilson, I.B.H., Altmann, F., and Duchêne, M. (2007). Nitroimidazole Action in *Entamoeba histolytica*: A Central Role for Thioredoxin Reductase. *PLoS Biol.* *5*, e211.

- Lemieux, R.U., Pavia, A.A., Martin, J.C., and Watanabe, K.A. (1969). Solvation effects on conformational equilibria. Studies related to the conformational properties of 2-methoxytetrahydropyran and related methyl glycopyranosides. *Can. J. Chem.*, 4427-39.
- Lockwood, B.C., and Coombs, G.H. (1991). Purification and characterization of methionine gamma-lyase from *Trichomonas vaginalis*. *Biochem. J.* 279 (Pt 3), 675-82.
- Loftus, B., Anderson, I., Davies, R., Alsmark, U.C., Samuelson, J., Amedeo, P., Roncaglia, P., Berriman, M., Hirt, R.P., Mann, B.J., Nozaki, T., Suh, B., Pop, M., Duchene, M., Ackers, J., Tannich, E., Leippe, M., Hofer, M., Bruchhaus, I., Willhoeft, U., Bhattacharya, A., Chillingworth, T., Churcher, C., Hance, Z., Harris, B., Harris, D., Jagels, K., Moule, S., Mungall, K., Ormond, D., Squares, R., Whitehead, S., Quail, M.A., Rabinowitsch, E., Norbertczak, H., Price, C., Wang, Z., Guillen, N., Gilchrist, C., Stroup, S.E., Bhattacharya, S., Lohia, A., Foster, P.G., Sicheritz-Ponten, T., Weber, C., Singh, U., Mukherjee, C., El-Sayed, N.M., Petri, W.A., Jr., Clark, C.G., Embley, T.M., Barrell, B., Fraser, C.M., and Hall, N. (2005). The genome of the protist parasite *Entamoeba histolytica*. *Nature* 433, 865-8.
- Manukhov, I.V., Mamaeva, D.V., Morozova, E.A., Rastorguev, S.M., Faleev, N.G., Demidkina, T.V., and Zavilgelsky, G.B. (2006). L-methionine gamma-lyase from *Citrobacter freundii*: cloning of the gene and kinetic parameters of the enzyme. *Biochemistry (Mosc)* 71, 361-69.
- Matsuo, Y. (1957). Pyridoxal Catalysis of Non-enzymatic Transamination in Ethanol Solution. *J. Am. Chem. Soc.* 79, 2016-19.
- McCoy, R.H., Meyer, C.E., and Rose, W.C. (1935). Feeding experiments with mixtures of highly purified amino acids. *J. Biol. Chem.* 112, 283-302.
- McDonough, B., Macdonald, P.M., Sykes, B.D., and McElhaney, R.N. (1983). Fluorine-19 nuclear magnetic resonance studies of lipid fatty acyl chain order and dynamics in *Acholeplasma laidlawii* B membranes. A physical, biochemical, and biological evaluation of monofluoropalmitic acids as membrane probes. *Biochemistry* 22, 5097-103.

- McKie, A.E., Edlind, T., Walker, J., Mottram, J.C., and Coombs, G.H. (1998). The primitive protozoon *Trichomonas vaginalis* contains two methionine gamma-lyase genes that encode members of the gamma-family of pyridoxal 5'-phosphate-dependent enzymes. *J. Biol. Chem.* *273*, 5549-56.
- McMillan, P.J., Patzewitz, E.M., Young, S.E., Westrop, G.D., Coombs, G.H., Engman, L., and Muller, S. (2009). Differential inhibition of high and low Mr thioredoxin reductases of parasites by organotelluriums supports the concept that low Mr thioredoxin reductases are good drug targets. *Parasitology* *136*, 27-33.
- Messerschmidt, A., Worbs, M., Steegborn, C., Wahl, M.C., Huber, R., Laber, B., and Clausen, T. (2003). Determinants of enzymatic specificity in the Cys-Met-metabolism PLP-dependent enzymes family: crystal structure of cystathionine gamma-lyase from yeast and intrafamilial structure comparison. *Biol. Chem.* *384*, 373-86.
- Metz, B., Kersten, G.F., Hoogerhout, P., Brugghe, H.F., Timmermans, H.A., de Jong, A., Meiring, H., ten Hove, J., Hennink, W.E., Crommelin, D.J., and Jiskoot, W. (2004). Identification of formaldehyde-induced modifications in proteins: reactions with model peptides. *J. Biol. Chem.* *279*, 6235-43.
- Metzler, D.E., Ikawa, M., and Snell, E.E. (1954a). A General Mechanism for Vitamin B6-catalyzed Reactions. *J. Am. Chem. Soc.* *76*, 648-52.
- Metzler, D.E., Longenecker, J.B., and Snell, E.E. (1954b). The Reversible Catalytic Cleavage of Hydroxyamino Acids by Pyridoxal and Metal Salts. *J. Am. Chem. Soc.*, 639-44.
- Metzler, D.E., and Snell, E.E. (1952). Deamination of serine. *Journal of Biological Chemistry. J. Biol. Chem.*, 353-61.
- Middleton, W.J. (1975a). New fluorinating reagents. Dialkylaminosulfur fluorides. *J. Org. Chem.* *40*, 574-78.
- Middleton, W.J. (1975b). Tetrafluorodithiosuccinyl difluoride. *J. Org. Chem.* *40*, 129-30.
- Miki, K., Xu, M., An, Z., Wang, X., Yang, M., Al-Refaie, W., Sun, X., Baranov, E., Tan, Y., Chishima, T., Shimada, H., Moossa, A.R., and Hoffman, R.M. (2000). Survival efficacy

- of the combination of the methioninase gene and methioninase in a lung cancer orthotopic model. *Cancer Gene Ther* 7, 332-8.
- Miki, K., Xu, M., Gupta, A., Ba, Y., Tan, Y., Al-Refaie, W., Bouvet, M., Makuuchi, M., Moossa, A.R., and Hoffman, R.M. (2001). Methioninase cancer gene therapy with selenomethionine as suicide prodrug substrate. *Cancer Res.* 61, 6805-10.
- Mills, J.E. (1986). A Mild, Convenient Preparation of N,N-Disubstituted Thioformamides From Secondary Amines. *Synthesis* 1986, 482-84.
- Mino, K., and Ishikawa, K. (2003). Characterization of a novel thermostable O-acetylserine sulfhydrylase from *Aeropyrum pernix* K1. *J Bacteriol* 185, 2277-84.
- Misaki, T., Nagase, R., Matsumoto, K., and Tanabe, Y. (2005). Ti-Crossed-Claisen Condensation between Carboxylic Esters and Acid Chlorides or Acids: A Highly Selective and General Method for the Preparation of Various β -Keto Esters. *J. Am. Chem. Soc.* 127, 2854-55.
- Miyake, T., and Shibamoto, T. (1995). Quantitative analysis by gas chromatography of volatile carbonyl compounds in cigarette smoke. *J. Chromatogr. A* 693, 376-81.
- Mo, Y. (2010). Computational evidence that hyperconjugative interactions are not responsible for the anomeric effect. *Nat. Chem.* 2, 666-71.
- Moltzen, E.K., Kramer, M.P., Senning, A., and Klabunde, K.J. (1987). Carbon monosulfide chemistry in solution. 4. Studies on the reactivity of carbon monosulfide toward amines and thiols. *J. Org. Chem.* 52, 1156-61.
- Moreno, S.N., Mason, R.P., and Docampo, R. (1984). Distinct reduction of nitrofurans and metronidazole to free radical metabolites by *Tritrichomonas foetus* hydrogenosomal and cytosolic enzymes. *J. Biol. Chem.* 259, 8252-9.
- Motoshima, H., Inagaki, K., Kumasaka, T., Furuichi, M., Inoue, H., Tamura, T., Esaki, N., Soda, K., Tanaka, N., Yamamoto, M., and Tanaka, H. (2000). Crystal structure of the pyridoxal 5'-phosphate dependent L-methionine gamma-lyase from *Pseudomonas putida*. *J Biochem* 128, 349-54.

- Moya, I.A., Su, Z., and Honek, J.F. (2009). Current and future perspectives on the chemotherapy of parasitic protozoa *Trichomonas vaginalis* and *Entamoeba histolytica*. *Future Med. Chem.* *1*, 619-43.
- Moya, I.A., Westrop, G.D., Coombs, G.H., and Honek, J.F. (2011). Mechanistic studies on the enzymatic processing of fluorinated methionine analogs by *Trichomonas vaginalis* methionine gamma-lyase. *Biochem. J.* *438*, 513-21.
- Muller, M. (1988). Energy metabolism of protozoa without mitochondria. *Annu. Rev. Microbiol.* *42*, 465-88.
- Nagle, J.K. (1990). Atomic polarizability and electronegativity. *J. Am. Chem. Soc.* *112*, 4741-47.
- Nakayama, T., Esaki, N., Tanaka, H., and Soda, K. (1988a). Chemical Modification of Cysteine Residues of L-Methionine γ -Lyase. *Agric. Biol. Chem.*, 177-83.
- Nakayama, T., Esaki, N., Tanaka, H., and Soda, K. (1988b). Specific labeling of the essential cysteine residue of L-methionine gamma-lyase with a cofactor analogue, N-(bromoacetyl)pyridoxamine phosphate. *Biochemistry* *27*, 1587-91.
- Nicolaou, K.C., Dethe, D.H., Leung, G.Y.C., Zou, B., and Chen, D.Y.K. (2008). Total Synthesis of Thiopeptide Antibiotics GE2270A, GE2270T, and GE2270C1. *Chem.-Asian J.* *3*, 413-29.
- Norhayati, M., Fatmah, M.S., Yusof, S., and Edariah, A.B. (2003). Intestinal parasitic infections in man: a review. *Med. J. Malaysia*, 296-305.
- Nozaki, T., Asai, T., Kobayashi, S., Ikegami, F., Noji, M., Saito, K., and Takeuchi, T. (1998). Molecular cloning and characterization of the genes encoding two isoforms of cysteine synthase in the enteric protozoan parasite *Entamoeba histolytica*. *Mol. Biochem. Parasitol.* *97*, 33-44.
- Nozaki, T., Asai, T., Sanchez, L.B., Kobayashi, S., Nakazawa, M., and Takeuchi, T. (1999). Characterization of the gene encoding serine acetyltransferase, a regulated enzyme of cysteine biosynthesis from the protist parasites *Entamoeba histolytica* and *Entamoeba*

- dispar. Regulation and possible function of the cysteine biosynthetic pathway in *Entamoeba*. *J. Biol. Chem.* *274*, 32445-52.
- Nozaki, T., Tokoro, M., Imada, M., Saito, Y., Abe, Y., Shigeta, Y., and Takeuchi, T. (2000). Cloning and biochemical characterization of genes encoding two isozymes of cysteine synthase from *Entamoeba dispar*. *Mol. Biochem. Parasitol.*, 129-33.
- Nudelman, A., and Nudelman, A. (1999). Convenient Syntheses of δ -Aminolevulinic Acid. *Synthesis*, 568-70.
- O'Connor, J.R., Johnson, S., and Gerding, D.N. (2009). *Clostridium difficile* infection caused by the epidemic BI/NAP1/027 strain. *Gastroenterology* *136*, 1913-24.
- O'Hagan, D. (2008). Understanding organofluorine chemistry. An introduction to the C-F bond. *Chem. Soc. Rev.* *37*, 308-19.
- O'Hagan, D., and Rzepa, H.S. (1997). ChemInform Abstract: Some Influences of Fluorine in Bioorganic Chemistry. *Chem. Commun.* *28*, 645-52.
- Ochman, H., Lawrence, J.G., and Groisman, E.A. (2000). Lateral gene transfer and the nature of bacterial innovation. *Nature* *405*, 299-304.
- Ohlinger, W.S., Klunzinger, P.E., Deppmeier, B.J., and Hehre, W.J. (2009). Efficient Calculation of Heats of Formation. *J. Phys. Chem. A.* *113*, 2165-75.
- Olivard, J., Metzler, D.E., and Snell, E.E. (1952). Catalytic racemization of amino acids by pyridoxal and metal salts. *J. Biol. Chem.*, 669-74.
- Pal, D., Banerjee, S., Cui, J., Schwartz, A., Ghosh, S.K., and Samuelson, J. (2009). *Giardia*, *Entamoeba*, and *Trichomonas* enzymes activate metronidazole (nitroreductases) and inactivate metronidazole (nitroimidazole reductases). *Antimicrob. Agents Chemother.* *53*, 458-64.
- Palm, D., Klein, H.W., Schinzel, R., Buehner, M., and Helmreich, E.J. (1990). The role of pyridoxal 5'-phosphate in glycogen phosphorylase catalysis. *Biochemistry* *29*, 1099-107.
- Papeo, G., Giordano, P., Brasca, M.G., Buzzo, F., Caronni, D., Ciprandi, F., Mongelli, N., Veronesi, M., Vulpetti, A., and Dalvit, C. (2007). Polyfluorinated amino acids for

- sensitive ^{19}F NMR-based screening and kinetic measurements. *J. Am. Chem. Soc.* *129*, 5665-72.
- Posner, B.I., and Flavin, M. (1972). Cystathionine β -synthase. Studies of hydrogen exchange reactions. *J. Biol. Chem.* *247*, 6402-11.
- Rablen, P.R., Hoffmann, R.W., Hrovat, D.A., and Borden, W.T. (1999). Is hyperconjugation responsible for the "gauche effect" in 1-fluoropropane and other 2-substituted-1-fluoroethanes? *J. Chem. Soc. Perkin Trans.*, 1719-26.
- Rablen, P.R., Lockman, J.W., and Jorgensen, W.L. (1998). Ab Initio Study of Hydrogen-Bonded Complexes of Small Organic Molecules with Water. *J. Phys. Chem. A.* *102*, 3782-97.
- Rasoloson, D., Tomkova, E., Cammack, R., Kulda, J., and Tachezy, J. (2001). Metronidazole-resistant strains of *Trichomonas vaginalis* display increased susceptibility to oxygen. *Parasitology* *123*, 45-56.
- Ravanel, S., Gakiere, B., Job, D., and Douce, R. (1998). The specific features of methionine biosynthesis and metabolism in plants. *Proc Natl Acad Sci U S A* *95*, 7805-12.
- Reeves, R.E. (1984). Metabolism of *Entamoeba histolytica* Schaudinn, 1903. *Adv. Parasitol.* *23*, 105-42.
- Ren, J. (2006). Polar Group Enhanced Gas-Phase Acidities of Carboxylic Acids: An Investigation of Intramolecular Electrostatic Interaction. *J. Phys. Chem. A* *110*, 13405-11.
- Rogers, M.T., and Burdett, J.L. (1965a). Keto-enol tautomerism in β -dicarbonyls studied by nuclear magnetic resonance spectroscopy. II. Solvent effects on proton chemical shifts and on equilibrium constants. *Can. J. Chem.* *43*, 1516-26.
- Rogers, M.T., and Burdett, J.L. (1965b). Keto-enol tautomerism in β -dicarbonyls studied by nuclear magnetic resonance spectroscopy. III. Studies of proton chemical shifts and equilibrium constants at different temperatures. *Can. J. Chem.* *43*, 1516-26.
- Rosenthal, B., Mai, Z., Caplivski, D., Ghosh, S., de la Vega, H., Graf, T., and Samuelson, J. (1997). Evidence for the bacterial origin of genes encoding fermentation enzymes of the amitochondriate protozoan parasite *Entamoeba histolytica*. *J. Bacteriol.* *179*, 3736-45.

- Sakai, T., Liu, Y., Ohta, H., Korenaga, T., and Ema, T. (2005). Lipase-Catalyzed Resolution of (2R*,3S*)- and (2R*,3R*)-3-Methyl-3-phenyl-2-aziridinemethanol at Low Temperatures and Determination of the Absolute Configurations of the Four Stereoisomers. *J. Org. Chem.* *70*, 1369-75.
- Samarawickrema, N.A., Brown, D.M., Upcroft, J.A., Thammapalerd, N., and Upcroft, P. (1997). Involvement of superoxide dismutase and pyruvate:ferredoxin oxidoreductase in mechanisms of metronidazole resistance in *Entamoeba histolytica*. *J. Antimicrob. Chemother.* *40*, 833-40.
- Sambrook, J., and Russell, D.W. (2001). Protocol 6: Site-specific mutagenesis by overlap extension. , Vol 2 (New York, Cold Spring Harbor Laboratory Press).
- Samuelson, J. (1999). Why metronidazole is active against both bacteria and parasites. *Antimicrob. Agents Chemother.* *43*, 1533-41.
- Sato, D., and Nozaki, T. (2009). Methionine gamma-lyase: the unique reaction mechanism, physiological roles, and therapeutic applications against infectious diseases and cancers. *IUBMB Life* *61*, 1019-28.
- Sato, D., Yamagata, W., Harada, S., and Nozaki, T. (2008). Kinetic characterization of methionine gamma-lyases from the enteric protozoan parasite *Entamoeba histolytica* against physiological substrates and trifluoromethionine, a promising lead compound against amoebiasis. *FEBS J.* *275*, 548-60.
- Savage, D.C. (1977). Microbial Ecology of the Gastrointestinal Tract. *Annu. Rev. Microbiol.* *31*, 107-33.
- Schneider, G., Käck, H., and Lindqvist, Y. (2000). The manifold of vitamin B6 dependent enzymes. *Structure* *8*, R1-R6.
- Schneider, W.F., Nance, B.I., and Wallington, T.J. (1995). Bond Strength Trends in Halogenated Methanols: Evidence for Negative Hyperconjugation? *J. Am. Chem. Soc.* *117*, 478-85.
- Schwebke, J.R. (2002). Update of trichomoniasis. *Sex Transm Infect* *78*, 378-9.

- Sebahia, M., Wren, B.W., Mullany, P., Fairweather, N.F., Minton, N., Stabler, R., Thomson, N.R., Roberts, A.P., Cerdeno-Tarraga, A.M., Wang, H., Holden, M.T., Wright, A., Churcher, C., Quail, M.A., Baker, S., Bason, N., Brooks, K., Chillingworth, T., Cronin, A., Davis, P., Dowd, L., Fraser, A., Feltwell, T., Hance, Z., Holroyd, S., Jagels, K., Moule, S., Mungall, K., Price, C., Rabinowitsch, E., Sharp, S., Simmonds, M., Stevens, K., Unwin, L., Whithead, S., Dupuy, B., Dougan, G., Barrell, B., and Parkhill, J. (2006). The multidrug-resistant human pathogen *Clostridium difficile* has a highly mobile, mosaic genome. *Nat. Genet.* *38*, 779-86.
- Seebach, D., Häner, R., and Vettiger, T. (1987). Nucleophile ringöffnung von α -nitrocyclopropan-carbonsäure-arylestern mit sterisch geschützter, aber elektronisch wirksamer carbonyl- und nitro-gruppe. Ein neues prinzip der α -aminosäure-synthese (2-aminobutansäure- α^4 -synthon). *Helv. Chim. Acta* *70*, 1507-15.
- Sekowska, A., Kung, H.F., and Danchin, A. (2000). Sulfur metabolism in *Escherichia coli* and related bacteria: facts and fiction. *J. Mol. Microbiol. Biotechnol.* *2*, 145-77.
- Shao, Y., Molnar, L.F., Jung, Y., Kussmann, J., Ochsenfeld, C., Brown, S.T., Gilbert, A.T.B., Slipchenko, L.V., Levchenko, S.V., O'Neill, D.P., DiStasio Jr, R.A., Lochan, R.C., Wang, T., Beran, G.J.O., Besley, N.A., Herbert, J.M., Yeh Lin, C., Van Voorhis, T., Hung Chien, S., Sodt, A., Steele, R.P., Rassolov, V.A., Maslen, P.E., Korambath, P.P., Adamson, R.D., Austin, B., Baker, J., Byrd, E.F.C., Dachsel, H., Doerksen, R.J., Dreuw, A., Dunietz, B.D., Dutoi, A.D., Furlani, T.R., Gwaltney, S.R., Heyden, A., Hirata, S., Hsu, C.-P., Kedziora, G., Khalliulin, R.Z., Klunzinger, P., Lee, A.M., Lee, M.S., Liang, W., Lotan, I., Nair, N., Peters, B., Proynov, E.I., Pieniazek, P.A., Min Rhee, Y., Ritchie, J., Rosta, E., David Sherrill, C., Simmonett, A.C., Subotnik, J.E., Lee Woodcock Iii, H., Zhang, W., Bell, A.T., Chakraborty, A.K., Chipman, D.M., Keil, F.J., Warshel, A., Hehre, W.J., Schaefer Iii, H.F., Kong, J., Krylov, A.I., Gill, P.M.W., and Head-Gordon, M. (2006). Advances in methods and algorithms in a modern quantum chemistry program package. *Phys. Chem. Chem. Phys.* *8*, 3172-91.

- Silverman, R.B., and Abeles, R.H. (1976). Inactivation of pyridoxal phosphate dependent enzymes by mono- and polyhaloalanines. *Biochemistry* 15, 4718-23.
- Soda, K. (1968). Microdetermination of D-amino acids and D-amino acid oxidase activity with 3-methyl-2-benzothiazolone hydrazone hydrochloride. *Anal. Biochem.* 25, 228-35.
- Soda, K., Yorifuji, T., Misono, H., and Moriguchi, M. (1969). Spectrophotometric determination of pyridoxal and pyridoxal 5'-phosphate with 3-methyl-2-benzothiazolone hydrazone hydrochloride, and their selective assay. *Biochem. J.* 114, 629-33.
- Soloshonok, V., Kukhar, V., Pustovit, Y., and Nazaretian, V. (1992). A new and convenient synthesis of S-trifluoromethyl-containing amino acids. *Synlett* 1992, 657-58.
- Squillacote, M.E., Sheridan, R.S., Chapman, O.L., and Anet, F.A.L. (1979). Planar s-cis-1,3-butadiene. *J. Am. Chem. Soc.* 101, 3657-59.
- Stanley, S.L., Jr. (2005). The *Entamoeba histolytica* genome: something old, something new, something borrowed and sex too? *Trends Parasitol.* 21, 451-3.
- Stern, P., and Hoffman, R. (1984). Elevated overall rates of transmethylation in cell lines from diverse human tumors. *In Vitro Cell Dev.-Pl.*, 663-70.
- Stipanuk, M.H. (1986). Metabolism of sulfur-containing amino acids. *Annu. Rev. Nutr.* 6, 179-209.
- Sturtevant, J.M., Ho, C., and Reimann, A. (1979). Thermotropic behavior of some fluorodimyristoylphosphatidylcholines. *Proc. Natl. Acad. Sci. USA* 76, 2239-43.
- Tachezy, J., Kulda, J., and Tomkova, E. (1993). Aerobic resistance of *Trichomonas vaginalis* to metronidazole induced *in vitro*. *Parasitology* 106, 31-37.
- Takada, H., Esaki, N., Tanaka, H., and Soda, K. (1988). The C₃-N bond cleavage of 2-amino-3-(N-substituted-amino)-propionic acids catalyzed by L-methionine gamma-lyase. *Agric. Biol. Chem.* 52, 2897-901.
- Tan, Y., Sun, X., Xu, M., Tan, X., Sasson, A., Rashidi, B., Han, Q., Wang, X., An, Z., Sun, F.X., and Hoffman, R.M. (1999). Efficacy of recombinant methioninase in combination with cisplatin on human colon tumors in nude mice. *Clin Cancer Res* 5, 2157-63.

- Tan, Y., Xu, M., Tan, X., Wang, X., Saikawa, Y., Nagahama, T., Sun, X., Lenz, M., and Hoffman, R.M. (1997). Overexpression and large-scale production of recombinant L-methionine-alpha-deamino-gamma-mercaptomethane-lyase for novel anticancer therapy. *Protein Expr Purif* 9, 233-45.
- Tanaka, H., Esaki, N., and Soda, K. (1977). Properties of L-methionine gamma-lyase from *Pseudomonas ovalis*. *Biochemistry* 16, 100-6.
- Tarleton, J.L., Haque, R., Mondal, D., Shu, J., Farr, B.M., and Petri, W.A., Jr. (2006). Cognitive effects of diarrhea, malnutrition, and *Entamoeba histolytica* infection on school age children in Dhaka, Bangladesh. *Am. J. Trop. Med. Hyg.* 74, 475-81.
- Thomas, D., and Surdin-Kerjan, Y. (1997). Metabolism of sulfur amino acids in *Saccharomyces cerevisiae*. *Microbiol. Mol. Biol. Rev.* 61, 503-32.
- Thomas, J.H., Dodgson, K.S., and Tudball, N. (1968). The pyridoxal- and pyridoxal 5'-phosphate-catalysed non-enzymic degradations of l-serine o-sulphate and related compounds. *Biochem. J.* 110, 687-92.
- Tisdale, M.J. (1980). Effect of methionine replacement by homocysteine on the growth of cells. *Cell Biol. Int. Rep.*, 563-70.
- Tokoro, M., Asai, T., Kobayashi, S., Takeuchi, T., and Nozaki, T. (2003). Identification and characterization of two isoenzymes of methionine gamma-lyase from *Entamoeba histolytica*: a key enzyme of sulfur-amino acid degradation in an anaerobic parasitic protist that lacks forward and reverse trans-sulfuration pathways. *J. Biol. Chem.* 278, 42717-27.
- Toraya, T., Nihira, T., and Fukui, S. (1976). Essential Role of Monovalent Cations in the Firm Binding of Pyridoxal 5'-Phosphate to Tryptophanase and β -Tyrosinase *Eur. J. Biochem.* 69, 411-19.
- Tovar, J., Fischer, A., and Clark, C.G. (1999). The mitosome, a novel organelle related to mitochondria in the amitochondrial parasite *Entamoeba histolytica*. *Mol. Microbiol.* 32, 1013-21.

- Trapp, M.L., Watts, J.K., Weinberg, N., and Pinto, B.M. (2006). Component analysis of the X-C-Y anomeric effect (X=O, S; Y=F, OMe, NHMe) by DFT molecular orbital calculations and natural bond orbital analysis. *Can. J. Chem.* *84*, 692-701.
- Trussell, R.E. (1946). Microagglutination Tests with *Trichomonas vaginalis*. *J. Parasitol.* *32*, 563-69.
- Tsushima, T., Ishihara, S., and Fujita, Y. (1990). Fluorine-containing amino acids and their derivatives. 9. Synthesis and biological activities of difluoromethylhomocysteine. *Tetrahedron Lett.* *31*, 3017-18.
- Tyrra, W. (2001). Die Desulfonierung-Fluorierung von Thiuramdisulfiden, [R₂NC(S)S]₂ und Silberdithiocarbamaten, Ag[SC(S)NR₂] (R = CH₃, CH₃CH₂, C₆H₅CH₂), mit Silber(I)fluorid, AgF - ein einfacher Zugang zu Diorgano(trifluormethyl)aminen, R₂NCF₃, und Thiocarbamoylfluoriden, R₂NC(S)F. *J. Fluor. Chem.* *109*, 189-94.
- Vallabhajosula, S. (2007). (18)F-labeled positron emission tomographic radiopharmaceuticals in oncology: an overview of radiochemistry and mechanisms of tumor localization. *Semin. Nucl. Med.* *37*, 400-19.
- Vaughan, M.D., Cleve, P., Robinson, V., Duetzel, H.S., and Honek, J.F. (1999). Difluoromethionine as a novel ¹⁹F NMR structural probe for internal amino acid packing in proteins. *J. Am. Chem. Soc.* *121*, 8475-78.
- Verstappen, M.M.H., Ariaans, G.J.A., and Zwanenburg, B. (1996). Asymmetric Synthesis of 2H-Azirine Carboxylic Esters by an Alkaloid-Mediated Neber Reaction. *J. Am. Chem. Soc.* *118*, 8491-92.
- Vicente, J.B., Ehrenkaufner, G.M., Saraiva, L.M., Teixeira, M., and Singh, U. (2008). *Entamoeba histolytica* modulates a complex repertoire of novel genes in response to oxidative and nitrosative stress: implications for amebic pathogenesis. *Cell Microbiol.* *11*, 51-69.
- Vila, A., Estévez, L., Mosquera, R.A., Estévez, L., and Mosquera, R.A. (2011). Influence of the solvent on the charge distribution of anomeric compounds. *J. Phys. Chem. A.* *115*, 1964-70.

- von Hofsten, B. (1961a). Acid phosphatase and the growth of *Escherichia coli*. *Biochim. Biophys. Acta* *48*, 171-81.
- von Hofsten, B. (1961b). Fluoro-d-galactosides as substrates and inducers of the [beta]-galactosidase of *Escherichia coli*. *Biochim. Biophys. Acta* *48*, 159-63.
- Wade, T.N., and Kheribet, R. (1980). New convenient synthesis of .beta.,.beta.-difluoro amines and .beta.,.beta.-difluoro-.alpha.-amino acid alkyl esters by the addition of hydrogen fluoride on 1-azirines. *J. Org. Chem.* *45*, 5333-35.
- Washtien, W., Cooper, A.J., and Abeles, R.H. (1977). Substrate proton exchange catalyzed by gamma-cystathionase. *Biochemistry* *16*, 460-3.
- Wassmann, C., Hellberg, A., Tannich, E., and Bruchhaus, I. (1999). Metronidazole Resistance in the Protozoan Parasite *Entamoeba histolytica* Is Associated with Increased Expression of Iron-containing Superoxide Dismutase and Peroxiredoxin and Decreased Expression of Ferredoxin 1 and Flavin Reductase. *J. Biol. Chem.* *274*, 26051-56.
- Wendel, K.A., and Workowski, K.A. (2007). Trichomoniasis: challenges to appropriate management. *Clin. Infect. Dis.* *44*, S123-29.
- West, S.B., Wislocki, P.G., Fiorentini, K.M., Alvaro, R., Wolf, F.J., and Lu, A.Y.H. (1982). Drug residue formation from ronidazole, a 5-nitroimidazole. I. Characterization of in vitro protein alkylation. *Chem.-Biol. Interact.* *41*, 265-79.
- Westrop, G.D., Goodall, G., Mottram, J.C., and Coombs, G.H. (2006). Cysteine biosynthesis in *Trichomonas vaginalis* involves cysteine synthase utilizing O-phosphoserine. *J. Biol. Chem.* *281*, 25062-75.
- Wiberg, K.B., and Murcko, M.A. (1988). Bond bending and hybridization. *J. Mol. Struct.* *169*, 355-65.
- Woehl, E.U., and Dunn, M.F. (1995). The roles of Na⁺ and K⁺ in pyridoxal phosphate enzyme catalysis. *Coord. Chem. Rev.* *144*, 147-97.
- Yan, L., and Spallholz, J.E. (1993). Generation of reactive oxygen species from the reaction of selenium compounds with thiols and mammary tumor cells. *Biochem. Pharmacol.* *45*, 429-37.

- Yang, Z., Wang, J., Lu, Q., Xu, J., Kobayashi, Y., Takakura, T., Takimoto, A., Yoshioka, T., Lian, C., Chen, C., Zhang, D., Zhang, Y., Li, S., Sun, X., Tan, Y., Yagi, S., Frenkel, E.P., and Hoffman, R.M. (2004). PEGylation confers greatly extended half-life and attenuated immunogenicity to recombinant methioninase in primates. *Cancer Res* *64*, 6673-8.
- Yarlett, N., Yarlett, N.C., and Lloyd, D. (1986). Metronidazole-resistant clinical isolates of *Trichomonas vaginalis* have lowered oxygen affinities. *Mol. Biochem. Parasitol.* *19*, 111-6.
- Yoshimura, M., Nakano, Y., and Koga, T. (2002). L-Methionine-gamma-lyase, as a target to inhibit malodorous bacterial growth by trifluoromethionine. *Biochem. Biophys. Res. Commun.* *292*, 964-8.
- Yoshioka, T., Wada, T., Uchida, N., Maki, H., Yoshida, H., Ide, N., Kasai, H., Hojo, K., Shono, K., Maekawa, R., Yagi, S., Hoffman, R.M., and Sugita, K. (1998). Anticancer efficacy in vivo and in vitro, synergy with 5-fluorouracil, and safety of recombinant methioninase. *Cancer Res.* *58*, 2583-87.
- Yu, S.-L., Sauer, D.T., and Shreeve, J.M. (1974). Oxidations of partially fluorinated alkyl sulfides. Preparation of methyltrifluoromethyl sulfoxide and methyl(trifluoromethyl)sulfur tetrafluoride. *Inorg. Chem.* *13*, 484-86.
- Zabinski, R.F., and Toney, M.D. (2001). Metal ion inhibition of nonenzymatic pyridoxal phosphate catalyzed decarboxylation and transamination. *J. Am. Chem. Soc.* *123*, 193-8.